ROYAUME DU MAROC
Université Mohammed V - RABAT -
جامعة محمد الخامس – الرباط –
Faculté des sciences
كلية العلوم

CENTRE D'ETUDES DOCTORALES-SCIENCES ET TECHNOLOGIES

N° d'ordre : 3856

THÈSE

En vue de l'obtention du : ***DOCTORAT***

Structure de recherche *: Équipe des sciences de la matière et du rayonnement*

Discipline *: Physique*

Spécialité *: Physique quantique*

Présentée et soutenue le 21/10/2023 par :

Oumayma EL BIR

Quantum correlations in an optomechanical ring cavity

Jury

Yassine HASSOUNI	PES, Université Mohammed V, Faculté des Sciences, Rabat	Président
Hamid EZ-ZAHRAOUY	PES, Université Mohammed V, Faculté des Sciences, Rabat	Rapporteur/Examinateur
Rachid AHL LAAMARA	PES, Université Mohammed V, Faculté des Sciences, Rabat	Rapporteur/Examinateur
Saad RFIFI	PH, Université Abdelmalek Essaâdi, Faculté Polydisciplinaire de Larache	Rapporteur/Examinateur
Adil BELHAJ	PH, Université Mohammed V, Faculté des Sciences, Rabat	Rapporteur/Examinateur
Özgür E. MUSTECAPLIOGLU	PES, Université Koç, Istanbul, Turkey	Examinateur
Morad EL BAZ	PES, Université Mohammed V, Faculté des Sciences, Rabat	Directeur de thèse

Année universitaire : 2023/2024

✉ Faculté des Sciences, avenue Ibn Battouta, BP. 1014 RP, Rabat-Maroc
☎ 00212 (05) 37 77 18 76 🖷 00212 (05) 37 77 42 61; http://www.fsr.um5.ac.ma

To my beloved father

Acknowledgements

The doctoral thesis presented hereafter could not have been completed without the support of people who had the utmost positive impact on my experience as a researcher.

Words cannot express my appreciation and gratitude to my supervisor, Prof. ***Morad EL BAZ****, for embracing me as a member of his research team. I could not have undertaken this research project without relying on his outstanding knowledge in Math and Physics. His in-depth insights guided me to solving complicated problems throughout the entire duration of the project. His compassion and supportive manners were also my refuge for positive energy when I did not have a clear vision and was lost in the array of my own scattered ideas. His leadership mind set helped grasp the idea that receiving a rejection letter for an article I have submitted, is in fact a learning curve rather than a failure.*

I want to express my deep appreciation to Professor ***Yassine HASSOUNI*** *for arousing my interest in scientific research and providing support with my studies.*

I am grateful to Professor ***Adil BELHAJ*** *director of theoretical physics laboratory who is always ready to give best guide.*

I am profoundly indebted to my mother, Mrs ***Latifa EL JIRARI*** *for believing in me and supporting me over the years of my academic journey. To her I say: I hope I made you proud.*

I would like also to express my special thanks to my brothers ***Tarik*** *and* ***Anas****, for providing me with the powerful encouragement needed during the hard times. Thanks to little* ***Salim*** *for his love and for making our house full of joy and happiness. And to the rest of my extended family members, I would like to say thank you for all the care and interest you demonstrated at every occasion when we met and you asked about how my project was coming along.*

My sincere thanks to Dr ***Mustapha ZIANE*** *for his guidance and help. His insights that helped me solving problems on the research subject. I hope that our valuable cooperation will continue.*

During my time as PHD research, I have had the pleasure and honor of attending numerous international scientific events. My deepest thanks to the International Centre for Theoretical Physics in Trieste-Italy for the travel grants, and for giving me and my colleagues the opportunity of networking with other junior and senior researchers from all over the world.

My sincere acknowledgement goes out to the following researchers whom I have enjoyed my exchange of ideas and discussions: ***Daniel BRAUN****,* ***Matteo G A PARIS****,* ***Mauro PATERNOSTRO****,* ***Michael THORWART****,* ***Florian MARQUADT****.*

A special thanks to all Professors and senior staff members of ***ESMAR*** *(Equipe Science de la Matière et Rayonnement) for creating a great research environment in the laboratory of theoretical physics. I would also like to thank my dear colleagues for the many great memories from trips and events that we attended together. In particular,* ***Sanae ABAACH****,* ***Zakaria MZAOUALI****,* ***Khadija EL ANOUZ****,* ***Hassna HAJJI****,* ***Khadija EL HOUWARY****,* ***Hicham AIT MANSOUR*** *and* ***Fadwa EL AYACHI****.*

A special thank you to my dear friend ***Meriem LAASSIRI*** *for her support during the hard times.*

Finally, I would like express my gratitude to the members of the jury who accepted to examine and evaluate my work.

Résumé

Cette thèse est consacrée à l'étude des corrélations quantiques au sein d'une cavité optomécanique en anneau. Cette étude met en lumière l'interaction extraordinaire entre la lumière et le mouvement mécanique au niveau quantique. Une étude théorique complète basée sur les principaux concepts de l'optomécanique est donnée. Les progrès récents dans ce domaine ont ouvert de nombreuses applications dans diverses structures. Dans ce contexte, On donne une description claire du choix d'une cavité annulaire, qui présente un milieu idéal pour étudier les effets coopératifs grâce à leur interaction commune avec le mode de la cavité. Les cavités annulaires diffèrent de la conception traditionnelle des cavités Fabry-Pérot par la présence de paires de miroirs mobiles. Cela ajoute une manipulation dynamique supplémentaire du déplacement des deux résonateurs, intensifiant ainsi le champ optique intra-cavité, contrairement au cas d'une cavité linéaire. Un autre type de système présenté dans cette thèse, considéré comme une source de grande variété de phénomènes physiques, est le système atome-optomécanique, où un ensemble d'atomes est confiné à l'intérieur de la cavité, permettant des interactions à longue distance et des corrélations multipartites. Dans la deuxième partie de la thèse, l'accent est mis sur la composante non linéaire de l'Hamiltonien optomécanique. La résolution de la dynamique est effectuée en excluant le traitement de linéarisation. Cette solution est basée sur l'identification d'une algèbre de Lie minimale et finie qui génère l'évolution temporelle du système, et dérive une solution analytique pour calculer la non-Gaussianité du système en fonction du temps.

Mots-clefs : Optomécanique, intrication, cavité en anneau, corrélations quantiques, non-Gaussianité.

Abstract

This thesis focuses on the fascinating realm of quantum correlations within a ring optomechanical cavity, shedding light on the extraordinary interplay between light and mechanical motion at the quantum level. A comprehensive theoretical framework based on the principal concepts of optomechanics. Recent advancements in this have opened up numerous applications in various structures. In this context, a clear description of choosing a ring cavity, which serves as an ideal testbed to exhibit cooperative effects through their common interaction with the cavity mode. Ring cavities differ from the traditional Fabry-Perot cavity design by having pairs of movable mirrors. This adds an extra dynamic manipulation of the displacement of the two resonators, thereby intensifying the intra-cavity optical field, unlike in the case of a linear cavity. Another type of system presented in this thesis, which serves as a source of a wide variety of physical phenomena, is the atom- optomechanical system, where an ensemble of atoms is confined inside the cavity, allowing for long range interactions and multipartite correlations. In the next part of the thesis, the nonlinear component of the optomechanical Hamiltonian is emphasized. The resolution of the dynamics is carried out excluding the linearization treatment. This solution is based on identifying a minimal and finite Lie algebra that generates the time-evolution of the system, and derive analytic solution to compute the non-Gaussianity of the system as function of the time.

Keywords: Optomechanics, entanglement, ring cavity, quantum correlations, non-Gaussianity.

List of Figures

1 (a) illustrates a linear configuration composed of two mirrors and (b) describes a ring cavity. 3

1.1 The figure shows the thermal photon statistics P_n^{th} as a function of the photon number n. In the left (right), we consider $\bar{n} = 2(\bar{n} = 4)$. 13

1.2 Fresnel representation of a squeezed state for different quadratures. 14

1.3 Plots of the Wigner function of coherent states having amplitude $\alpha = 2$ and phase $\varphi = \frac{\pi}{4}$. 16

2.1 Schematic diagram of the motion of the mechanical object made by the electromagnetic field due to the radiation pressure force. 28

2.2 Gallery of cavity optomechanics devices. From top left, down : N. Mavalvala, A. Heidmann, M. Aspelmeyer, D. Bouwmeester, J. Harris, P. Treutlein, T. J. Kippenberg, I. Favero, M. Lipson, T. J. Kippenberg/E. Weig/J. Kotthaus, H. Tang, K. Vahala/T. Carmon, J. Teufel/K. Lehnert, I. Robert, O. Painter, O. Painter, I. Favero/E. Weig/K. Karrai, and D. Stamper-Kurn 29

2.3 A schematic of a Fabry-Perot cavity. Formed of two mirrors each mirror has an associated reflection and transmission field amplitude coefficients r_1,r_2 and t_1,t_2 respectively. 30

2.4 Energy Levels of the one-dimensional harmonic oscillator, the Wavefunction representations for the first eight bound eigenstates, n = 0 to 7. 35

2.5 Schematic representation of the coupling $\hat{H}_{coupl}$ between the harmonic oscillator $\hat{H}_m$ and the environment $\hat{H}_e$. 36

2.6 Schematic representation of the optomechanical interaction between the electromagnetic field and the mechanical mirror. 38
2.7 Schematic diagram of Stokes and Anti-Stokes sideband. Here a moving mirror driving by laser with frequency ω_L. 40
2.8 Modeling of the studied system: standard Fabry-Perot cavity with a laser-driven. 41
2.9 Plot of E_N as a function of Δ/ω_m for three different values of m, m_3(cyan Thik curves), m_2(orange dashed curves) and m_1(rainbow curves). 49
2.10 Entanglement E_N Vs the temperature $T(K)$ for two different values of m the mass of the mechanical oscillator. 49
2.11 Contour plot of E_N versus temperature T and optomechanical cooperativity C_{op}. We use $\Delta = \omega_m$, $m = 5\,ng$ and finesse $F = 3.4\,10^4$ 2.16, the other parameters similar to those in Fig. 2.10. 50
2.12 3D Plot of entanglement as function of laser power P and temperature T. 51

4.1 Schematic illustration of the Atom-optomechanical system. 63
4.2 Single atom interacting mechanically with a coherently electromagnetic cavity field. 64
4.3 Plot of the bipartite entanglement E_{m_1a}, between m_1 and a, versus the thermal bath temperature $T(K)$, for different values of the input field squeezing parameter r. 70
4.4 The logarithmic negativity E_{m_1op}, between m_1 and op versus the thermal bath temperature $T(K)$; the other parameters are chosen as in Figure 4.3. 72
4.5 Effect of the normalized atomic detuning on the (a) tripartite logarithmic negativities $\mathcal{E}_1$, $\mathcal{E}_2$ and $\mathcal{E}_3$ and (b) bipartite negativities ($E_{m_1m_2}$, E_{m_1op}, E_{m_1a} and E_{opa}) . In all the cases we choose $\Delta = \omega_m$, $P = 10mW$, $r = 0.1$ and the temperature $T = 0.1mK$. 73
4.6 (a) $\mathcal{E}_3$ and (b) $\mathcal{E}_2$ as a function of the temperature $T(mK)$ for different values of the pumping power P (measured in mW). $\Delta = 0.5\omega_m$ and the other parameters are chosen as in Figure 4.5. 75
4.7 The influence of the atom-cavity coupling G_a on $\mathcal{E}_1$ and $\mathcal{E}_2$ as a function of the temperature $T(mK)$. We choose $P = 35mW$, $r = 0.6$, $\Delta = \omega_m$. 76

5.1 Scheme of the optomechanical system under analysis. 80

5.2 The measure of non-Gaussianity $\delta(\tau)$ versus time τ for different values of μ_c. (a) corresponds to the non-Gaussianity of the optical and the mechanical mode 1. (b) represent the non-Gaussianity between the two mechanical modes. (c) corresponds to the 3 modes non-Gaussianity of the optomechanical system (optical, mechanical 1 and mechanical 2). 90

Table of Contents

Dedication i

Acknowledgements iii

Résumé iv

Abstract vi

List of Figures vii

Introduction 1

1 Quantum measures 6

1.1 Quantum optics in continuous variable 6

1.2 Quantum information basics 7

1.2.1 Quantum state 8

1.3 Definition of Gaussian states 9

1.3.1 Coherent state 10

1.3.2 Thermal state 12

1.3.3 Squeezed state 13

1.4 Mathematical description of N-mode Gaussian systems 14

1.4.1 Covariance matrix formalism 14

1.4.2 Wigner function 15

1.4.3 Symplectic formalism 17

1.4.4 Summary 18

1.5 Notion of quantum correlations 19

1.5.1 Definition of quantum entanglement . . . 19
1.5.2 Entanglement detection . . . 20
1.5.3 Quantifying quantum entanglement in Gaussian state . . . 22
1.5.4 Genuine tripartite entanglement . . . 24
1.5.5 Quantum discord . . . 25

2 Cavity Optomechanics : The theory behind 28
2.1 Optical resonators . . . 29
2.1.1 Intensity or Field transmission . . . 30
2.1.2 Stability . . . 32
2.1.3 The optical finesse . . . 32
2.1.4 Quality factor of the optical resonator . . . 33
2.2 Quantum harmonic oscillator . . . 33
2.2.1 Basic properties . . . 33
2.2.2 Mechanical quality factor . . . 35
2.2.3 Thermal bath environment of quantum harmonic oscillator . . . 36
2.3 Characterization of the optomechanical coupling . . . 37
2.4 Stokes and Anti-Stokes process . . . 39
2.5 Theoretical Fabry-Perot cavity model . . . 41
2.5.1 Hamiltonian formulation . . . 41
2.5.2 Quantum Langevin Equations . . . 43
2.5.3 Stability of the system . . . 45
2.5.4 Covariance Matrix . . . 46
2.5.5 Entanglement analysis . . . 47

3 Quantum correlations under the effect of a thermal environment in a triangular optomechanical cavity 52
3.1 Model and Hamiltonian . . . 52

4 Detection of genuine tripartite entanglement of an atoms-optomechanical cavity 62
4.1 Model and Hamiltonian . . . 63
4.1.1 Model . . . 63
4.1.2 Basics of light-atom interaction . . . 63

4.1.3 Hamiltonian . . . 65
4.2 System dynamics . . . 66
4.3 Entanglement analysis . . . 69
4.3.1 Bipartite entanglement . . . 69
4.3.2 Tripartite entanglement . . . 73

5 Observation of Non-Gaussianity on nonlinear optomechanical cavity 79
5.1 System and model . . . 80
5.2 Dynamics . . . 80
5.3 Measures of deviation from quantum Gaussianity . . . 88
5.4 Summary . . . 91

Conclusion and future works 92

Introduction

This dissertation delves into the intricacies of quantum measures, both as a tool for exploring the interplay between light and mechanical motion and as a potential hindrance in this project. The motion of objects stands as a cornerstone in our understanding of the natural world. Throughout the ages, from early astronomy through the modern scientific revolution. The examination of dynamical objects has been at the heart of numerous greatest scientific discoveries. Presently, manipulating mechanical motion of massive objects via light finds wide application in various fields, such as the measures probing quantumness remains an efficient used method. The optical manipulation over mechanical systems and the reciprocal impact of material objects on the propagation of light fall within the field of optomechanics which this work falls into.

The theory of optomechanical systems lies in the study of the interaction between electromagnetic radiation and mechanical motion. These systems are, to date, the most substantial platforms to achieve quantum control over mechanical motion while preserving their quantum properties. Therefore, one of the key goals of this thesis is to provide a complete mathematical description of optomechanical systems and generate quantum correlations with a focus on the stability conditions. Additional goals include proposing various practical schemes to enhance quantum correlations in such systems.

History of optomechanics:

Optomechanics encompasses the study of interactions between light and moving object. It stems from the idea that light can exert a force on a material object, an idea first postulated by Kepler in 17th century, who believed that the tails of comets were caused by the outward pressure of sunlight [1]. Light-induced force was solidified by a theoretical foundation in 20th century by both Maxwell and Bartoli, based on electromagnetic theory and the second Law of

thermodynamics, respectively. The first unambiguous experimental demonstration of the radiation pressure force was in 1901 [2,3]. The physicits, indeed, performed pioneering experiments using a light mill configuration. A careful analysis of these experiments became necessary to differentiate the phenomenon from thermal effects that had dominated earlier observations. As early as 1909, Einstein deduced the statistical characteristics of the force fluctuations caused by radiation pressure on a moving mirror [4]. Over half a century later, a seminal investigation found that light-induced pressure could alter the mechanical properties of a moving object. This remarkable result paved the way for what is today a dynamic field of experimental physics, with significant implications for both fundamental and practical science. In this thesis, I provide recent developments of optomechanics. My perspective on the progression of optomechanics, however, is not exhaustive; only a select subset of crucial research undertakings.

The role of radiation pressure and its potential for cooling larger objects were already investigated earlier by Braginsky within the context of interferometers. In 1970s, when Braginsky and co-workers considered the dynamic impact of radiation pressure on an harmonically suspended end mirror of a cavity [5–9].

Throughout the 1980s, optomechanics became applicable to various branches of physics, each adopting distinct and specialized manifestations within their respective domains. In optical physics [10]. In atomic physics [11–13], and in the context realizations of laser-driven deceleration of atoms [14,15].

The remainder of my dissertation essentially proceed with the ring optomechanical cavities, which represents a specialized configuration within the field of optomechanics. I consider myself very fortunate to have entered the world of optomechanics at such an effervescent stage of its evolution, enabling me to make meaningful contributions to some of its pivotal advancements.

Ring optomechanical cavity:

Cavities are generally categorized into two sections, linear and ring cavities as shown in figure 1. Linear cavities are composed by two mirrors aligned in front of each other (figure 1a), one of the mirrors of the cavity is free to move and thus acts as a mechanical resonator interacting with the cavity field. This interaction is caused by the radiation pressure force between scattered photons and suspended mirror [16–18], cavity photons modifies the motion of the movable mirror. As a result, it changed the length of cavity, which in turn affects the cavity resonance frequency and thus the intensity of the cavity field. The strength of the radiation pressure force is therefore

coupled with the mechanical motion. This type of optical cavity is known as the Fabry-Pérot resonator [19–21]. Other geometries employing a large number of mirrors are widely used [22–24]. To achieve the desired optical properties, careful selection of mirror focal lengths and spacing between them is essential. In this thesis, I chose to employ a cavity composed of three mirrors in a ring design.

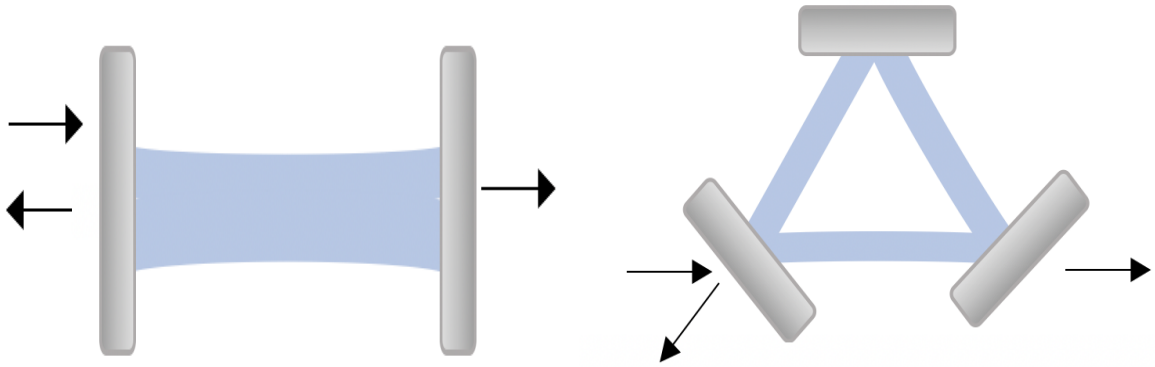

(a) (b)

Figure 1: (a) illustrates a linear configuration composed of two mirrors and (b) describes a ring cavity.

As shown in Figure 1b, ring cavities have three mirrors, a fixed one and two movable ones, driving by an electromagnetic field that circulate inside cavity. This design can support two propagation modes in opposite directions as opposed to the more common two-mirror linear cavity. Furthermore, a ring configuration not only enhances the optomechanical coupling by the displacement of the two movable mirrors, but also the circulation of the optical power inside the cavity enhances the intensity of the pumping power, in contrast with the case of a linear cavity. In addition, the structure of the cavity can minimize optical losses compared to other cavity geometries, leading to higher finesse and powerful interaction against decoherence. Besides, the closed-loop configuration for the light circulating within the cavity facilitate the generation of entanglement, that can be strengthened by the displacement of the mirror and an increase of the photon number. This topic will be frequently studied in next chapter.

Motivation:

This thesis aims to study the quantum correlations in a ring optomechanical cavity. Cavity optomechanics is a branch of physics that explores the interaction between mechanical motion and electromagnetic fields confined within high-quality optical cavity. The traditional optomechanical cavity, widely employed in research, consists of two highly reflective mirrors separated by a distance 'd', called Fabry-Perot cavity. However, this thesis focuses on ring cavities, which represent a specialized configuration within the field of optomechanics, in contrast to the predominantly studied Fabry-Perot cavities. Ring cavities feature a triangular design with three mirrors. The closed-loop configuration for the light circulating within the cavity facilitate the generation of quantum correlations. These correlations can be enhanced through mirror displacement and an increase in the photon number. Moreover, throughout this dissertation, I emphasize the nonlinearity inherent in the optomechanical Hamiltonian and solve the dynamics excluding the linearization treatment. Additionally, I derive an analytic solution to calculate the amount of non-Gaussianity among different modes of the system as a function of the time.

Outline of Thesis:

This thesis reports the quantum measures within a ring optomechanical cavity. In the following, I present the outline of the thesis by including a description about the content of each chapter of the thesis. There are a total five chapters.

Chapter 1: This chapter covers the fundamental notions and basic concepts of continuous variable systems that will be used to quantify the quantumness of various correlations that occur in optomechanical systems. It is followed by a complet description of the properties of quantum entanglement.

Chapter 2: This chapter gives an overview of the basic theoretical language used to describe cavity optomechanics. Notation and preliminary concepts of optical resonators and mechanical oscillators are established. In the second part of the chapter, I studied the entanglement of an optomechanical system where the optical resonator is coupled to the mechanical oscillator via the radiation pressure interaction.

Chapter 3: In this chapter, I analyze the entanglement generated between the optical mode and the relative mechanical mode in a ring cavity composed of a fixed mirror and two movable ones in a triangular design. In addition to entanglement, I investigate the behavior of Gaussian

quantum discord and the mutual information in a ring cavity.

Chapter 4: This chapter is devoted to the study of genuine tripartite entanglement. The system under consideration corresponds to an hybrid optomechanical system formed of a ring cavity where an atomic ensemble is placed inside. The central idea of this chapter is to explore the impact of the atomic ensemble on the entanglement, since, a strong quantum entanglement can be generated between the atomic ensemble and a vibrating mirror by increasing the coupling strength. Another point of interest is to investigate the genuine tripartite entanglement being possibly shared by the four subsystems (cavity field – atomic ensemble and two vibrating mirrors).

Chapter 5: In this chapter, I solved the time-evolution of a non-linear optomechanical ring cavity to quantify the non-Gaussianity of both the two-mode and three-mode of the system. Our solution is based on identifying a closed Lie algebra that facilitates calculations for the quantification of non-Gaussianity. The measure relies on the relative entropy of a state to characterize the deviation from Gaussianity within the system.

I conclude the thesis with a summary of the major findings of the research works, and a brief description of the future studies.

Chapter 1

Quantum measures

This chapter is meant to familiarize the reader with fundamental notions and basic concepts of continuous variable systems that will be used to quantify the quantumness of various correlations that occur in optomechanical systems.

In the beginning, we will present some mathematical foundations of quantum information with the main focus on continuous variable system [25, 26], then we will investigate the notion of quantum correlations. We end up this chapter with the properties of quantum entanglement to clears the way for the manipulation of entangled states in cavity optomechanical systems. Recent developments of the generation of entanglement in this field will be discussed in the next chapters which is the main subject of this thesis.

1.1 Quantum optics in continuous variable

In recent years, quantum information has focused on continuous spectrum variables. These variables are more precise than the discrete variables. The first example of such variables in quantum mechanics are the position and momentum of a particle, whose analogue in quantum optics are the conjugate quadrature components of a mode of the electromagnetic field. This analogy obtained directly from the quantization of the field, makes it possible to write a mode as a quantum harmonic oscillator. In this part, are presented the most useful aspects for the experimenter of continuous variables in quantum optics. First, we will start with the quantization of the electromagnetic field, the quantum states of the field and their representation. And we will focus on the theoretical study of quantum correlations in continuous-variable systems.
We consider an electromagnetic field mode corresponding to a plane wave of pulsation ω for

fixed polarization and direction.

$$E(t) = E_0 \cos(\omega t + \phi) = E_p \cos(\omega t) + E_q \sin(\omega t), \tag{1.1}$$

where, E_0 and ϕ are respectively the amplitude and the phase of the wave. E_p and E_q are the amplitudes of the two quadratures of the field in the Fresnel representation. For a description in terms of quadratures, where the position and momentum can be quantized, one can give a quantum description of the electromagnetic field

$$\hat{E} = \epsilon_0(\hat{q}\cos(\omega t)) + \hat{p}\sin(\omega t)), \tag{1.2}$$

where ϵ_0 is a normalization constant corresponds to the electric field associated with one photon. Thus, we define the operators of creation and annihilation of a photon at the frequency ω :

$$\begin{aligned} \hat{a} &= \frac{\hat{q} + \hat{p}}{\sqrt{2}}, \\ \hat{a}^\dagger &= \frac{\hat{q} - i\hat{p}}{\sqrt{2}}, \end{aligned} \tag{1.3}$$

which allows us to write 1.2 as :

$$\hat{E}(t) = \epsilon_0(\hat{a}\,\mathrm{e}^{-i\omega t} + \hat{a}^\dagger\,\mathrm{e}^{i\omega t}). \tag{1.4}$$

1.2 Quantum information basics

In this introductory Chapter, we give a detailed study of the concepts of quantum information theory on the usefulness on how to manipulate quantum systems. To that, we start by defining a quantum system and to facilitate the readers to understand quantum theory, we investigate the quantum measures. Indeed, a quantum system is any physical system assign to it a space of normed complex inner product, called Hilbert space $\mathcal{H}$ of some dimension d, with the physical state of the considered system being described by a vector $|\psi\rangle \in \mathcal{H}^d$, known as the quantum state, in that Hilbert space. The definition used in this part are taken from the textbook by Nielsen and Chuang [27].

1.2.1 Quantum state

A quantum state is any possible state represented by a vector in a Hilbertian vector space; the space to be considered depends on the system studied. Any quantum state $|\psi\rangle$ can be expressed in terms of a sum of basis states (also called basis kets). Knowledge that, A mixture of quantum states is again a quantum state. Quantum states that cannot be written as a mixture of other states are called pure quantum states, while all other states are called mixed quantum states.

pure state

A pure quantum state $|\psi\rangle$ is a state which can be described by a single ket vector, or as a sum of basis states. Let consider $|\psi\rangle$ that can be expressed as :

$$|\psi\rangle = \sum_{i=1}^{n} c_i |k_i\rangle \tag{1.5}$$

where c_i are the complex coefficients representing the probability amplitude, such that, $|c_i|^2$ is the probability of a measurement yielding the state $|k_i\rangle$. The normalization condition mandates that the total sum of probabilities is equal to one, $\sum_{i=1}^{n} c_i^2 = 1$. Another way to express this pure quantum state is in the matrix form. This can be done by using the density operator representation, which is given by:

$$\hat{\rho} = |\psi\rangle \langle\psi| = \sum_{i,j} c_i^* c_j |k_i\rangle \langle k_j| . \tag{1.6}$$

The matrix elements are defined as

$$\rho_{ij} = \langle k_i| \hat{\rho} |k_j\rangle . \tag{1.7}$$

Mathematically, the density matrix of a pure state has rank 1, while a mixed state has rank greater than 1. The best way of calculating this is via $Tr(\hat{\rho}^2) = Tr(\hat{\rho}) = 1$. It important to emphasize that $\hat{\rho}$ is an hermetien operator i.e, $\hat{\rho}^\dagger = \hat{\rho}$.
Let us now define the expectation value of an operator $\hat{A}$ as a function of $\hat{\rho}$:

$$\langle \hat{A} \rangle = \sum_{i,j} c_i^* c_j A_{ij} = \sum_{i,j} \rho_{ij} \langle k_j| \hat{A} |k_i\rangle = Tr[\hat{\rho}\hat{A}] \tag{1.8}$$

We have defined quantum systems in terms of pure states, but not all quantum systems have a well-defined pure quantum state at each point in time. However, any realistic quantum systems

cannot be perfectly isolated. In fact, this interaction will always lead to some mixedness. In order to describe a statistical distribution of pure states, we describe in the next part the density operator ρ of a mixed state. Notice that, any quantum system unavoidably interacts with other quantum systems (environment), they are open quantum systems.

Mixed state

A mixed quantum state is a statistical ensemble of pure states. By introducing 'mixtures' of pure states $|\psi_i\rangle$ with probability p_i, we get :

$$\hat{\rho} = \sum_{i=1}^{n} p_i \rho_i \tag{1.9}$$

with

$$\rho_i = |\psi_i\rangle \langle\psi_i| \tag{1.10}$$

we get

$$\hat{\rho} = \sum_{i=1}^{n} p_i |\psi_i\rangle \langle\psi_i| = \sum_{i=1}^{n} p_i P_i \tag{1.11}$$

P_i design the projection operator. Notice that, the density matrix operator satisfies the following proprieties,

- $\hat{\rho} \geq 0$
- $Tr\hat{\rho} = 1$
- $Tr\hat{\rho}^2 < 1$
- $\hat{\rho}^2 \neq \hat{\rho}$

1.3 Definition of Gaussian states

In the context of continuous-variable system each mode $k = 1, ...n$ lives in the Hilbert space $\mathcal{H} = \otimes_{k=1}^{n} \mathcal{H}_k$ resulting from the tensor product structure of infinite dimensional Fock spaces $\mathcal{H}_k$. In our case, the modes are those of the electromagnetic field emphasize in the previous part, for each mode k we can define the annihilation operator $\hat{a}_k^\dagger$ and the creation operator $\hat{a}_k$, with commutation relations $[\hat{a}_k, \hat{a}_l^\dagger] = \delta_{kl}$. The free Hamiltonian of the system may be simply

written as : $H = \sum_{k=1}^{n}(\hat{a}_k^\dagger \hat{a}_k + \frac{1}{2})$ and the corresponding position-momentum operators are :

$$\hat{q}_k = \frac{1}{\sqrt{2}}(\hat{a}_k + \hat{a}_k^\dagger) \quad and \quad \hat{p}_k = \frac{1}{i\sqrt{2}}(\hat{a}_k - \hat{a}_k^\dagger). \tag{1.12}$$

The commutation relations $[\hat{q}_k, \hat{p}_l] = i\delta_{kl}$. Let theses operators be grouped in the column vector $\hat{R}$

$$\hat{R} = \begin{pmatrix} \hat{q}_1 \\ \hat{p}_1 \\ \vdots \\ \hat{q}_n \\ \hat{p}_n \end{pmatrix}. \tag{1.13}$$

The canonical commutation relations for the $\hat{R}$ can be expressed in terms of the symplectic form Ω:

$$[\hat{R}_l, \hat{R}_m] = 2i\Omega_{lm}, \tag{1.14}$$

we define Ω as :

$$\Omega = \begin{pmatrix} \begin{pmatrix} 0 & 1 \\ -1 & 0 \end{pmatrix} & & (0) \\ & \ddots & \\ (0) & & \begin{pmatrix} 0 & 1 \\ -1 & 0 \end{pmatrix} \end{pmatrix} = \oplus_{i=1}^{n}\omega, \qquad \omega = \begin{pmatrix} 0 & 1 \\ -1 & 0 \end{pmatrix}. \tag{1.15}$$

Note that, $\Omega^T = -\Omega = \Omega^{-1}$.

The symplectic form will play crucial role in our next discussion. Later we will provide a clear exposition of N-mode Gaussian systems.

Now that we have present the general formalism of Gaussian states, let us give some important class of states (which includes coherent, squeezed, thermal states of the electromagnetic field).

1.3.1 Coherent state

Coherent state is considered one of the most classical quantum states. Refers to a state of the quantized electromagnetic field, it is used to describe a coherent laser beam [28]. Characterizing a classical kind of behavior and a maximal kind of coherence.

Mathematically, a coherent state $|\alpha\rangle$ is defined to be the eigenstate of the annihilation operator $\hat{a}$ with corresponding eigenvalue α. This reads,

$$\hat{a}\,|\alpha\rangle = \alpha\,|\alpha\rangle \quad \longleftrightarrow \quad \langle\alpha|\,\hat{a}^\dagger = \langle\alpha|\,\alpha^*. \tag{1.16}$$

Notice that, α satistfies $\langle\alpha|\alpha\rangle = 1$. The average value of photons number in a coherent state is given by:

$$\langle\hat{a}^\dagger\hat{a}\rangle = |\alpha|^2. \tag{1.17}$$

Coherent state can be expressed over the Fock basis, using this representations the states are defined as an infinite superposition of the number states :

$$|\alpha\rangle = \mathrm{e}^{-|\alpha|^2/2}\sum_{n=0}^{\infty}\frac{\alpha^n}{\sqrt{n!}}\,|n\rangle\,. \tag{1.18}$$

The same state can be obtained from the vacuum state $|0\rangle$ by applying the displacement operator

$$|\alpha\rangle = \hat{D}(\alpha)\,|0\rangle\,, \qquad\qquad \hat{D}(\alpha) = \exp\Big(\alpha\hat{a}^\dagger - \alpha^*\hat{a}\Big) \tag{1.19}$$

the parameter α is a complex number, and $\hat{D}(\alpha)$ is the displacement operator that verifies the following properties:

- $\hat{D}^\dagger(\alpha) = \hat{D}^{-1}(\alpha)$
- $\hat{D}^{-1}(\alpha) = \hat{D}(-\alpha)$
- $\hat{D}^\dagger(\alpha)\hat{a}\hat{D}(\alpha) = \hat{a} + \alpha$

We notice that, coherent states have mathematical characteristics that are different from Fock state. For example, two different coherent states are not orthogonal,

$$\langle\beta|\alpha\rangle = \mathrm{e}^{-\frac{1}{2}(|\beta|^2+|\alpha|^2-2\beta^*\alpha)} \neq \delta(\alpha-\beta). \tag{1.20}$$

Finally, it is appropriate to specify that the coherent states form a generative family on which one can decompose any other state in the same mode. In particular, we show the following closure relation:

$$\frac{1}{\pi}\int d^2\alpha\,|\alpha\rangle\,\langle\alpha| = \hat{I}, \tag{1.21}$$

with $d^2\alpha = dRe(\alpha)dIm(\alpha)$. This latter allows to easily calculate certain operations of the identity and the partial traces.

Notice that, coherent states present maximum coherence, as opposed to thermal states-another class of displaced states that will be studied in the next part. Coherent states are often considered as "quasi-classical" states of the field and their use is current in quantum optics.

1.3.2 Thermal state

The second state to consider is the thermal state. These states are statistical mixtures of Fock states. Their density matrices do not represent a coherence. As known any quantum system $\in H$ at thermal equilibrium is in thermal state reads,

$$\hat{\rho}^{th} = \frac{\mathrm{e}^{-\hat{H}/K_B T}}{Tr[\mathrm{e}^{-\hat{H}/K_B T}]}, \tag{1.22}$$

where,$\hat{H}$ is Hamiltonian operator, k_B is the Boltzmann constant, and T is the temperature of the state. Their representation in the Fock basis reads,

$$\hat{\rho}^{th} = \frac{1}{\bar{n}\pi} \int |\alpha\rangle \langle\alpha| \exp\left(-\frac{|\alpha|^2}{\bar{n}}\right) d^2\alpha \tag{1.23}$$

$\bar{n}$ is the average photon number, that reads $\bar{n} = \frac{1}{\mathrm{e}^{(\hat{H}/K_B T)} - 1}$.

Another useful representation is:

$$\hat{\rho}^{th} = \sum_n P_n^{th} |n\rangle \langle n|, \tag{1.24}$$

with P_n^{th} is the thermal photon statistics given by

$$P_n^{th} = \frac{\bar{n}^n}{(\bar{n}+1)^{n+1}} \tag{1.25}$$

We illustrate in figure 1.1, the thermal photon statistics it has the form of a Bose-Einstein distribution [29]. The state with the maximum probability is always the vacuum state with n = 0. It follows that the fluctuation in the photon number is typically larger than the mean photon number.

Lastly, such states have a simple covariance matrix that completely defines these states.

$$\sigma = (2\bar{n} + 1)I. \tag{1.26}$$

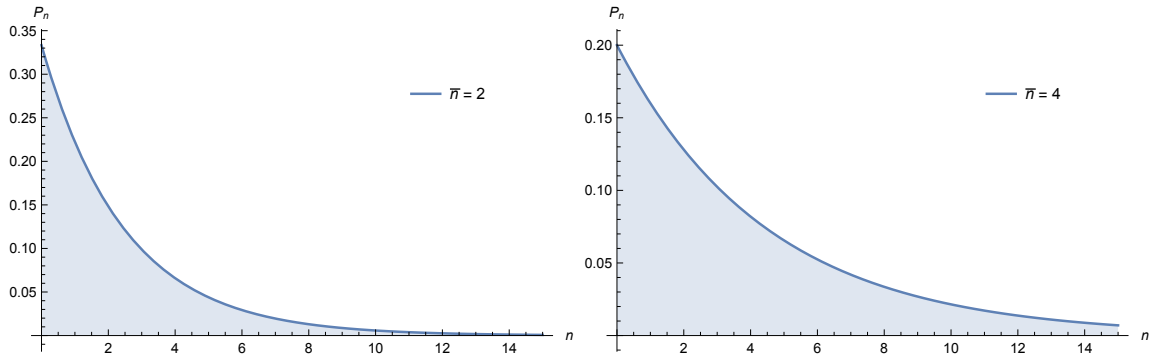

Figure 1.1: The figure shows the thermal photon statistics P_n^{th} as a function of the photon number n. In the left (right), we consider $\bar{n} = 2(\bar{n} = 4)$.

with I is the identity matrix. Next, a more detailed description of the covariance matrix will be discussed.

1.3.3 Squeezed state

Squeezed states are an important class of photonic states that are mostly used in quantum optics. Squeezed states are physically created by pumping a non-linear crystal with a bright laser [30]. Mathematically, squeezed state is obtained by applying the squeezing operator $\hat{S}_\xi$ to a coherent state $|\alpha\rangle$, i.e $|\alpha, \xi\rangle := \hat{S}_\xi |\alpha\rangle$. Notice, $\hat{S}_\xi := \mathrm{e}^{\frac{1}{2}(\xi^* \hat{a}^2 - \xi \hat{a}^{\dagger 2})}$ with the quantity ξ is the squeezing parameter.

The single-mode squeezing operator corresponds to the following mode evolutions:

$$\begin{aligned} \hat{S}_\xi^\dagger \, \hat{a} \, \hat{S}_\xi &= \cosh r \hat{a} + \mathrm{e}^{i\psi} \sinh r \hat{a}^\dagger, \\ \hat{S}_\xi^\dagger \, \hat{a}^\dagger \, \hat{S}_\xi &= \cosh r \hat{a}^\dagger + \mathrm{e}^{-i\psi} \sinh r \hat{a}, \end{aligned} \tag{1.27}$$

with $\xi = r \, \mathrm{e}^{i\psi}$. The squeezing phase ψ determines which quadrature will be (anti-)squeezed and the parameter r is known as the squeezing degree of the state. High squeezing degree is one of the most desirable resources in CV quantum information.

Therefore, we can obtain the squeezed vacuum state from the vacuum state, as:

$$|\xi\rangle = \hat{S}_\xi |0\rangle = \frac{1}{\sqrt{\cosh r}} \sum_{m=0}^{\infty} \frac{\sqrt{(2m)!}}{2^m m!} \, \mathrm{e}^{im\psi} (-\tanh r)^m \, |2m\rangle \, . \tag{1.28}$$

Similarly, the squeezed coherent states is generated by displacing the squeezed vacuum state:

$$|\alpha, \xi\rangle = \hat{D}(\alpha) \, |0, \xi\rangle = \hat{D}(\alpha) \hat{S}_\xi \, |0\rangle \, . \tag{1.29}$$

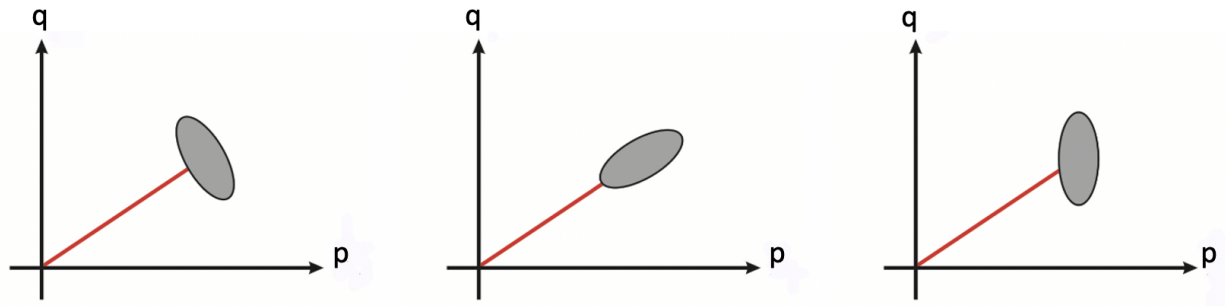

Figure 1.2: Fresnel representation of a squeezed state for different quadratures.

Lastly, we present in figure 1.2 the squeezed states in the Fresnel diagram by a field where the fluctuation zone takes the form of an ellipse. From left to right : the noise squeezing of intensity, the noise squeezing of phase and the noise squeezing for any quadrature. The direction of the minor axis of the ellipse indicates that of the most squeezed quadrature.

1.4 Mathematical description of N-mode Gaussian systems

The set of Gaussian states are characterized by Gaussian characteristic functions and Gaussian quasi-probability distributions such as the Wigner function on the multimode quantum phase space [31–34]. Therefore, they are of central of information processing in CV systems and are the subject of our analysis.

1.4.1 Covariance matrix formalism

By definition a Gaussian state ρ is completely characterized by the first and second moments of the quadrature field operators, which will be identified respectively, by the vector of first moments $\overline{R} = (\langle \hat{R}_1 \rangle, \langle \hat{R}_1 \rangle, ..., \langle \hat{R}_N \rangle, \langle \hat{R}_n \rangle)$ and by the covariance matrix (CM) σ of elements

$$\sigma_{ij} = \frac{1}{2}\langle \hat{R}_i \hat{R}_j + \hat{R}_j \hat{R}_i \rangle - \langle \hat{R}_i \rangle \langle \hat{R}_j \rangle. \tag{1.30}$$

Where, for any observable $\hat{o}$, the expectation value $\langle \hat{o} \rangle \equiv Tr(\rho \hat{o})$. In the following, σ will be assumed indifferently to denote the matrix of second moments of a Gaussian state.

Now given a CM σ, we can expect some constraints to exist to be obeyed by any bona fide CM. Indeed, any density matrix ρ must be positive and semi-definite. Such condition associated

with the commutation relations implies [35]

$$\sigma + i\Omega \geq 0. \tag{1.31}$$

The commutation relation given in 1.31, is equivalent to Simon's condition applies to any CM describing a physical state. For Gaussian state this is however not only necessary but also the sufficient condition for a state to be physically realizable. For non-Gaussian states, this condition is not sufficient, but remains necessary [36].

For future convenience, the CM 1.30 can be define and write in the form of 2×2 sub-matrix as :

$$\begin{pmatrix} \sigma_1 & \varepsilon_{1,2} & \cdots & \cdots & \varepsilon_{1,N} \\ \varepsilon_{1,2}^T & \ddots & \ddots & & \vdots \\ \vdots & \ddots & \ddots & \ddots & \vdots \\ \vdots & & \ddots & \ddots & \varepsilon_{N-1,N} \\ \varepsilon_{1,N}^T & \cdots & \cdots & \varepsilon_{N-1,N}^T & \sigma_N \end{pmatrix}, \tag{1.32}$$

where, $\sigma_k = \begin{pmatrix} \langle \hat{p}_k^2 \rangle & \langle \hat{p}_k \hat{q}_k \rangle_s \\ \langle \hat{p}_k \hat{q}_k \rangle_s & \langle \hat{q}_k^2 \rangle \end{pmatrix}$ and $\varepsilon_{i,j} = \begin{pmatrix} \langle \hat{p}_i \hat{p}_j \rangle_s & \langle \hat{p}_i \hat{q}_j \rangle_s \\ \langle \hat{q}_i \hat{p}_j \rangle_s & \langle \hat{q}_i \hat{q}_j \rangle_s \end{pmatrix}$ represent respectively the individual covariance matrices of kth mode with $k \in \{1, ..., N\}$ and the off-diagonal elements $\varepsilon_{i,j}$ are the symmetric correlation matrices between the modes i and j with $(\{i, j\} \in [1, ..., N])$.

In the following, the properties of Gaussian state $\hat{\rho}$ are easily expressed in terms of its covariance matrix σ.

1.4.2 Wigner function

The Wigner distribution function is a quasi-probability distribution function in phase space (q, p). It as introduced by Eugene Wigner in 1932 to study quantum corrections to classical statistical mechanics. This latter, is a special representation of the density matrix ρ. In this part, we give a short description of Wigner function of Gaussian states.

The Wigner function for N mode Gaussian state can be written in term of phase-space quadrature variables as [34]:

$$W(R) = \frac{\mathrm{e}^{-\frac{1}{2} R^T (\sigma^N)^{-1} R}}{\pi^N \sqrt{\det \sigma^N}} \tag{1.33}$$

where R represent the real phase-space vector 1.13 beloning to Γ(phase-space) and σ^N is the

correlation matrix $2N \times 2N$ given by

$$\sigma_{ij}^{N} = \int W(R)\hat{R}_i\hat{R}_j \, d^{2N}R = \langle\{\hat{R}_i, \hat{R}_j\}\rangle \tag{1.34}$$

we define the anti-commutator $\{\hat{R}_i, \hat{R}_j\} = (\hat{R}_i\hat{R}_j + \hat{R}_j\hat{R}_i)/2$.
The wigner function stands for some properties for N modes :

- W is real ($\Longleftrightarrow$ ρ is Hermitian)
- W can be negative (it is a quasi-probability distribution)
- W is normalized : $\int_{\mathbb{R}^{2N}} W(R)\, dR = 1 (\Longleftrightarrow\ tr\rho = 1)$

As an example of Wigner function, we choose to present in figure 1.3 the Wigner quasiprobability distribution of coherent state in phase space. Therefore, it is categorized as a Gaussian state and given by

$$W_{coh}(q, p, \alpha, \varphi) = \frac{2}{\pi}\, \mathrm{e}^{-2((q-\alpha\cos\varphi)^2+(p-\alpha\sin\varphi)^2)}, \tag{1.35}$$

where the coherent state amplitude $\alpha = |\alpha|\, \mathrm{e}^{i\varphi}$ and φ represents the phase angle of the coherent state

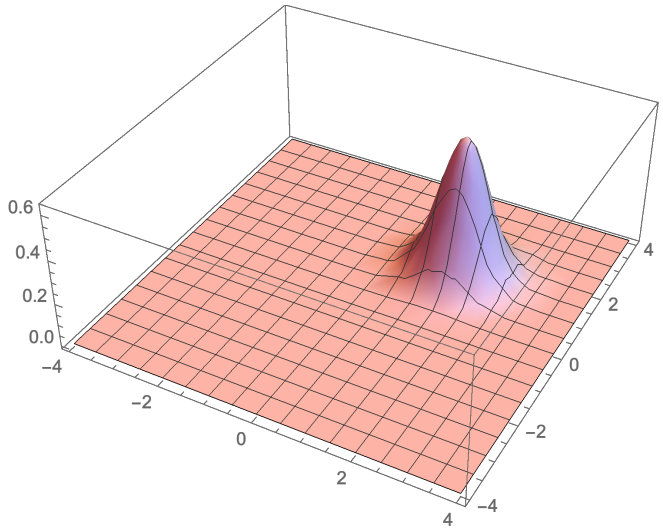

Figure 1.3: Plots of the Wigner function of coherent states having amplitude $\alpha = 2$ and phase $\varphi = \frac{\pi}{4}$.

Figure 1.3, present a visualisation of the Wigner function of coherent states which has a Gaussian in shape. The function is positive and centered at different points in phase space.

This result might illustrate the use so far of the Gaussian states in the majority of quantum optics experiments, and which serve as a resource for conditional preparation protocols.

1.4.3 Symplectic formalism

A crucial role in the theoretical and experimental manipulation of Gaussian states is played by unitary operations since they preserve their Gaussian character. The simplest and most common of such operations are those generated by Hamiltonian terms at most quadratic in the field operators. Each of these unitary operations acting on the Hilbert space corresponds to a symplectic transformation, acting on the phase space, i.e., to a linear transformation S which preserves the symplectic form Ω, and so

$$S^T \Omega S = \Omega, \tag{1.36}$$

the definition in eq 1.36 implies $\det S = 1, \forall S \in S_{P(2N,R)}$ it corresponds to a symplectic transformations on a $2N$-dimensional phase space form the real symplectic group $S_{P(2N,R)}$ [34]. Such transformation preserve the commutation relation between $\hat{Q}$ and $\hat{P}$. Their action on the vector $\hat{R}$ is linear, so that they act on the covariance matrices in the form:

$$\sigma \mapsto S \sigma S^T \tag{1.37}$$

S represents the Gaussian unitary operation in the space of first and second moments. All the symplectic transformations that can act on the covariance matrix σ of a given system, there is one that is of particular importance: the one that diagonalizes the covariance matrix. Thanks to Williamson theorem [37], the covariance matrix of an N-mode Gaussian state can always be written in the form known as "Williamson normal form" or "diagonal form":

$$\sigma = S^T \nu S \tag{1.38}$$

where ν is defined as

$$\nu = \bigoplus_{k=1}^{N} \begin{pmatrix} \nu_k & 0 \\ 0 & \nu_k \end{pmatrix} \tag{1.39}$$

ν is the covariance matrix of a state with N modes fully decorrelated, corresponding to a diagonal density matrix $\rho^{\otimes}$:

$$\rho^{\otimes} = \bigotimes_{k=1}^{N} \frac{2}{\nu_k + 1} \sum_{n=1}^{\infty} \left(\frac{\nu_k - 1}{\nu_k + 1} \right) |n\rangle_k \langle n| \,, \tag{1.40}$$

with ν_k is the number state of order n in the Fock space $\mathcal{H}_k$. The quantities ν_k's form the symplectic spectrum of the covariance matrix σ, and they can be calculated as eigenvalues of the matrix $|i\Omega\sigma|$. Such eigenvalues are in fact invariant under the action of symplectic transformations on the matrix σ. Indeed, using the fact that the inverse of a symplectic transformation is also symplectic and therefore preserves the matrix σ and the definition 1.38, we can show that the relation 1.31 is equivalent to :

$$\nu + i\Omega \geq 0 \tag{1.41}$$

which we can immediately rewrite in terms of the symplectic eigenvalues:

$$\nu_k \geq 1. \tag{1.42}$$

A major symplectic invariants is simply the determinant of the covariance matrix, whose invariance is a consequence of the fact that $\det S = 1$. Using the Williamson diagonal form, we have :

$$\det(\sigma) = \prod_{k=1}^{N} \nu_k^2. \tag{1.43}$$

Another important invariant is given by the quantity called "seralian", denoted Δ [38] defined as the sum of the determinants of all the 2×2 sub-matrices of the covariance matrix σ. The Seralian can be expressed as a function of the symplectic eigenvalues:

$$\Delta(\sigma) = \sum_{k=1}^{N} \nu_k^2. \tag{1.44}$$

1.4.4 Summary

Table 1.1 summarizes the mapping of properties and tools between Hilbert $\mathcal{H}$ and phase space Γ discussed all over the previous sections for the set of Gaussian states.

	Hilbert space $\mathcal{H}$	**Phase space Γ**
Dimension	∞	2N
Structure	$\bigotimes$	$\bigoplus$
Description	Density matrix ρ	Covariance matrix σ
Physical condition	$\rho \geq 0$	$\sigma + i\Omega \geq 0$
Unitary transformation	$U^\dagger U = \mathbb{1}$ $\rho \mapsto U\rho U^\dagger$	$S^T \Omega S = \Omega$ $\sigma \mapsto S\sigma^T S$
Spectrum	$U\rho U^\dagger = diag\{\lambda_k\}$ $0 \leq \lambda_k \leq 1$	$S\sigma^T S = diag\{\nu_k\}$ $1 \leq \nu_k \leq \infty$

Table 1.1: Schematic comparison between Hilbert space $\mathcal{H}$ and Phase space Γ for N mode Gaussian states in continuous variable systems [34].

1.5 Notion of quantum correlations

In this section, we will introduce the notion of quantum correlations. Indeed, the proper nature of quantum correlations exist when a two quantum systems are in interaction, some quantum correlations are generated between the two of them [39–41]. This latter keep on even when the interaction is interrupted or the two subsystems are spatially separated. Given a bipartite or multipartite quantum state an evident question arises. Does this state contain quantum correlations ? if yes how much it possess? For the following, we will clearly examine these questions.

Quantum correlations come in many forms, each form has its, own degree of strengths. A particular type of strong quantum correlations is called "**Entanglement**". This latter is understood as purely quantum correlations between quantum states of the system.

1.5.1 Definition of quantum entanglement

In quantum information, quantum entanglement is defined as a phenomenon that yields when two or group of particles generate or share the same proprieties and they are no longer independent. In other words, the quantum state of each particle cannot be described independently of the state of the others even separated by a large distance. In general, when one or more quantum states are entangled, they behave like a single inseparable quantum system [42–45].

In recent years, entanglement plays a leading role in many different domains such as the field of universal quantum computers which can solve complicated equations difficult to be solved by classical machine. The implementation of quantum states is experimentally observed in quantum communication, quantum teleportation, quantum cryptography applications, as well

as in quantum metrology.

Let us consider two different quantum systems A and B describe by $|\psi\rangle_A$ and $|\psi\rangle_B$ in Hilbert space $\mathcal{H}_A$ and $\mathcal{H}_B$ respectively. The Hilbert space of the composite system is the tensor product $\mathcal{H}_{AB} = \mathcal{H}_A \otimes \mathcal{H}_B$. If the composite system can be represented in the form

$$|\psi\rangle_{AB} = |\psi\rangle_A \otimes |\psi\rangle_B \tag{1.45}$$

we say that the state are separable or non-entangled. Accordingly, if a state $|\psi\rangle_{AB}$ cannot be written as a product of the states,i.e, $|\psi\rangle_{AB} = |\psi\rangle_A \neq |\psi\rangle_B$, then the state is entangled. Physically speaking, the two subsystems A and B are dependent and the corresponding observable perform a measure on one of the subsystems cannot be fully described without considering the other. Denotes that, there is many different techniques to detect entanglement. This will be highlighted in the next section with the main focus being Gaussian states.

1.5.2 Entanglement detection

Several operational criteria have been developed in order to detect entanglement [46, 47]. Here, we are going to present some of them, covenable to Gaussian states of Continuous Variable systems.

PPT criterion

One of the most important separability criteria at present is the Peres-Horodecki criterion (PPT) [48, 49]. The principle of this criterion is that any bipartite state remains a valid quantum state if we consider the operation of partial transposition of the density matrix of a bipartite system. In quantum phase space, we consider the covariance matrix σ. Here, we focus on two-mode Gaussian state.

The covariance matrix σ in terms of the three 2×2 matrices α, β, γ takes the form :

$$\sigma = \begin{pmatrix} \alpha & \gamma \\ \gamma^T & \beta \end{pmatrix} \tag{1.46}$$

α and β are the local covariance matrix of the single-mode subsystems, and γ represents their correlations. We define, the invariant

$$\Delta(\sigma) = \det(\alpha) + \det(\beta) - 2\det(\gamma) \tag{1.47}$$

The PPT(Positive Partial Transpose) criterion is necessary and sufficient for the separability of $(1 \times N) - mode$ Gaussian states. Under partial transposition, the covariance matrix σ is transformed into a new matrix $\tilde{\sigma}$

$$\sigma = \begin{pmatrix} \alpha & \gamma \\ \gamma^T & \beta \end{pmatrix} \rightarrow \tilde{\sigma} = \begin{pmatrix} \alpha & \tilde{\gamma} \\ \tilde{\gamma}^T & \beta \end{pmatrix} \tag{1.48}$$

$\tilde{\sigma}$ can be obtained as follow :

$$\tilde{\sigma} \equiv \Lambda \sigma \Lambda \tag{1.49}$$

with $\Lambda = diag(1, 1, 1, -1)$. For the case of N mode, (Adesso, G., Illuminati, F. (2007) [34]) provide the positive partial transpose covariance matrix of N mode Gaussian state. The PPT criterion implied that a Gaussian state is separable if and only if the partially transposed $\tilde{\sigma}$ is physically realizable i.e satisfies the inequality

$$\tilde{\sigma} + i\Omega \geq 0. \tag{1.50}$$

The covariance matrix $\tilde{\sigma}$ differs from σ by a sign flip in $\det(\gamma)$ of the eq. 1.47. Therefore the invariant $\Delta(\sigma)$ is changed to $\tilde{\Delta}(\sigma)$:

$$\tilde{\Delta}(\sigma) = \det(\alpha) + \det(\beta) + 2\det(\tilde{\gamma}) = \det(\alpha) + \det(\beta) - 2\det(\gamma). \tag{1.51}$$

The PPT criterion can be expressed in terms of the symplectic eigen values $\tilde{\nu}_{\pm}$ of the partially transposed covariance matrix $\tilde{\sigma}$. We define $\tilde{\nu}_{\pm}$ as:

$$\tilde{\nu}_{\pm} = \sqrt{\frac{\tilde{\Delta}(\sigma) \pm \sqrt{\tilde{\Delta}(\sigma)^2 - 4\det\sigma}}{2}}. \tag{1.52}$$

For separability, the PPT condition 1.50 can be reduces to a simple inequality that must be satisfied by the smallest symplectic eigenvalue of the partially transposed state,

$$\tilde{\nu}_{-} \geq 1. \tag{1.53}$$

If $\tilde{\nu}_{-} < 1$, the corresponding Gaussian state σ is entangled. Which is equivalent to $\det(\gamma) < 0$. The above inequality imply a necessary condition for two-mode Gaussian state to be entangled.

Werner and wolf criterion

For a bipartite Gaussian state of a system $N_A \times N_B$, a necessary and sufficient condition to a state to be separable if and only if the covariance matrix of the two-mode system σ realize the corresponding inequality [36]:

$$\sigma \geq \sigma_A \otimes \sigma_B \tag{1.54}$$

the pair of covariance matrices σ_A and σ_B correspond respectively to the subsystems S_A and S_B. Unfortunately, this creterion is not very useful in practice. Accordingly, we bring other separability criteria based on non-linear map.

Giedke et al.

The operational criterion introduced by Giedke et al. is based on the iterative applications of a nonlinear map, that is stronger and independent to the PPT criterion. This latter completely qualifies separability for all bipartite Gaussian states.

1.5.3 Quantifying quantum entanglement in Gaussian state

In addition to the detection of entangled state, an important topic is the quantification of entanglement. This part is aimed at shedding light on entanglement measurements, we will give some functions used to quantify the amount of entanglement in the set of quantum Gaussian state.

A state can be either separable or entangled, most of functions assign the entanglement numbers ranging from 0 to 1, 0 when the state is separable(unentangled) and 1 when the state is maximally entangled. So then, there is a degree of entanglement where we can differentiate between states. Some states are strongly entangled than others. The first natural generalization of the quantification of entanglement is the entanglement of formation.

Entanglement of formation

The entanglement of formation E_F was introduced by (Bennett et al., 1996c [50]). For a mixed quantum state ρ, E_F is defined as the average entanglement of pure states of the decomposition, minimized over all decompositions of ρ:

$$E_F(\rho) = \min \sum_i p_i E(|\psi_i\rangle), \tag{1.55}$$

the minimization is taken over all the pure states realizations of ρ :

$$\rho = \sum_i p_i \left|\psi_i\right\rangle \left\langle\psi_i\right| . \tag{1.56}$$

The optimal convex decomposition of Eq.(1.55) has been found for a two-mode symmetrical Gaussian states. The minimum is achieved within the set of pure two-mode Gaussian states, which yields to the expression

$$E_F = \max[0, g(\tilde{\nu}_-)], \tag{1.57}$$

with $\tilde{\nu}_-$ is the smallest symplectic eigenvalue and the function $g(x)$ is given by:

$$g(x) = \frac{(1+x)^2}{4x} \ln\left[\frac{(1+x)^2}{4x}\right] - \frac{(1-x)^2}{4x} \ln\left[\frac{(1-x)^2}{4x}\right]. \tag{1.58}$$

Negativity

A standard quantitative measure of quantum entanglement is the negativity. The measure is based on the Peres-Horodecki (PPT) criterion. If a Gaussian bipartite state is entangled then the partially transposed state have a negative symplectic eigen values $\tilde{\nu}_-$. The negativity is defined as [51]:

$$E_N = \max[0, -\ln 2\tilde{\nu}_-]. \tag{1.59}$$

Therefore, the state is entangled if and only if $E_N > 0$, which corresponds to $\tilde{\nu}_- < 1/2$, the stronger the entanglement, the resilience of entanglement to noise becomes [52–55]. Negativity satisfy various properties :

- E_N vanishes for all separable states.
- Is additive on tensor products $E_N(\rho \otimes \sigma) = E_N(\rho) + E_N(\sigma)$.
- Is an upper bound to the distillable entanglement.
- Provides an upper bound to teleportation capacity.

We see that, the negativity satisfies all basic postulates that make it a good candidate for evaluating entanglement in a quantitative way.

Gaussian Rényi-2 entanglement

Besides the negativity, the Gaussian Rényi-2 entanglement entropy is another measure of entanglement. This measure is based on the concept of Rényi-α entropies [56]. This latter were first introduced by Alfred Rényi as a generalisation of the usuel concept of entropy, as its name signifies, which are defined for a given quantum state ρ as

$$S_\alpha(\hat{\rho}) = (1-\alpha)^{-1} \ln \mathrm{Tr}(\rho^\alpha), \tag{1.60}$$

where $0 < \alpha < \infty$. The entanglement measure we consider here is based on the Rényi-2 entropy, by replacing α by 2 in Eq.(1.60),

$$S_2(\hat{\rho}) = -\ln \mathrm{Tr}\left(\rho^2\right). \tag{1.61}$$

Rényi-2 entropy can be expressed in terms of covariance matrix,

$$S_2(\hat{\rho}) = \frac{1}{2} \ln (\det \sigma), \tag{1.62}$$

for pure state, $\det \sigma = 1$, and growing with increasing mixedness of the state. For generally pure or mixed Gaussian states , the Gaussian Rényi-2 entanglement admits the following formula by extending the Rényi-2 entropy via a Gaussian convex-roof procedure, [56, 57]:

$$\varepsilon(\hat{\rho}_{AB}) = \inf_{\{p_i, |\psi_i\rangle\}} \sum_i p_i S_2(\mathrm{Tr}_B \, |\psi_i\rangle \langle\psi_i|), \tag{1.63}$$

where the minimization is over all Gaussian decompositions $\{p_i, |\psi_i\rangle\}$ of the state $\hat{\rho}_{AB} = \sum_i p_i \, |\psi_i\rangle \langle\psi_i|$.

1.5.4 Genuine tripartite entanglement

In this part, we present a detailed study of entanglement in three-mode Gaussian states of continuous variable (CV). For the following, let us write the covariance matrix σ of tripartite system (ABC) in terms of two submatrices :

$$\sigma = \begin{pmatrix} \sigma_A & \varepsilon_{AB} & \varepsilon_{AC} \\ \varepsilon_{AB}^T & \sigma_B & \varepsilon_{BC} \\ \varepsilon_{AC}^T & \varepsilon_{BC}^T & \sigma_C \end{pmatrix}. \tag{1.64}$$

The genuine tripartite entanglement adopt a quantitative measure of tripartite negativity [58–60]

$$E_{ABC} = (E_{A|BC} E_{B|AC} E_{C|AB})^{1/3} \tag{1.65}$$

$E_{A|BC} = \max[0, -\ln 2\nu_{A|BC}]$ is the logarithmic negativity of the one mode-versus-two modes bi-partitions in the system, where $\nu_{A|BC} = \min\left\{\text{eig} \mid \oplus_{j=1}^{3} (-\sigma_y) P_{A|BC}\ \sigma\ P_{A|BC}|\right\}$, with $P_{A|BC} = \sigma_z \oplus 1 \oplus 1$, $P_{B|AC} = 1 \oplus \sigma_z \oplus 1$, and $P_{C|AB} = 1 \oplus 1 \oplus \sigma_z$ are the matrices of the partial transposition of the tripartite covariance matrix, σ_y and σ_z are the Pauli matrices, and σ is the 6×6 covariance matrix of the tripartite system.

Let us also recall the contangle $C_{u|v}$, as an entanglement measure of the tripartite entanglement. $C_{u|v}$ defined as the convex roof of the squared logarithmic negativity, i.e., $C_{u|v} = E^2_{u|v}$, here the notation $u|v$ refers to some pair of subsystems. For three-mode, the contangle satisfies the monogamy inequality of quantum entanglement $C_{A|BC} - C_{A|B} - C_{A|C} \geq 0$. A proper quantification of genuine tripartite entanglement is given by the minimum residual contangle

$$R_{min} \equiv \min[C_{A|BC} - C_{A|B} - C_{A|C}], \tag{1.66}$$

where (A, B, C) denotes all the permutations of the three-mode indexes. One can also define the Gaussian contangle $G_{j|k}$, that reads

$$G_{min} \equiv \min[G_{A|BC} - G_{A|B} - G_{A|C}], \tag{1.67}$$

Such a measure is monotonic under Gaussian local operations and can be adopted to quantify the genuine tripartite entanglement of three-mode Gaussian states.

1.5.5 Quantum discord

Alternatively, to entanglement, the quantum correlations can be also quantified by the quantum discord. Quantum discord corresponds to a measure of quantum correlation originally suggested in Refs. [61, 62]. The main idea behind the presentation of the quantum discord is to prove that for mixed states, quantum discord corresponds to a measure of quantum correlation which does not include quantum entanglement however, for pure states quantum entanglement is equivalent to quantum discord. In other words, quantum discord can be different from zero even if the state is non-entangled(separable), which prove that entanglement is not the only source of quantum correlations.

This measure is defined as the difference between the mutual information and the classical correlation. By definition, quantum discord of a bipartite system A and B is given by :

$$\mathcal{D}_G(\hat{\rho}_{AB}) = \mathcal{I}_M(\hat{\rho}_{AB}) - \mathcal{C}(\hat{\rho}_{AB}), \tag{1.68}$$

$\mathcal{C}(\hat{\rho}_{AB})$ refers to the classical correlation and $\mathcal{I}_M(\hat{\rho}_{AB})$ is the quantum mutual information that read:

$$\mathcal{I}_M(\hat{\rho}_{AB}) = S_V(\hat{\rho}_A) + S_V(\hat{\rho}_B) - S_V(\hat{\rho}_{AB}), \tag{1.69}$$

where, $S_V(\hat{\rho}_{AB}), S_V(\hat{\rho}_A)$ and $S_V(\hat{\rho}_B)$ are the von Neumann entropies of the two mode Gaussian state $\hat{\rho}_{AB}$ and that of subsystems $\hat{\rho}_A$ and $\hat{\rho}_B$. It can be easily expressed in terms of the symplectic eigenvalues of the covariance matrix σ (defined in 1.46) as follow [63] :

$$\mathcal{I}_M(\hat{\rho}_{AB}) = f(\sqrt{I_1}) + f(\sqrt{I_2}) - f(\nu_+) - f(\nu_-) \tag{1.70}$$

with, the symplectic invariants is define as :

$$I_1 = \det[\alpha], I_2 = \det[\beta], I_3 = \det[\gamma], I_4 = \det[\sigma], \tag{1.71}$$

and the function f is given by :

$$f(x) \equiv (x + \frac{1}{2}) \ln \left[x + \frac{1}{2} \right] - (x - \frac{1}{2}) \ln \left[x - \frac{1}{2} \right]. \tag{1.72}$$

and the two symplectic eigenvalues $\nu_\pm$ are computed as :

$$\nu_\pm \equiv \sqrt{\frac{\Delta(\sigma) \pm \sqrt{\Delta(\sigma)^2 - 4 \det \sigma}}{2}}. \tag{1.73}$$

By performing Gaussian measurement, the Gaussian quantum discord for Gaussian bipartite systems can be expressed as [63, 64] :

$$\mathcal{D}_G = f(\sqrt{I_2}) - f(\nu_+) - f(\nu_-) + f(\sqrt{W}), \tag{1.74}$$

$$W = \begin{cases} \dfrac{2|I_3| + \sqrt{4I_3^2 + (4I_2 - 1)(4I_4 - I_1)}}{(4I_2 - 1)}^2 & \text{if } \dfrac{4(I_1 I_2 - I_4)^2}{(I_1 + 4I_4)(1 + 4I_2)I_3^2} \leq 1 \\ \dfrac{I_1 I_2 + I_4 - I_3^2 - \sqrt{(I_1 I_2 + I_4 - I_3^2)^2 - 4I_1 I_2 I_4}}{2I_2} & \text{otherwise.} \end{cases} \tag{1.75}$$

These measures of Gaussian quantum discord and quantum entanglement will be used in the following chapters.

In summary, quantum discord is a measure of quantum correlations including entanglement. In fact, both of them can be considered as a crucial key to quantify quantum correlations in many tasks in quantum information theory. For this reason, we study in this chapter the basic measures of quantum correlations related to Gaussian states in continuous variable systems that will be presented in different physical models throughout this thesis.

Chapter 2

Cavity Optomechanics : The theory behind

The field of optomechanics, explores the interaction between electromagnetic radiation and a moving object [65]. It covers the basics aspect of optical cavities and mechanical resonators as needed to describe cavity-optomechanical systems. This interaction, i.e., photons interacting with phonons, by making use of a cavity stems from the idea that light can exert a force on a mechanical object due to the radiation pressure force as shown in figure 2.1. Indeed, when the cavity is coherently driven by an external laser field, the photons induces a small displacement of the motion of the material object proportional to the instantaneous photon number in the cavity [66]. Thus the motion of the movable mirrors induced by the radiation pressure changes the cavity's length, and alters the intensity of the cavity field, which in turn modifies the radiation pressure force itself [67].

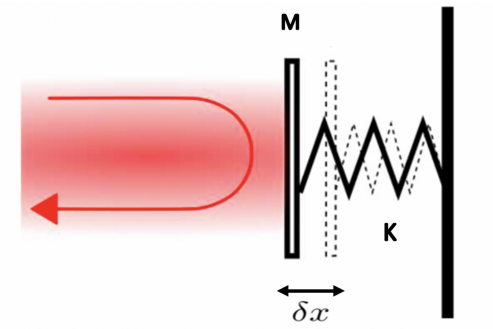

Figure 2.1: Schematic diagram of the motion of the mechanical object made by the electromagnetic field due to the radiation pressure force.

To investigate the influence of the optomechanical interaction between the electromagnetic field and mechanical object, an optical resonator is usually used to enhance the photon's circulation that interacts with the mechanics. For this reason, we study the basic aspect of optical

resonators and mechanical objects as required to describe a generic cavity optomechanical system.

2.1 Optical resonators

Here we aim for a proper analysis of the optical properties and mathematical formulas that provide a unifying description of an optical cavity pumped with a monochromatic laser source. Optical resonators can be realized experimentally [68, 69], Fig 2.2 shows a several forms of optomechanical cavities. All these types can be modelled by a Fabry-Pérot cavity that will be discussed in detail in the next part.

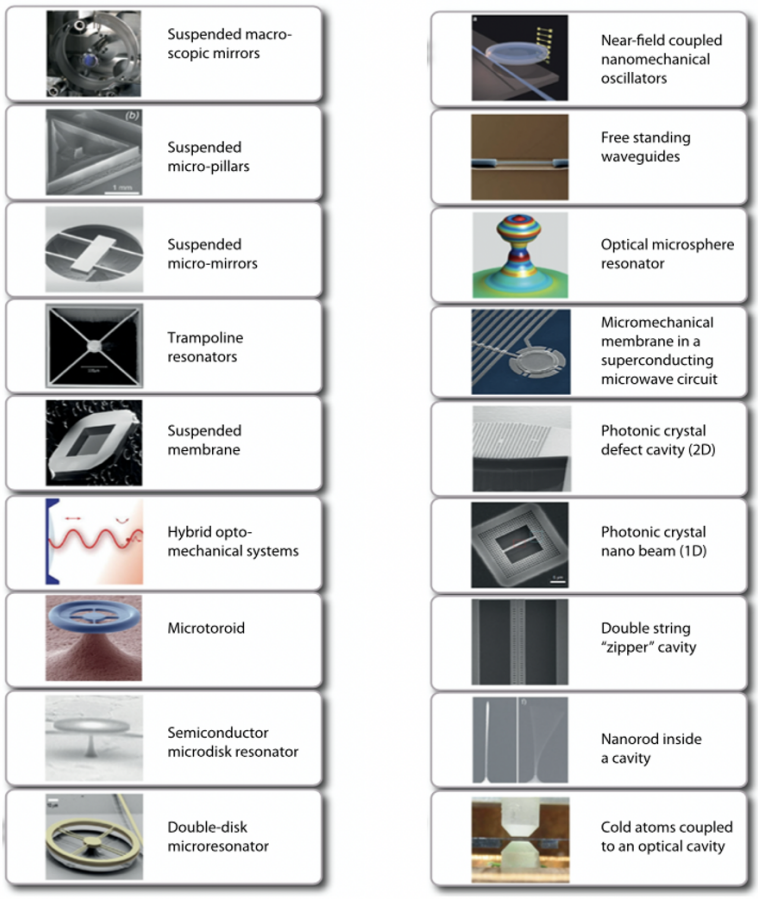

Figure 2.2: Gallery of cavity optomechanics devices. From top left, down : N. Mavalvala, A. Heidmann, M. Aspelmeyer, D. Bouwmeester, J. Harris, P. Treutlein, T. J. Kippenberg, I. Favero, M. Lipson, T. J. Kippenberg/E. Weig/J. Kotthaus, H. Tang, K. Vahala/T. Carmon, J. Teufel/K. Lehnert, I. Robert, O. Painter, O. Painter, I. Favero/E. Weig/K. Karrai, and D. Stamper-Kurn

2.1.1 Intensity or Field transmission

Optical cavities are formed when light propagates in a closed path between two or more reflecting surfaces i.e mirrors separated by a distance with length l. To characterize this latter, I consider a prototypical cavity optomechanical system, i.e., a Fabry-Perot cavity that made up of two highly reflective mirrors separated by a distance d. When the cavity is driven by a plane wave and encounters the input mirror, this latter is divided into two partial waves. One part is transmitted and the other one is reflected this character is well illustrates in Fig 2.3.

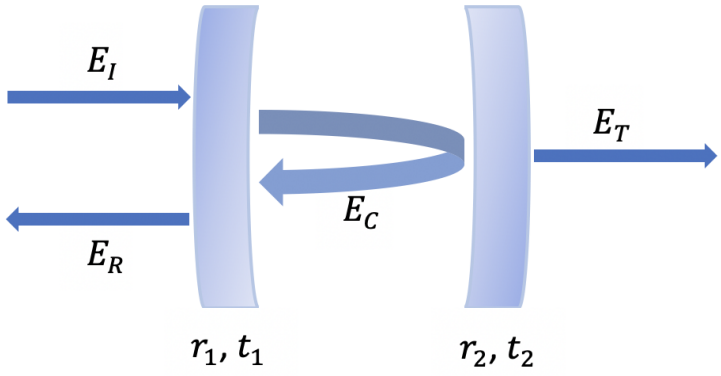

Figure 2.3: A schematic of a Fabry-Perot cavity. Formed of two mirrors each mirror has an associated reflection and transmission field amplitude coefficients r_1,r_2 and t_1,t_2 respectively.

The transmitted and reflected electrical amplitudes can be written as [70] :

$$E_T = -itE_I, \tag{2.1}$$

$$E_R = rE_I, \tag{2.2}$$

where E_I is the incident electric field amplitude. The circulating field inside the cavity is noted as E_C. After one round trip E_C will return a complex round trip gain $G(\omega)$, where $\mathrm{e}^{\frac{i\omega l}{c}}$ is the phase shift that the wave accumulate after each round trip. Notice that, ω is the angular frequency and c is the speed of light.

$$G(\omega) = R\,\mathrm{e}^{\varphi}, \tag{2.3}$$

where, $\varphi = [i\omega l/c]$ and $R = r_1 r_2 (r_3 ...)$.

The circulationg field equal the sum of the the initial wave that transmitted through the input

mirror $-it_1E_I$ plus the circulating field E_C which left the same point one round trip earlier

$$E_C = -it_1E_I + G(\omega)E_C, \tag{2.4}$$

Dividing the circulating field to the incident field we get the expression

$$\frac{E_C}{E_I} = \frac{-it_1}{1 - G(\omega)}. \tag{2.5}$$

A simiular treatment can be done for the reflected and transmitted fields, we get

$$E_R = r_1E_I - it_1(G(\omega)/r_1)E_C. \tag{2.6}$$

Relating the reflected field to the incident field we get the expression

$$\frac{E_R}{E_I} = r_1 - \frac{t_1^2}{r_1}\frac{G(\omega)}{1 - G(\omega)}. \tag{2.7}$$

The portion of the circulating field that gets transmitted through the mirror M_2, we get the transmitted field

$$E_T = -it_2\,\mathrm{e}^{\frac{\varphi}{2}}\,E_C. \tag{2.8}$$

Relating the reflected field to the incident field we get

$$\frac{E_T}{E_I} = \frac{t_1t_2\,\mathrm{e}^{\frac{i\varphi}{2}}}{1 - G(\omega)} \tag{2.9}$$

$$\frac{I_{R,T}}{I_0} = \left|\frac{E_{R,T}}{E_0}\right|^2 \tag{2.10}$$

we adopt the intensity of the fields using the quadratic dependence of the intensity upon the field, given by

$$I_T = I_0(\frac{T}{1 - R})^2\,\frac{1}{1 + \frac{4R}{(1-R)^2}\sin^2(\varphi/2)} \tag{2.11}$$

with $T = t_1t_2$, neglecting the absorption, we have $T = 1 - R$, hence the result :

$$I_T = \frac{I_0}{1 + m_R\sin^2(\varphi/2)}, \tag{2.12}$$

with $m_R = \frac{4R}{(1-R)^2}$.

2.1.2 Stability

Only certain ranges of values for R_1, R_2 and the distance l produce stable resonators. Notice that R_1 and R_2 the radii of curvature of the two mirrors. When the stability condition is satisfied, a periodic refocussing of the intracavity beam is produced. Otherwise, the beam size will grow without limit, eventually growing larger than the size of the cavity mirrors and being lost. The stability condition criterion can be expressed as [71]:

$$0 < (1 - \frac{l}{R_1})((1 - \frac{l}{R_2}) < 1 \tag{2.13}$$

values which satisfy the inequality correspond to stable resonators.

2.1.3 The optical finesse

A further useful quantity is the optical finesse F, which is a measure of the cavity quality and typically is determined by the reflectivity of the mirrors

$$F = \frac{\pi\sqrt{R}}{1-R}, \tag{2.14}$$

A Fabry-Perot resonator, composed of two highly reflective mirrors, separated by a distance l, contains a series of resonances given by the angular frequency $\omega_c \approx q.\pi(c/l)$, q is an integer. The separation of two longitudinal resonances is denoted as the free spectral range (FSR) of the cavity

$$\Delta\omega = \pi\frac{c}{l}, \tag{2.15}$$

the optical finesse gives the average number of round-trips before a photon leaves the cavity :

$$F = \Delta\omega/\kappa, \tag{2.16}$$

with κ, the decay rate the losses during one cycle divided by the roundtrip time. It is worth mentioning that, the cavity decay rate can have two contributions $\kappa = \kappa_{ex} + \kappa_0$, κ_0 is due to the internal losses and κ_{ex} from the losses that are associated to the input coupling.

2.1.4 Quality factor of the optical resonator

Another important parameter is the optical quality factor,

$$Q_{opt} = \omega_c \tau, \tag{2.17}$$

with, $\tau = \kappa^{-1}$ is the photon lifetime. The quality factor is also used to characterize the damping rate of mechanical objects. This will be more illustrate in the next part.

2.2 Quantum harmonic oscillator

The optomechanical cavity, i.e., a Fabry-Perot cavity where one of the end mirrors is fixed while the other one is free to move along the cavity axis due to the radiation pressure force and its center of mass motion can be modelled as a mechanical harmonic oscillator. The harmonic oscillator is one of the few analytical solvable systems in quantum mechanics. It has an important impact in most of the branches of modern physics solid-state physics, quantum field theory, quantum optics and will also describe our optomechanical systems. Notice that, harmonic motion is one of the most important examples of motion in all of physics and has been successively described classically then quantumly. One problem with this classical formulation is that it is not general. We cannot use it, for example, to describe vibrations of diatomic molecules, where quantum effects are important. In this part, we only consider the review of the quantum harmonic oscillator.

2.2.1 Basic properties

Let start by the basic Hamiltonian of a mechanical harmonic oscillator, read as:

$$\hat{H}_m = \frac{\hat{p}^2}{2m} + \frac{m{\omega_m}^2\hat{x}^2}{2}, \tag{2.18}$$

where, m represents the mass and ω_m the angular frequency of the oscillator. The variables $\hat{x}$ and $\hat{p}$ are the position and momentum for the particle, respectively. That verify the canonical commutation relation $[\hat{x}, \hat{p}] = i\hbar$ [72].

To give another useful representation of Eq.2.18, we introduce the non-hermitian bosonic anni-

hilation operator for a single particle ($[\hat{b}, \hat{b}^\dagger] = 1$):

$$\hat{b} = \sqrt{\frac{m\omega_m}{2\hbar}}(\hat{x} + \frac{i\hat{p}}{m\omega_m}), \tag{2.19}$$

$$\hat{b}^\dagger = \sqrt{\frac{m\omega_m}{2\hbar}}(\hat{x} - \frac{i\hat{p}}{m\omega_m}), \tag{2.20}$$

and therefore we can get:

$$\hat{x} = \sqrt{\frac{\hbar}{2m\omega_m}}(\hat{b}^\dagger + \hat{b}), \tag{2.21}$$

$$\hat{p} = i\sqrt{\frac{m\hbar\omega_m}{2}}(\hat{b}^\dagger - \hat{b}), \tag{2.22}$$

we define also the number $\hat{N}_b$ operator as :

$$\hat{N}_b = \hat{b}^\dagger\hat{b}, \tag{2.23}$$

that satisfy the following commutation relations :

$$\begin{aligned} [\hat{N}_b, \hat{b}] &= [\hat{b}^\dagger\hat{b}, \hat{b}] = -\hat{b}, \\ [\hat{N}_b, \hat{b}^\dagger] &= [\hat{b}^\dagger\hat{b}, \hat{b}^\dagger] = \hat{b}^\dagger. \end{aligned} \tag{2.24}$$

Using Eqs(2.18, 2.23), we can rewrite the Hamiltonian as :

$$\hat{H}_m = \hbar\omega_m(\hat{N}_b + \frac{1}{2}). \tag{2.25}$$

The basis related to the creation and annihilation operator is the Fock basis $|n\rangle$, with n is the photons number in the quantum state. If $\hat{b}(\hat{b}^\dagger)$ acts on $|n\rangle$ this can annihilate (create) one photon :

$$\begin{aligned} \hat{b}\,|n\rangle &= \sqrt{n}\,|n-1\rangle\,, \\ \hat{b}^\dagger\,|n\rangle &= \sqrt{n+1}\,|n+1\rangle\,, \\ \hat{N}_b\,|n\rangle &= n\,|n\rangle\,. \end{aligned} \tag{2.26}$$

Notice that, $\hat{H}_m\,|n\rangle = E_n\,|n\rangle$, where the eigenvalues of $\hat{N}$ represents the number of quanta energy present in the mode in consideration. The corresponding energy levels are

$$E_n = \hbar\omega_m(n + \frac{1}{2}), \tag{2.27}$$

with $n = 0, 1, 2, \ldots$. The energy spectrum is represented in Figure 2.4. We denote that, the lowest energy level is ground state and its wavefunction in the x representations reads

$$\psi_0(x) = (\frac{m\omega_m}{\pi\hbar})^{1/4} \mathrm{e}^{-m\omega_m x^2/2\hbar} \tag{2.28}$$

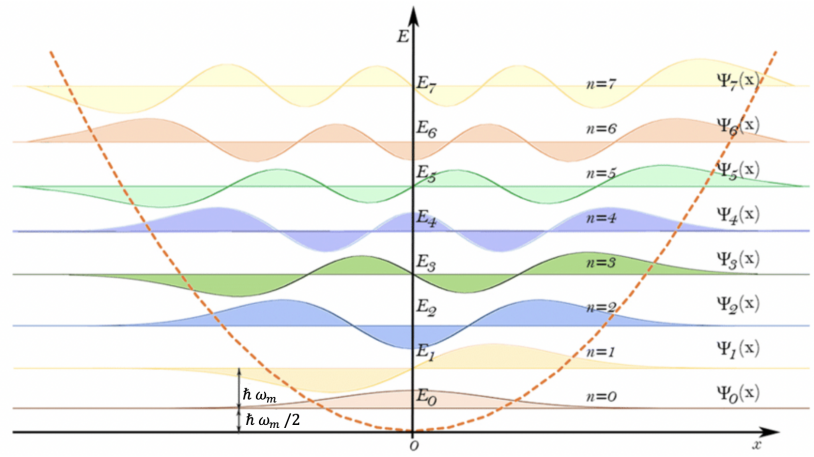

Figure 2.4: Energy Levels of the one-dimensional harmonic oscillator, the Wavefunction representations for the first eight bound eigenstates, n = 0 to 7.

which to satisfies the schrödinger wave equation [73]:

$$\hat{H}_m\psi_n(x) = (n + \frac{1}{2})\hbar\omega_m\psi_n(x) \tag{2.29}$$

with the eigenfunction $\psi_n(x)$ reads :

$$\psi_n(x) = \frac{1}{\sqrt{2^n n!}}(\frac{m\omega}{\pi\hbar})^{1/4} \mathrm{e}^{-m\omega_m x^2/2\hbar} H_n(\sqrt{\frac{m\omega}{\hbar}}x), \tag{2.30}$$

where $H_n(x) = (-1)^n \mathrm{e}^{-x^2} \frac{d^n}{dx^n}(\mathrm{e}^{-x^2})$ are the Hermite polynomials. To each eigenfunction $\psi_n(x)$ corresponds an energy level $(n+\frac{1}{2})\hbar\omega_m$. This evently spaced energy levels correspond to discrete quanta of excitation of the system [74], photons for electromagnetic field and phonons for a mechanical oscillator.

2.2.2 Mechanical quality factor

The key parameters used to describe a mechanical resonator are its mass m, resonant frequency ω_m, and its quality factor Q_m, which defines the ratio of energy stored in the oscillator compared to energy dissipated per radian of oscillation. It gives how many oscillations the resonator it

undergoes before losing its coherence. This useful quantity is given by:

$$Q_m = \frac{\omega_m}{\gamma_m} \tag{2.31}$$

γ_m is the energy damping rate, which is on one hand related to the mechanical excitation loss of the phonons and on the other hand, the energy in which the damping is occurs [75].
In general, for low mechanical quality factor the mechanical dissipation can be significant, leading to a less efficient quantum correlations [76]. The dissipative factor in optomechanical system, is considered to have negative effect on the performance of quantum manipulation of mechanical modes. Which requires very high mechanical quality factor.

2.2.3 Thermal bath environment of quantum harmonic oscillator

Any realistic physical system is never truly isolated but coupled to an environment as shown in the scheme 2.5. Notice that, total Hamiltonian of the system is $\hat{H}_{tot} = \hat{H}_m + \hat{H}_e + \hat{H}_{coupl}$.
In the next chapters, this coupling will be taken into consideration. In this part, i will study the temporal evolution of quantum harmonic oscillator coupled to this environment in thermal bath with temperature T.
The quantum state of the harmonic oscillator is not a pure state, but a statistical state defined by an energy $\hat{H}_m$ described by a density matrix ρ.

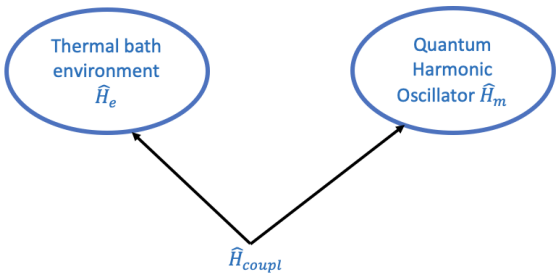

Figure 2.5: Schematic representation of the coupling $\hat{H}_{coupl}$ between the harmonic oscillator $\hat{H}_m$ and the environment $\hat{H}_e$.

Initially, let us assume the density operator [77]:

$$\hat{\rho} = \frac{1}{Z}\, \mathrm{e}^{-\hat{H}_m/K_B T}, \tag{2.32}$$

where K_B is Boltzmann's constant and Z is the canonical partition function defined as :

$$Z = Tr(\mathrm{e}^{-\hat{H}_m/K_BT}) = \sum_{n=0}^{\infty} \mathrm{e}^{-(n+1/2)\hbar\omega_m/K_BT} = \frac{\mathrm{e}^{-\hbar\omega_m/2K_BT}}{1-\mathrm{e}^{-\hbar\omega_m/K_BT}} \tag{2.33}$$

we adopt the definition of the thermal phonons numbers as shown in Eq(2.34) to give a complete description of a mechanical model.

$$n_{th} = (\mathrm{e}^{\frac{\hbar\omega_m}{K_BT}} - 1)^{-1} = \frac{1}{2}\coth\left(\frac{\hbar\omega_m}{2K_BT}\right) - \frac{1}{2}. \tag{2.34}$$

This equation links the mode temperature of a resonator to its phonon occupation and will be more illustrates in the next part.

The usefulness of the partition function, allows as to calculate the total energy using the trace of $\hat{H}_m$ and $\hat{\rho}$ [78]:

$$\langle \hat{H}_m \rangle_T = Tr(\hat{H}_m\hat{\rho}) = \hbar\omega_m(n_{th} + 1/2) \tag{2.35}$$

When a quantum system is coupled to an environment, the pilot equation which defines the evolution of the density matrix, makes it possible to calculate all the average values of observable of this system [79]. This equation, although exact, is often complicated to solve. To study the fluctuations of the system, we will therefore use the Heisenberg representation to obtain the Langevin equations, the latter will be studied later.

2.3 Characterization of the optomechanical coupling

Now, let us have a look at radiation pressure effects occurring in cavity optomechanical system. In an optomechanical cavity one of the mirrors is free to move and thus acts as a mechanical resonator and when the cavity is coherently driven by an external laser field. Knowing that, any electromagnetic field is made up of particles called photons, and while photons have no mass, they do carry a very small amount of energy. Once the photons reach the mirror, they bounce off it and give it a small push. The impacts of the photons cause the mirror to move slightly due to the radiation pressure force, this latter is proportional to the instantaneous photon number in the cavity. This, in turn, changes the length of the cavity, and alters the intensity of the cavity field, which in turn modifies the radiation pressure force itself. This interaction gives a complete description of the wavelengths of light we can trap inside the cavity.

Each photon that arise on the movable mirror yield a momentum of $2h/\lambda$, with λ is the wave-

length of the photon and h is Planck's constant. Due to this interaction knowing by the radiation pressure force that changes the resonant frequency of the cavity. This frequency shift per unit displacement is given by the optomechanical coupling strength g_0. As shown in figure 2.1 the oscillator moves it changes the length L of the cavity subsequently changing the cavity frequency ω_c over time. This is well explained by the following equation

$$\omega_c(x(t)) = \omega_c + x(t)\frac{\partial\omega_c(x(t))}{\partial x} = \omega_c - g_0 x(t), \tag{2.36}$$

we define the optical frequency shift per displacement as $g_0 = -\frac{\partial\omega_c(x(t))}{\partial x}$ (but different in some cases)

The optomechanical coupling rate defined as a function of the frequency shift per zero-point oscillation of the mechanical resonator :

$$g = g_0 x_{ZPM} \tag{2.37}$$

where $x_{ZPM} = \sqrt{\frac{\hbar}{2m\omega_m}}$, m and ω_m are respectively the mass and frequency of the mechanical oscillator.

As the photons exert a radiation pressure force on the surfaces of the movable mirror proportional to the instantaneous photon number in the cavity n_{cav}, we have

$$G = g\sqrt{n_{cav}} \tag{2.38}$$

A strong coupling regime is satisfied when the condition $G > \kappa$ is met.

For a clear illustration of the coupled system, figure 2.6 shows, an optomechanical system where the optical field couples to the mechanical object by using the concept of radiation pressure.

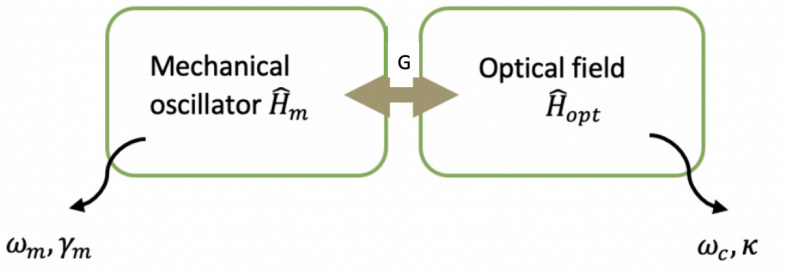

Figure 2.6: Schematic representation of the optomechanical interaction between the electromagnetic field and the mechanical mirror.

The Hamiltonian of the present system is :

$$\hat{H}_{tot} = \hat{H}_m + \hat{H}_{opt} + \hat{H}_{int} \tag{2.39}$$

where, $\hat{H}_m$ the Hamiltonian of the mechanical object as described in eq. 2.25, we define the Hamiltonian of the optical field $\hat{H}_{opt}$ using 2.36 :

$$\hbar\omega_c(x(t))\,\hat{a}^\dagger\hat{a} \approx \hbar(\omega_c - g_0 x_{ZPM}(\hat{b}+\hat{b}^\dagger))\hat{a}^\dagger\hat{a} \tag{2.40}$$

with $\hat{x} = x_{ZPM}(\hat{b}+\hat{b}^\dagger)$ as defined before. Then we get

$$\begin{cases} \hat{H}_{opt} = & \hbar\omega_c\hat{a}^\dagger\hat{a} \\ \hat{H}_{int} = & -\hbar g\hat{a}^\dagger\hat{a}(\hat{b}+\hat{b}^\dagger) \end{cases} \tag{2.41}$$

$\hat{H}_{int}$ the Hamiltonian of the coupling that allows to get the expression of the radiation-pressure force since is simply the derivative of $\hat{H}_{int}$

$$\hat{F}_{rad} = -\frac{d\hat{H}_{int}}{d\hat{x}} = \hbar\frac{g}{x_{ZPM}}\hat{a}^\dagger\hat{a} = \hbar\, g_0\,\hat{a}^\dagger\hat{a}, \tag{2.42}$$

for a simple cavity of length L, we have $g_0 = \frac{\omega_c}{L}$. Then, we get

$$\hat{F}_{rad} = \hbar\frac{\omega_c}{L}\hat{a}^\dagger\hat{a} \tag{2.43}$$

this expression is equivalent to

$$\hat{F}_{rad} = 2\hbar\,\kappa\,\frac{\hat{a}^\dagger\hat{a}}{\tau}. \tag{2.44}$$

Notice that, $\hbar\omega_c/L$ describes the radiation-pressure force caused by one intracavity photon. Here $\tau = 2L/c$ denotes the cavity round-trip time [65].

2.4 Stokes and Anti-Stokes process

In this part of chapter, we shall focus on Stokes and Anti-Stokes scattering. In fact, as explained in previous, optomechanical interaction induced by the radiation pressure force can generate quantum correlations when the cavity is driven by strong laser with frequency ω_L.

Ok, so what does this have to do with Stokes and Anti-Stokes process? the answer to this question will be understood by thinking of two harmonic oscillator with an arbitrary states

$|n, m\rangle$(n, m represents the photon and phonon numbers respectively).

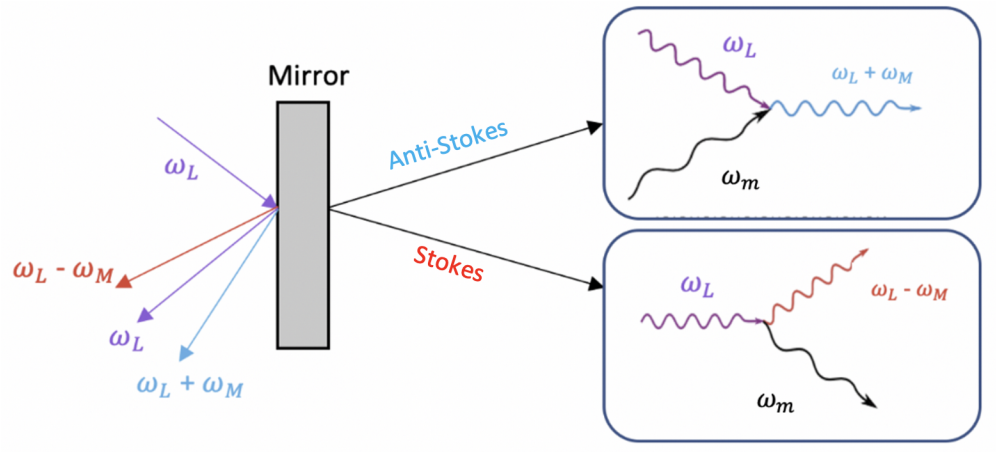

Figure 2.7: Schematic diagram of Stokes and Anti-Stokes sideband. Here a moving mirror driving by laser with frequency ω_L.

As shown in figure 2.7, the reflection of a photon on a moving mirror lead to a modification of the photon frequency by two different regimes. The first one (Stokes process) corresponds to a loss of energy from the photon by creation of a phonon, this interaction couples a state $|n, m\rangle$ to $|n-1, m+1\rangle$. When this regime is enhanced, the laser photons shed energy, increasing the number of phonons and becoming resonant with the cavity in the process. The second regime (Anti-Stokes) correspond to absorption of a phonon and transfert of energy $\hbar\omega_m$ from the resonator to the photon, one eventually gets a transition from $|n, m\rangle$ to $|n+1, m-1\rangle$. Photons leaking from the cavity take the system to $|n, m-1\rangle$. These two elementary processes create sidebands $\omega_L \pm \omega_m$. A quantitative description of a resonant cavity depending on Δ, the detuning between the laser frequency and the cavity resonance frequency is provided by considering scattering of laser photons. The cavity is detuned to the stokes sideband, i.e., $\Delta = -\omega_m$ or to the Anti-Stokes sideband that correspond to $\Delta = \omega_m$. In the next, we choose a system by driving the cavity with a detuning $\Delta = \omega_m$, this sideband is used to achieve quantum entanglement.

In the previous sections, we introduce the main basics of the optical resonators and the harmonic oscillators that present the mechanical part of the term optomechanics. In addition, the coupling strength of the coupled optomechanical system due to the radiation pressure, trying to give a complete description of the dynamics behind optomechanical systems. For clarity and simplicity, we provide in the next section a specific example that incorporates recent advances.

2.5 Theoretical Fabry-Perot cavity model

A generic optomechanical cavity have been realized experimentally in a variety of systems. More complete description including Fabry-Perot cavity with moving mirror(s) can be found in [80–85]. Let as consider a prototypical cavity optomechanical system, consists of a Fabry-Perot cavity with a fixed end-mirror while the other one is movable and oscillates harmonically. The interaction of light with a mechanical object is enhanced via the radiation pressure, when the cavity is driven by a powerful laser. The schematic of the system is depicted in fig 2.8.

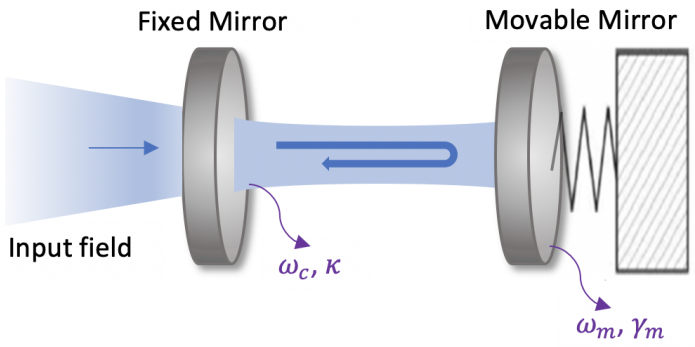

Figure 2.8: Modeling of the studied system: standard Fabry-Perot cavity with a laser-driven.

For a comprehensive treatment of the generic optomechanical system, we start with the standard Hamiltonian of the system [86], before a well-developed method based on the equation of motion of the cavity field and the mirror. Subsequently, the quantum Langevin approach is derived. Next, we numerically simulate the degree of stationary entanglement and show that it depends on some parameters with respect to the certain environment temperature.

2.5.1 Hamiltonian formulation

The Hamiltonian of the system $\hat{H}_{om}$ reads [86],

$$\hat{H}_{om} = \hat{H}_o + \hat{H}_m + \hat{H}_{int} + \hat{H}_{driv}, \tag{2.45}$$

we can identify four terms : $\hat{H}_m$ the mechanical side representing the movable mirror that can be modeled as an harmonic oscillator, it's Hamiltonian have already been introduced in 2.18, $\hat{H}_o$ the optical side, representing the energy of the cavity mode, the equation of motion is obtained

by treating the optical field as an harmonic oscillator, $\hat{H}_{int}$ design the interaction part caused by the radiation pressure force between the scattered photons and the mirror, the last term $\hat{H}_{driv}$ describe the input driving field since the cavity is pumped with a single monochromatic laser source. Indeed, the input-output theory allows us to takes into account any coherent laser drive that may be present [65]. Thus the resulting Hamiltonian reads

$$\hat{H}_{om} = \hbar\omega_c\,\hat{a}^\dagger\hat{a} + \frac{\hbar\omega_m}{2}(p^2+q^2) - \hbar g\hat{a}^\dagger\hat{a}q + i\hbar E(\mathrm{e}^{-i\omega_L t}\,\hat{a}^\dagger - \mathrm{e}^{i\omega_L t}\,\hat{a}). \tag{2.46}$$

In this coupled optomechanical system, it is convenient to transform the above Hamiltonian into the rotating frame at the frequency ω_L of the driving laser field. Applying the unitary transformation $\hat{U} = \mathrm{e}^{i\omega_L\hat{a}^\dagger\hat{a}t}$, we can generate the new Hamiltonian using $\hat{H} = \hat{U}\hat{H}_{om}\hat{U}^\dagger - i\hbar\dot{\hat{U}}\hat{U}^\dagger$. We rewrite the system Hamiltonian as

$$\hat{H} = \hbar\Delta_0\hat{a}^\dagger\hat{a} + \frac{\hbar\omega_m}{2}(p^2+q^2) - \hbar g\hat{a}^\dagger\hat{a}q + i\hbar E(\hat{a}^\dagger - \hat{a}). \tag{2.47}$$

with $\Delta_0 = \omega_L - \omega_c$, the other parameters and operators used in 2.47 are defined in 2.1, where we adopt the set of notations and symbols used in this thesis.

Symbol	Description
K_B	Boltzmann constant
$\hbar$	$h/(2\pi)$ reduced Planck constant
c	speed of light
ε_0	the vacuum permittivity
T	temperature
m	mass
κ	cavity total loss rate
L	cavity length
ω_L	laser frequency
ω_c	cavity frequency
ω_m	mechanical oscillator frequency
p	laser power
E	$E = \sqrt{\frac{2p\kappa}{\hbar\omega_L}}$ input laser power
g	$g = \frac{\omega_c}{L}\sqrt{\frac{\hbar}{m\omega_m}}$ optomechanical coupling
γ_m	mechanical damping rate
γ_a	decay rate of the atomic excited level
Q_m	$Q_m = \frac{\omega_m}{\gamma_m}$ mechanical quality factor
n_{th}	mean thermal excitation number
Δ_0	$\Delta_0 = \omega_c - \omega_L$ laser field detuning from the cavity resonance
Δ_a	$\Delta_a = \omega_a - \omega_L$ atomic detuning
Δ	effective detuning

Table 2.1: Table of the symbols and formulas used in this thesis.

2.5.2 Quantum Langevin Equations

In this part, we study the dynamics of the system, by considering the Heisenberg's equation of motion

$$\frac{d\hat{Y}(t)}{dt} = \frac{i}{\hbar}[\hat{H}, \hat{Y}(t)] + \frac{\partial \hat{Y}(t)}{\partial t}, \tag{2.48}$$

where $\hat{Y}(t)$ generic operator satisfying the commutation relation $[\hat{Y}, \hat{Y}^\dagger] = 1$.

A proper analysis of the dynamics must include the fluctuation-dissipation processes. The photon losses in the cavity and the thermal bath noise acting on the mirror can be taken into account. By adding the dissipation decay term $\sqrt{2\eta}\hat{D}(t)$, where η is a dissipation coefficient we gets

$$\frac{d\hat{Y}(t)}{dt} = \frac{i}{\hbar}[\hat{H}, \hat{Y}(t)] - \eta\hat{D}(t) + \sqrt{2\eta}\hat{D}(t), \tag{2.49}$$

the equation (2.49), is known as the Quantum Langevin equation. Using the Hamiltonian of the system 2.47 the set of nonlinear quantum-Langevin equations are defined as

$$\begin{aligned}
\dot{q} &= \omega_m\, p, \\
\dot{p} &= -\omega_m q - \gamma_m\, p + g\hat{a}^\dagger\hat{a} + \xi, \\
\dot{\hat{a}} &= -(\kappa + i\Delta_0)\hat{a} + ig\hat{a}q + E + \sqrt{2\kappa}a^{in},
\end{aligned} \tag{2.50}$$

the mechanical mode is affected by ξ, the Brownian stochastic force with zero mean values and possessing the correlation function

$$< \xi(t)\xi(t^{'}) >= \frac{\gamma_m}{\omega_m}\int \frac{\omega}{2\pi}\, \mathrm{e}^{-i\omega(t-t^{'})}[1 + \coth\left(\frac{\hbar\omega}{2k_BT}\right)]d\omega. \tag{2.51}$$

However, quantum effects are achievable only for the mechanical oscillator with high quality factor (2.31), i.e., $Q_m \gg 1$. In this limit, this non-Markovian process can be approximated as a Markovian one, $\xi(t)$ becomes delta-correlated [87, 88]

$$\langle \xi(t)\xi(t^{'}) + \xi(t^{'})\xi(t)\rangle/2 \simeq \gamma_m(2n_{th}+1)\delta(t-t^{'}) \tag{2.52}$$

In addition, the cavity mode decays at the rate κ and is affected by the vacuum radiation input noise a_{in}. Its correlation functions obey the relation [89]

$$\langle a_{in}(t)a_{in}^{\dagger}(t^{'})\rangle = \delta(t-t^{'}) \tag{2.53}$$

The linearization treatment of the nonlinear quantum Langevin equations can be realized around the steady state by rewriting each Heisenberg operator as a sum of its steady-state mean value plus an additional fluctuation operator with zero mean value

$$\begin{aligned}
q &= q_s + \delta q, \\
p &= p_s + \delta p, \\
a &= a_s + \delta a.
\end{aligned} \tag{2.54}$$

Inserting these expressions into 2.50, we gets the exact quantum Langevin equations for the fluctuations. The cavity is coherently driven by an external laser field, with a very large input power P, so that the intracavity fields have a large amplitude $|a_s| \gg 1$. In this case, we neglect the high order terms of the fluctuation $\delta a^\dagger \delta a$ and $\delta a \delta q$, and gets the following Langevin equations

of motion fully linear:

$$\begin{aligned}
\delta\dot{q} &= \omega_m \delta p, \\
\delta\dot{p} &= -\omega_m \delta q - \gamma_m \delta p + g(a_s^* \delta a + a_s \delta a^\dagger) + \xi, \\
\delta\dot{a} &= -(\kappa + i\Delta)\delta a + i g a_s\, \delta q + \sqrt{2\kappa}\, a_{in}
\end{aligned} \tag{2.55}$$

with $\Delta = \Delta_0 - \frac{g^2|a_s|^2}{\omega_m}$. The parameters p_s, q_s and a_s are the solutions of the nonlinear algebraic equations in the steady state, it satisfies

$$\begin{aligned}
p_s &= 0 \\
q_s &= \frac{g|a_s|^2}{\omega_m} \\
a_s &= \frac{E}{\kappa + i\Delta}
\end{aligned} \tag{2.56}$$

We define the cavity field quadratures $\delta X \equiv (\delta a + \delta a^\dagger)/\sqrt{2}$ and $\delta Y \equiv (\delta a - \delta a^\dagger)/i\sqrt{2}$ and the corresponding Hermitian input noise operators $x_{in} \equiv (a_{in} + a_{in}^\dagger)/\sqrt{2}$ and $y_{in} \equiv (a_{in} - a_{in}^\dagger)/i\sqrt{2}$, we rewrite the linearized equations of motion 2.55

$$\begin{aligned}
\delta\dot{q} &= \omega_m \delta p, \\
\delta\dot{p} &= -\omega_m \delta q - \gamma_m \delta p + G_{eff} \delta X + \xi, \\
\delta\dot{X} &= -\kappa \delta X + \Delta \delta Y + \sqrt{2\kappa}\, x_{in}, \\
\delta\dot{Y} &= -\kappa \delta Y - \Delta \delta X + G_{eff} \delta q + \sqrt{2\kappa}\, y_{in}
\end{aligned} \tag{2.57}$$

with $G_{eff} = g\, a_s \sqrt{2}$.

2.5.3 Stability of the system

The resulting equations of motion for the fluctuations in 2.57 can be written in compact form as

$$\dot{U}(t) = AU(t) + W \tag{2.58}$$

where the vector of four component quadrature fluctuations $U = (\delta q, \delta p, \delta X, \delta Y)^T$, similarly the vector of noise $W = (0, \xi(t), \sqrt{2\kappa}x_{in}, \sqrt{2\kappa}y_{in})^T$ and the drift matrix A is given by

$$A = \begin{pmatrix} 0 & \omega_m & 0 & 0 \\ -\omega_m & -\gamma_m & G_{eff} & 0 \\ 0 & 0 & -\kappa & \Delta \\ G_{eff} & 0 & -\Delta & -\kappa \end{pmatrix}, \tag{2.59}$$

the solution of eq 2.58 is $U(t) = M(t)U(0) + \int_0^t dsM(s)W(t-s)$, where $M(t) = \mathrm{e}^{AT}$. The system is stable and reaches it steady state when all the eigenvalues of A have negative real parts [90]. By applying the Routh-Hurwitz criterion [91], we obtain the following conditions in order to achieve the stability of the system

$$\begin{aligned} &C_1 = \gamma_m + 2\kappa > 0, \\ &C_2 = -G_{eff}^2 \Delta\, \omega_m + \Delta^2\, \omega_m^2 + \kappa^2\, \omega_m^2 > 0, \\ &C_3 = 2\kappa\gamma_m(\Delta^4 + \Delta^2(\gamma_m^2 + 2\kappa\gamma_m + 2\kappa^2 - 2\omega_m^2) + (\kappa\gamma_m + \kappa^2 + \omega_m^2)^2) + \omega_m G_{eff}^2 \Delta(\gamma_m + 2\kappa)^2 > 0 \end{aligned} \tag{2.60}$$

this latter will be taken into consideration from now on. From 2.60, we define the multistability parameter [92]:

$$\chi = 1 - \frac{G_{eff}^2 \Delta}{\omega_m(\Delta^2 + \kappa^2)} \tag{2.61}$$

2.5.4 Covariance Matrix

In this hybrid optomechanical system, the optical mode and the mechanical mode form a bipartite continuous variable system (CV). The Gaussian nature of the noise operators, is a zero-mean Gaussian state, completely characterized by covariance matrix that represents the steady-state correlation matrix. When the stability conditions are satisfied, the covariance matrix V_s can be derived from the Lyapunov equation

$$AV_s + V_s A^T = -D, \tag{2.62}$$

where D the noise correlations matrix obtained from the relation $D_{kl}\delta(t-t^{'}) = \langle W_k(t)W_l(t^{'}) + W_l(t^{'})W_k(t)\rangle/2$. We found D a diagonal matrix :

$$D = \begin{pmatrix} 0 & 0 & 0 & 0 \\ 0 & \gamma_m(2n_{th}+1) & 0 & 0 \\ 0 & 0 & \kappa & 0 \\ 0 & 0 & 0 & \kappa \end{pmatrix} \tag{2.63}$$

In the following, the covariance matrix V_s can be written as the form of 2×2 block matrix

$$V_s = \begin{pmatrix} V_m & V_{ma} \\ V_{ma}^T & V_a \end{pmatrix} \tag{2.64}$$

where m and a index the coupled system {oscillating mirror, optical cavity}. This latter also allows to calculate the entanglement of the steady state. In the next section, we adopt the logarithmic negativity E_N [93] in order to study numerically the quantum entanglement properties of the coupled optomechanical system.

2.5.5 Entanglement analysis

The interaction between the mechanical motion and the light beam or between any systems that fall under the category of optomechanics, are used to engineer quantum entanglement. In order to establish the conditions under which the mechanical mode and the optical cavity are entangled, we consider the logarithmic negativity E_N a quantity that has been highlighted in the previous chapter. For Gaussian Continuous variable systems E_N is defined as [93] [51]:

$$E_N = \max[0, -\ln 2\tilde{\nu}_-]. \tag{2.65}$$

Here, $\tilde{\nu}_-$ is the minimum symplectic eigenvalue of the covariance matrix given by $\tilde{\nu}_- = 2^{-1/2}(\tilde{\Gamma} - (\tilde{\Gamma}^2 - 4\det V_s)^{1/2})^{1/2}$, where the symbol $\tilde{\Gamma}$ is the symplectic invariant $\tilde{\Gamma} = \det V_m + \det V_a - 2\det V_{ma}$. We notice that, a gaussian state is entangled if and only if $\tilde{\nu}_- < \frac{1}{2}$, which is consistent with Simon's necessary and sufficient criterion [94].

We have made a careful numerical simulation of the stationary optomechanical entanglement in a wide parameter range, for which a significant amount of entanglement is achievable. The parameters used are taken from (Vitali et al. (2007) 2.2). We summarizes in table 2.2, the most relevant experiments parameters for some hybrid optomechanical system.

Model	**Reference**	$\omega_{\mathbf{m}}/\mathbf{2}\pi(H_z)$	$\mathbf{m}(K_g)$	$\gamma_{\mathbf{m}}/\mathbf{2}\pi(H_z)$	$\kappa/\mathbf{2}\pi(H_z)$	$\mathbf{g}/\mathbf{2}\pi(H_z)$
Atomic gas	Murch et al.(2008) [95]	$4.2.10^4$	1.10^{-22}	1.10^3	$6.6.10^5$	6.10^5
Photonic crystal	Chan et al. (2011) [96]	$3.9.10^9$	$3.1.10^{-16}$	$3.9.10^4$	5.10^8	9.10^5
Microwave resonator	Teufel et al. (2011) [97]	$1.1.10^7$	$4.8.10^{-14}$	32	2.10^5	2.10^2
Circular resonator	Verhagen et al. (2012) [98]	$7.8.10^7$	$1.9.10^{-12}$	$3.4.10^3$	$7.1.10^6$	$3.4.10^3$
Fabry-Perot	Cuthbertson et al. (1996) [99]	1.10^3	1.85	$2.5.10^{-6}$	275	$1.2.10^{-3}$
	Arcizet et al. (2006) [66]	$8.14.10^5$	$1.9.10^{-7}$	81	1.10^6	1.2
	Gröblacher, et al. (2009) [100]	$9.5.10^5$	$1.4.10^{-10}$	$1.4.10^2$	2.10^5	3.9
	Kleckner et al. (2011) [101]	$9.7.10^3$	$1.4.10^{-10}$	$1.3.10^{-2}$	$4.7.10^5$	$2.2.10^1$
	Vitali et al. (2007) [90]	10^7	5.10^{-12}	10^2	$1.4.10^7$	$2.1.10^-3$

Table 2.2: Overview of numerical values of physical parameters used in optomechanical cavities experiments.

We show in figure 2.9 and 2.10 the importance of the parameter of mass. We plot in 2.10 the entanglement E_N versus the temperature T for two different values of m the mass of the mechanical oscillator. The other parameters are taken : $\Delta = \omega_m, p = 50\,mW, L = 1mm$ and the laser wavelength $810\,nm$ that correspond to $\omega_L = 2\pi\,3.7\,10^{14}H_z$. Knowing that, the optical mode and the mechanical mode are entangled when the logarithmic negativity E_N is positive. We see from figure 2.10 the entanglement decreases monotonically with temperature. We notice that, as expected, the quantum correlations do not resist the environment effects as E_N decreases with temperature. This is due to the environment-induced decoherence. We see also from the figure that, the largest stationary entanglement is the one corresponding to $m = 10\,ng$, where the entanglement persists for temperatures above $13K$. While, for $m = 50\,ng$ the entanglement vanishes at lower temperatures $(3K)$. As a matter of fact, the smaller it is, the more robust the system becomes against the thermal bath's temperature. This in turn is due to the fact that the optomechanical coupling, due to the radiation pressure, gets stronger as the displacement of the mirrors increases.

Next, fixing the temperature $T = 0.4K$. We study in figure 2.9 the entanglement E_N as a function of the normalized detuning Δ/ω_m for three values of m. We observe that, the entanglement is present only in the vicinity of $\Delta \sim \omega_m$. In fact, we see from the figure that the entanglement $(E_N = 0.04$ for $m_3 = 50ng)$, $(E_N = 0.18$ when $m_2 = 10ng)$ and $(E_N = 0.32$ when $m_1 = 5ng)$. Increasing the parameter of mass the entanglement becomes much less robust against tempera-

ture. Indeed, for small values of m not only the entanglement is increasingly stronger but also the region of the effective detuning that entanglement exists is more broader.

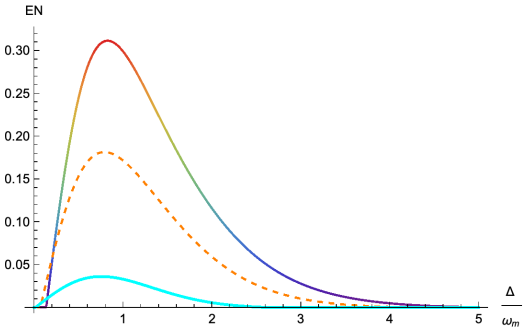

Figure 2.9: Plot of E_N as a function of Δ/ω_m for three different values of m, m_3(cyan Thik curves), m_2(orange dashed curves) and m_1(rainbow curves).

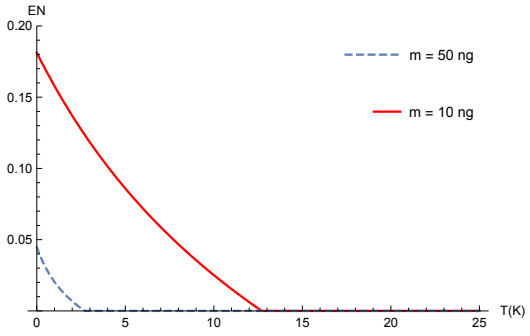

Figure 2.10: Entanglement E_N Vs the temperature $T(K)$ for two different values of m the mass of the mechanical oscillator.

We also investigate the behavior of the entanglement as a function of the optomechanical cooperativity C_{op}. This latter is getting using $C_{op} = 4\,G_{eff}^2/\gamma_m\kappa$. The contour plot 2.11 shows that entanglement is achievable at few kelvin degrees if C_{op} is sufficiently large. This result can be understood as following. Clearly, C_{op} depends on both the effective optomechanical coupling G_{eff} and the dissipative factors (γ_m and κ). Generally, the mechanical damping rate and the optical decay rate, are considered to have negative effect on the performance of quantum manipulation. contrariwise, a strong effective coupling G_{eff}, leads to a remarkable entanglement and a significant reduction of fluctuations. This can be achieved by increasing the photon numbers that interact in the surface of the movable mirror. It seems that a great number of these leads to photon–phonon interaction, which does enhance the optomechanical coupling due to the radiation pressure that consequently allows for robust entanglement. By using a powerfull input laser field characterized by a high photon numbers a strong optomechanical interaction is established. For a high values of this latter the system requires high values of T to switch from entangled to separable states, which illustrates well the strict necessity of using a bright laser field that resonates inside the cavity. For this reason, we show in the next part that, a strong laser power P have an important influence on quantum correlations.

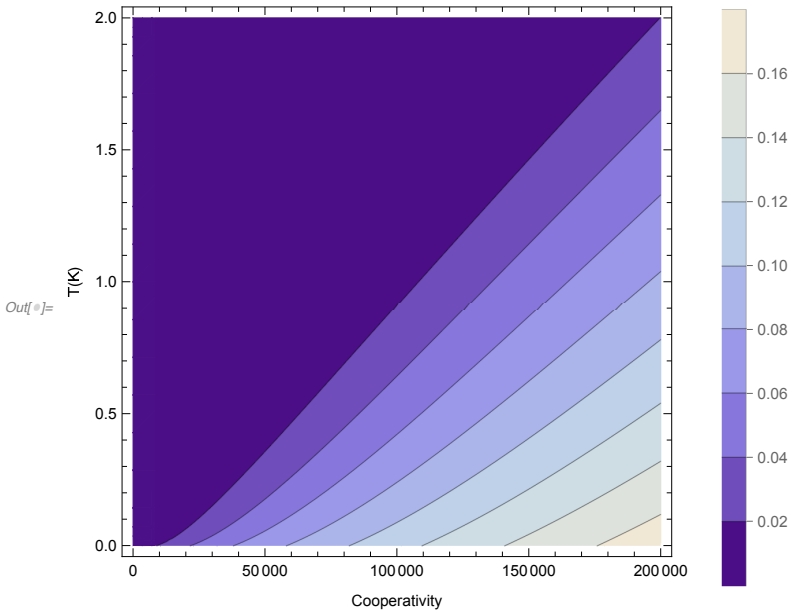

Figure 2.11: Contour plot of E_N versus temperature T and optomechanical cooperativity C_{op}. We use $\Delta = \omega_m$, $m = 5\,ng$ and finesse $F = 3.4\,10^4$ 2.16, the other parameters similar to those in Fig. 2.10.

To analyze the influence of the pumping power P, we plotted in figure 2.12 E_N as a function of the laser power P and the temperature T. We notice, for instance, that for a fixed temperature, the driving laser power has a favorable effect on the quantum correlations as captured by the logarithmic negativity. For example, with the power $P = 2mW$, E_N vanishes at $T \simeq 11K$. However, for $P = 5mW$, E_N vanishes at $T \simeq 24K$. It is clearly seen that, large driving strength increases the circulation inside the cavity which can contribute to enhance the optomechanical interaction which in turns enhances the entanglement. The higher the input powers, the wider the width of entanglement region becomes. Furthermore, there exists a minimum pump power strength for which the movable mirrors are entangled.

The minimum power required to observe mirror-field entanglement can be derived from 2.56, which yields

$$P \gg \frac{\hbar\omega_L(\kappa^2 + \Delta^2)}{2\kappa} \tag{2.66}$$

With the increase of driving power, the values of logarithmic negativity increase and, relatively, resist better the environment-induced decoherence.

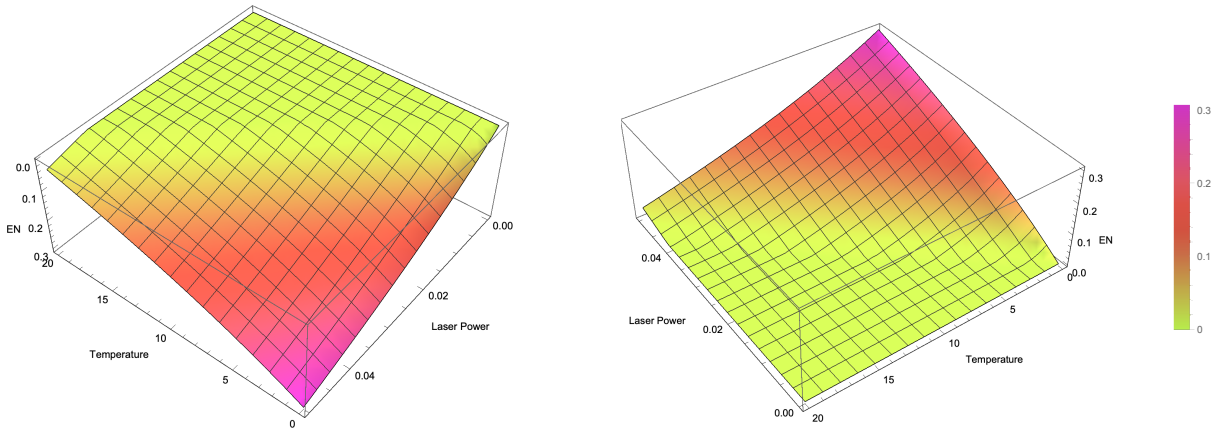

Figure 2.12: 3D Plot of entanglement as function of laser power P and temperature T.

It is worthwhile noting that with the increase in thermal phonon number, entanglement gradually decreases, but it can persist up to a much higher number as it is quantified by some parameters such as the laser pumping power and the mass of the movable mirrors. Adjusting and optimizing a bipartite entanglement in a thermal environment might contribute to various applications in quantum information processing and communication.

In this chapter, I have tried to give an overview of the basic theoretical language used to describe cavity optomechanics. Notation and preliminary concepts of optical resonators and mechanical oscillators are established. The practical analysis of an optomechanical system requires that it satisfy the stability criteria and then for a complete description it is important to characterize the degree of nonclassical correlation. To that, in the second part of the chapter, we adopted an optomechanical system where the optical resonator is coupled to the mechanical oscillator via the radiation pressure interaction. Then, to characterize the degree of entanglement we adopt the set of equations of motion. By linearizing the quantum Langevin equations in the steady state within the full parameter range of stable cavity we generate a robust entanglement. Notice that, cavity optomechanics comes in many other forms lengthening the cavity provides further enhancement of the interaction. By using a ring cavity configuration not only the circulating optical power is enhanced inside the cavity but also the optical phase detection is enhanced by the cavity's finesse. Subsequently, the next chapter is dedicated to a study of the stability and entanglement in ring cavity. Such systems can be realized experimentally. By linearizing the equation of motion, we characterize the entanglement present in the system, using the logarithmic negativity as a measure. The details are illustrated in the next chapter.

Chapter 3

Quantum correlations under the effect of a thermal environment in a triangular optomechanical cavity

In this chapter, we generate quantum correlations between the optical mode and the relative mechanical mode in a ring cavity composed of a fixed mirror and two movable ones in a triangular design. Using a ring configuration not only enhances the optomechanical coupling by the displacement of the two movable mirrors, but also the circulation of the optical power inside the cavity enhances the intensity of the pumping power, not as in the case of a linear cavity. As shown in previous chapter a linear optomechanical cavity is typically composed of an optical cavity with a moving mechanical object that can interact with the electromagnetic field confined in the cavity by the radiation pressure force.
In addition to entanglement, we investigate the behavior of Gaussian quantum discord and the mutual information in a ring cavity.

3.1 Model and Hamiltonian

The optomechanical system used in this chapter is a ring cavity as schematized below in Fig. 1. This latter is composed of a fixed partially transmitting mirror and two movable perfectly reflecting mirrors, with arm length L and frequency ω_c. The two movable mirrors are identical and are considered as quantum harmonic oscillators with frequencies ω_{m1}, ω_{m2} and effective masses m_1, m_2.

The Hamiltonian of the system is given by [67]

$$\hat{H} = \hbar\Delta_0\hat{a}^\dagger\hat{a} + \frac{\hbar\omega_{m1}}{2}(p_1^2+q_1^2) + \frac{\hbar\omega_{m2}}{2}(p_2^2+q_2^2) + \hbar g_1\hat{a}^\dagger\hat{a}\cos(\theta/2)^2 q_1 - \hbar g_2\hat{a}^\dagger\hat{a}\cos(\theta/2)^2 q_2 + i\hbar E(\hat{a}^\dagger - \hat{a}), \tag{3.1}$$

the first term as defined in previous, characterizes the optical mode, the second and third terms describe the energy of the mechanical resonator. The fourth and fifth terms denote the interaction between the cavity field and the movable mirror, which is due to the radiation pressure. The last term describes the laser driving input.

To study the quantum correlations that are present in the system, we have to analyze the dynamics of the coupled system. These can be obtained by linearizing the quantum Langevin equations as presented in section 2.5.2. The same procedure is done in the PdF below in order to obtain the drift matrix, that allows as to get the covariance matrix.

The drift matrix A reads,

$$A = \begin{pmatrix} 0 & \omega_m & 0 & 0 \\ -\omega_m & -\gamma_m & -\sqrt{2}g\cos(\theta/2)^2(\alpha_s+\alpha_s^*) & i\sqrt{2}g\cos(\theta/2)^2(\alpha_s-\alpha_s^*) \\ -i\frac{g}{\sqrt{2}}\cos(\theta/2)^2(\alpha_s-\alpha_s^*) & 0 & -\kappa & \Delta \\ -\frac{g}{\sqrt{2}}\cos(\theta/2)^2(\alpha_s+\alpha_s^*) & 0 & -\Delta & -\kappa \end{pmatrix}, \tag{3.2}$$

α_s is the classical steady state operator of the optical mode. To quantify the stationar correlations between the optical mode and the relative mechanical mode of the coupled system. The logarithmic negativity is used as a measure of entanglement, Gaussian quantum discord as a measure of total quantum correlations, and the mutual information as a measure of the overall correlations. The behavior of these quantities with respect to the environment's temperature as well as other parameters, such as the laser pumping power and mass of the movable mirrors, is discussed in detailed in the PdF below.

Research Article Vol. 37, No. 11 / November 2020 / Journal of the Optical Society of America B A237

Journal of the Optical Society of America B

OPTICAL PHYSICS

Quantum correlations under the effect of a thermal environment in a triangular optomechanical cavity

OUMAYMA EL BIR[1,*] AND MORAD EL BAZ[1,2,3]

[1]ESMaR, Faculty of Sciences, Mohammed V University, Rabat, Morocco
[2]The Abdus Salam International Center for Theoretical Physics, ICTP-Trieste, Italy
[3]e-mail: morad.elbaz@um5.ac.ma
*Corresponding author: oumayma.elbir@um5s.net.ma

Received 22 May 2020; revised 24 July 2020; accepted 24 July 2020; posted 27 July 2020 (Doc. ID 398308); published 20 August 2020

We quantify the stationary correlations between the optical mode and the relative mechanical mode of a ring cavity composed of a fixed mirror and two movable ones in a triangular design. Using a ring cavity configuration not only enhances the optomechanical coupling by the displacement of the two movable mirrors, but also the circulation of the optical power inside the cavity enhances the intensity of the pumping power, not as in the case of a linear cavity. The bipartite covariance matrix is used to evaluate the logarithmic negativity as a measure of entanglement, the Gaussian quantum discord as a measure of total quantum correlations, and the mutual information as a measure of the overall correlations. The behavior of these quantities with respect to the environment's temperature as well as other parameters, such as the laser pumping power and mass of the movable mirrors, is discussed.

https://doi.org/10.1364/JOSAB.398308

1. INTRODUCTION

In recent years, quantum information has attracted a lot of attention because of some of its surprising, unexpected, and remarkable properties. One of the most interesting characteristics at the foundations of this field is "entanglement" [1–3], which is, specifically, a quantum property. Recently, several propositions in using nonclassical entangled states of continuous variable (CV) systems in the realization of quantum memories for CV quantum information processing were presented [4]. These developments motivated advancements in quantitative entanglement measures [5] and CV entangled state preparation [6]. However a full description of the nonclassical properties of entangled states exists only for the class of the Gaussian state. These play a crucial role in quantum information theory of CV systems since they can be easily generated and controlled experimentally. So far, the production and manipulation of entangled states have been achieved with success in microscopic systems such as atoms, photons, ions [7–9], etc. Because the validity of entanglement in the macroscopic domain is not yet completely clear, this question made it an interesting subject for physicists. In this context, optomechanical systems manifest a new platform to investigate the entanglement between a macroscopic mechanical object and an optical field. Several studies covering this topic have been proposed to generate entanglement in mesoscopic systems [10–13]. In fact, the generation of entanglement between one or two mechanical modes and one or two optical modes has been proposed from many different angles, such as entangling two mirrors of two different cavities driven by entangled light beams [14], entangling two mirrors in a ring cavity [15], entangling two mirrors in a ring cavity by using a phase-sensitive feedback loop [16], enhancing quantum correlation and entanglement via cross-Kerr nonlinearity [17], qubit assisted enhancement of quantum correlations in an optomechanical system [18], entanglement in the four-mirror ring cavity [19], and optomechanially induced transparency (OMIT) in a ring cavity [20]. OMIT is a quantum interference effect caused by radiation pressure and observed in atoms in an optomechanical system, where the optical response of an atomic medium is controlled by an electromagnetic field, and they can become transparent by illuminating it with a second strong laser. Substantial progress has been made in OMIT theoretically [21,22] and experimentally [23,24].

The optomechanical systems [25,26] are typically composed of an optical cavity with a moving mechanical object that can interact with the electromagnetic field confined in the cavity via the radiation pressure force [27,28]. Indeed this latter is due to the momentum transfer of the photons during their reflection on the surface of the mechanical object. This force induces small displacements of the motion of the mechanical object that change the length of the cavity and modify the state of the cavity

field. The optomechanical coupling can be well observed when the cavity is driven by a strong laser source [29].

In this paper, we study the quantum correlations that are present in a ring cavity with two movable mirrors, the motion of which is due to the effect of the radiation pressure force. This allows to model the mirrors' motion as a mechanical harmonic oscillator and thus can be considered as a CV system. We found that the quantum correlations are present when the cavity is pumped by an external coherent laser source and even with the absence of squeezed light as in Ref. [19]. The degree of entanglement is probed using logarithmic negativity; we describe also the quantum mutual information that gives the total amount of correlations contained in a quantum state, which is equal to the sum of classical correlations and the quantum discord [30,31]. In fact, quantum discord has drawn much attention recently as another measure of quantum correlations that differs from entanglement, as the latter can be seen as contained in the former. Indeed quantum discord was first presented by Refs. [32,33], where it has been proved that some separable states do contain some amount of quantum correlations and have a nonzero value of the quantum discord. This notion was generalized to the field of CV systems in Refs. [34,35].

The structure of this work is as follows. In Section 2, we describe the model and present the Hamiltonian, then we solve the nonlinear quantum Langevin equations for the optical mode and the relative quadratures of the two mechanical modes which leads to obtain the bipartite covariance matrix. In Section 3, we study the stationary entanglement by using logarithmic negativity, and discuss the effect of some parameters on it. Beyond entanglement, we study the Gaussian quantum discord in Section 4 to measure quantum correlations, especially in the case where the state is separable. We simulate also the mutual information to quantify the total correlations present in the system considered. We conclude with some remarks to close the paper.

2. SYSTEM AND MODEL

A. System

We consider the ring cavity schematized in Fig. 1, with arm length L and frequency ω_c. This type of cavity was introduced in many different ways [15,16] and further studied in Ref. [19]. The cavity has three mirrors in a triangular configuration, such that one of the mirrors is fixed and partially transmitting, whereas the other two are movable and perfectly reflecting. These moving mirrors are considered as quantum harmonic oscillators with frequencies ω_{m1}, ω_{m2} and effective masses m_1, m_2. Their loss of mechanical energy is described by the damping rates γ_{m1}, γ_{m2}, respectively. The cavity is pumped by a coherent laser field with frequency ω_L, and the mean amplitude of the input laser is given by $E=\sqrt{\frac{2\kappa P}{\hbar\omega_L}}$, where P is the input pump power, $\hbar$ is the Planck constant, and κ is the total optical decay rate of the cavity: $\kappa=\kappa_{ex}+\kappa_0$ [25]. Here κ_{ex} denotes the losses at the input of the cavity, and κ_0 is due to internal losses.

An important parameter is the optical finesse F, which gives the average number of round-trips before a photon leaves the cavity:

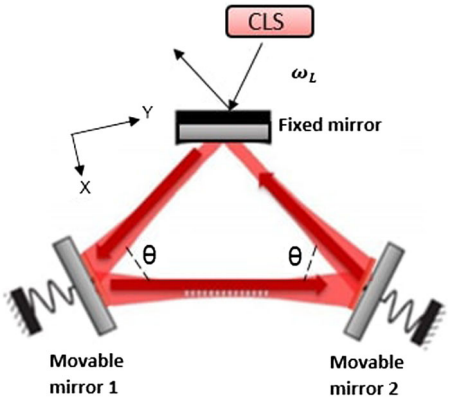

Fig. 1. Scheme of the optomechanical system under study including a ring cavity pumped by a coherent laser source (CLS) with frequency ω_L.

$$F=\frac{\pi c}{\kappa L}, \tag{1}$$

where c denotes the speed of light.

The reflection of each photon on the movable mirror gives rise to the transfer of momentum equal to $2\hbar k_y$, where $k_y=k\cos\frac{\theta}{2}$, θ is the angle between the incident and the reflected light on the surfaces of the movable mirrors (see Fig. 1), and k is the wave vector of the cavity field with $k=\omega_c/c$. This transfer produces a radiation pressure force F_{rad} that is exerted on the mirror; the photons emitted on the surface of the movable mirrors are $n_{cav}\cos(\theta/2)$ photons, during round-trip time inside the cavity ($t=2L/c$). This force is equal to the momentum exchanged per photon, multiplied by the number of photons reflected per second:

$$F_{rad}=n_{cav}\hbar\frac{\omega_c}{L}\cos^2(\theta/2). \tag{2}$$

This force induces a displacement on the movable mirrors that makes it possible to have a correlation between the optical mode and the mechanical modes.

B. Hamiltonian

The Hamiltonian of the system is given by [19]

$$\begin{aligned}H=&\hbar\Delta_0 a^\dagger a+\frac{\hbar\omega_{m1}}{2}(q_1^2+p_1^2)+\frac{\hbar\omega_{m2}}{2}(q_2^2+p_2^2)\\&+\hbar g_1 a^\dagger a\cos^2(\theta/2)q_1-\hbar g_2 a^\dagger a\cos^2(\theta/2)q_2\\&+i\hbar E(a^\dagger-a),\end{aligned} \tag{3}$$

where a and $a^\dagger$ are, respectively, the annihilation and creation operators of the optical mode, with $[a,a^\dagger]=1$, and $\Delta_0=\omega_c-\omega_L$ denotes the detuning between the cavity and the laser radiation. The first term in (3) describes the energy of the cavity mode, while the second and third terms describe the energy of the mechanical resonator. We defined q_i and $p_i (i=1,2)$ as being, respectively, the dimensionless position and momentum operators of the oscillator with $[q_j,p_k]=i\delta_{jk}$ $(j,k=1,2)$. The fourth and fifth terms denote the interaction between the cavity field and the movable mirror, which is due to

the radiation pressure, and $g_i (i = 1, 2)$ is the optomechanical coefficient given by $g_i = \frac{\omega_c}{L}\sqrt{\frac{\hbar}{m_i \omega_{m_i}}}$ in units of s^{-1}. The last term describes the laser driving input.

C. Quantum Langevin Equations

The analysis of the dynamics of the two coupled relative mechanical modes and the cavity field are determined by the Heisenberg equations of motion, which are derived from (3), and by adding the fluctuation-dissipation terms, we obtain the following set of Heisenberg–Langevin equations:

$$\begin{aligned}
\dot{q}_1 &= \omega_{m_1} p_1,\\
\dot{q}_2 &= \omega_{m_2} p_2,\\
\dot{p}_1 &= -g_1 a^\dagger a \cos^2(\theta/2) - \omega_{m_1} q_1 - \gamma_{m1} p_1 + f_1,\\
\dot{p}_2 &= g_2 a^\dagger a \cos^2(\theta/2) - \omega_{m_2} q_2 - \gamma_{m2} p_2 + f_2,\\
\dot{a} &= -i[\Delta_0 + g_1 \cos^2(\theta/2) q_1 - g_2 \cos^2(\theta/2) q_2] a\\
&\quad + E - \kappa a + \sqrt{2\kappa} a_{\rm in},\\
\dot{a}^\dagger &= i[\Delta_0 + g_1 \cos^2(\theta/2) q_1 - g_2 \cos^2(\theta/2) q_2] a^\dagger\\
&\quad + E - \kappa a^\dagger + \sqrt{2\kappa} a_{\rm in}^\dagger.
\end{aligned} \tag{4}$$

We have introduced the input vacuum noise $a_{\rm in}$ at temperature T_i with nonzero time domain correlation functions [36]:

$$\langle a_{\rm in}(t) a_{\rm in}^\dagger(t')\rangle = \delta(t - t'). \tag{5}$$

In addition to that, we have the Brownian noise expressed by the operator $f_i (i = 1, 2)$, which describes the coupling of the $i^{\rm th}$ movable mirror to its own environment, with zero mean values and characterized by the following correlation functions [37]:

$$\langle f_i(t) f_j(t')\rangle = \frac{\delta_{jk}}{2\pi}\frac{\gamma_m}{\omega_m}\int \omega e^{-i\omega(t-t')}\left[1 + \coth\left(\frac{\hbar\omega}{2k_B T}\right)\right] {\rm d}\omega. \tag{6}$$

The quality factor obeying $Q_i = \frac{\omega_{m_i}}{\gamma_{m_i}} \gg 1$ means that one can assume that the mechanical baths are Markovian. Hence, the f_i nonzero correlation functions [38] are given by

$$\langle f_i(t) f_i(t') + f_i(t') f_i(t)\rangle/2 \simeq \gamma_m (2n_{{\rm th}_i} + 1)\delta(t - t'), \tag{7}$$

where $n_{{\rm th}_i} = [e^{(\frac{\hbar\omega_{m_i}}{k_B T_i})} - 1]^{-1}$ is the $i^{\rm th}$ thermal phonon number, and k_B is the Boltzmann constant, $i,\ j = 1, 2$.

Without loss of generality, we choose $\omega_{m_1} = \omega_{m_2} = \omega_m$, $\gamma_{m_1} = \gamma_{m_2} = \gamma_m$, $m_1 = m_2 = m$, $g_1 = g_2 = g$, and $T_1 = T_2 = T (n_{{\rm th}_1} = n_{{\rm th}_2} = n_{\rm th})$.

Introducing the relative distance, $q_- = q_1 - q_2$, and the relative momentum, $p_- = p_1 - p_2$, of the movable mirrors, we obtain the reduced equations

$$\begin{aligned}
\dot{q} &= \omega_m p,\\
\dot{p} &= -2g n_{\rm cav} \cos^2(\theta/2) - \omega_m q - \gamma_m p + f_1 - f_2,\\
\dot{a} &= -i[\Delta_0 + g\cos^2(\theta/2) q] a + E - \kappa a + \sqrt{2\kappa} a_{\rm in},\\
\dot{a}^\dagger &= i[\Delta_0 + g\cos^2(\theta/2) q] a^\dagger + E - \kappa a^\dagger + \sqrt{2\kappa} a_{\rm in},
\end{aligned} \tag{8}$$

where $n_{\rm cav}$ is the average number of the photons inside the cavity.

D. Linearization of the Quantum Langevin Equations

To study the quantum correlations that are present in the system, we have to analyze the dynamics of the coupled system. These can be obtained by linearizing the quantum Langevin Eq. (8). This is achieved by expanding each Heisenberg operator as a sum of its c-number classical steady-state value plus an additional small fluctuation operator with zero-mean value [36]:

$$a = \alpha_s + \delta a, \quad q = q_s + \delta q, \quad p = p_s + \delta p. \tag{9}$$

The steady-state values are given by the following nonlinear algebraic equations:

$$\begin{aligned}
p_s &= 0,\\
(i\Delta + \kappa)\alpha_s - E &= 0,\\
q_s + \frac{2g\cos^2(\theta/2)|\alpha_s|^2}{\omega_m} &= 0,
\end{aligned} \tag{10}$$

where $\Delta = \Delta_0 + g q_s \cos^2(\theta/2)$ is the effective cavity detuning.

Inserting Eq. (9) into Eq. (8), and introducing the cavity field quadratures $\delta x = \frac{\delta a + \delta a^\dagger}{\sqrt{2}}$ and $\delta y = \frac{i(\delta a^\dagger - \delta a)}{\sqrt{2}}$, and the input noise quadratures $\delta x_{\rm in} = \frac{a_{\rm in} + a_{\rm in}^\dagger}{\sqrt{2}}$ and $\delta y_{\rm in} = \frac{i(a_{\rm in}^\dagger - a_{\rm in})}{\sqrt{2}}$, allows to obtain the linearized quantum Langevin equations

$$\begin{aligned}
\delta\dot{q} &= \omega_m \delta p,\\
\delta\dot{p} &= -\omega_m \delta q - \gamma_m \delta p - \sqrt{2} g\cos^2(\theta/2)(\alpha_s^* + \alpha_s)\delta x\\
&\quad + i\sqrt{2} g\cos^2(\theta/2)(\alpha_s - \alpha_s^*)\delta y + f_1 - f_2,\\
\delta\dot{x} &= -i\frac{g}{\sqrt{2}}\cos^2(\theta/2)(\alpha_s - \alpha_s^*)\delta q - \kappa\delta x + \Delta\delta y + \sqrt{2\kappa}\delta x_{\rm in},\\
\delta\dot{y} &= -\frac{g}{\sqrt{2}}\cos^2(\theta/2)(\alpha_s^* + \alpha_s)\delta q - \Delta\delta x - \kappa\delta y + \sqrt{2\kappa}\delta y_{\rm in}.
\end{aligned} \tag{11}$$

This system of equations can be rewritten in the matrix form

$$\dot{u}(t) = A u(t) + \eta(t), \tag{12}$$

where $u^T(\infty) = (\delta q(\infty), \delta p(\infty), \delta x(\infty), \delta y(\infty))$ is the column vector of the fluctuations, $\eta^T(t) = (0, f_1 - f_2, \sqrt{2\kappa}\delta x_{\rm in}, \sqrt{2\kappa}\delta y_{\rm in})$ is the column vector of noise operators, and the drift matrix A reads

$$A=\begin{pmatrix} 0 & \omega_m & 0 & 0 \\ -\omega_m & -\gamma_m & -\sqrt{2}g\cos^2(\theta/2)(\alpha_s+\alpha_s^*) & i\sqrt{2}g\cos^2(\theta/2)(\alpha_s-\alpha_s^*) \\ -i\frac{g}{\sqrt{2}}\cos^2(\theta/2)(\alpha_s-\alpha_s^*) & 0 & -\kappa & \Delta \\ -\frac{g}{\sqrt{2}}\cos^2(\theta/2)(\alpha_s+\alpha_s^*) & 0 & -\Delta & -\kappa \end{pmatrix}. \quad (13)$$

The solution to Eq. (12) is $u(t)=Y(t)u(0)+\int_0^t dx\,Y(x)\eta(t-x)$, where $Y(t)=\exp At$.

E. Covariance Matrix

When the stability conditions are verified according to the Routh–Hurwitz criteria [6,39,40], the steady-state covariance matrix satisfies the Lyapunov equation

$$AV+VA^T=-D, \quad (14)$$

where D is a diagonal matrix that represents the noise correlations; it is given by $D=\mathrm{Diag}[0,\,2\gamma_m(2n_{\mathrm{th}}+1),\,\kappa,\,\kappa]$.

In the following, we express the covariance matrix V in a 2×2 block form:

$$V=\begin{pmatrix} V_m & V_c \\ V_c^T & V_a \end{pmatrix}, \quad (15)$$

where V_a, V_m, and V_c are, respectively, the covariance matrix of the optical cavity mode, the relative mechanical mode, and the non-local correlations between them.

For later use, we define the following set of four symplectic invariants derived from the covariance matrix V:

$$I_1=\mathrm{Det}\,V_m,\quad I_2=\mathrm{Det}\,V_a,$$
$$I_3=\mathrm{Det}\,V_c,\quad I_4=\mathrm{Det}\,V. \quad (16)$$

For the bipartite system, the symplectic eigenvalues of the partial transpose of the covariance matrix V [41,42] are given by

$$\tilde{\nu}_{\pm}=\sqrt{\frac{\tilde{\Gamma}\pm\sqrt{\tilde{\Gamma}^2-4I_4}}{2}}, \quad (17)$$

where the symbol $\tilde{\Gamma}$ is the symplectic invariant given by $\tilde{\Gamma}=I_1+I_2-2I_3$.

Knowledge of the covariance matrix in the stationary state from Eq. (14) and use of the quantities Eq. (17) allow to evaluate the quantum correlations between the optical mode and the relative mechanical mode. This is studied in the next section.

3. ENTANGLEMENT ANALYSIS

In this part, we want to quantify the bipartite stationary entanglement between the mechanical mode and the optical mode, for that we use the logarithmic negativity E_N. This quantity is defined for Gaussian CV systems as [43,44]

$$E_N=\max[0,\,-\mathrm{Ln}2\tilde{\nu}_-]. \quad (18)$$

The two modes are entangled when $E_N>0$, which is equivalent to $\tilde{\nu}_-<\frac{1}{2}$. If not, the states are separable, which is consistent with Simon's necessary and sufficient criterion for bipartite entanglement [45].

In order to study the behavior of the quantum correlations, as captured by logarithmic negativity, some parameters are taken from the most relevant experiments [46], where the length of the cavity $L=35$ mm, the laser wavelength is $\lambda=1064$ nm, $\omega_m=2\pi\times 947\times 10^3\,H_z$, $\theta=\frac{\pi}{3}$, the mechanical quality factor $Q=\frac{\omega_m}{\gamma_m}=6700$, and $\kappa=2\pi\times 215\times 10^3\,H_z$. All the parameters chosen have been verified to satisfy the stability conditions.

Figure 2 shows the logarithmic Negativity E_N versus the thermal bath's temperature T for different values of m. The amount of entanglement monotonically decreases with temperature; we notice that, as expected, the quantum correlations do not resist the environment effects as E_N decreases with temperature. This is due to the environment-induced decoherence, since the two mechanical modes are subject to the thermal fluctuations from their bath. We see also from the figure that for $m=20$ ng, it survives until $T>0.8$ mK, while for $m=50$ ng, it vanishes at $T=0.4$ mK. On the other hand, for a fixed temperature, logarithmic negativity decreases with mass, e.g., when $T=0.2$ mK, $E_N=0.10$ (respectively 0.026) for $m=20$ ng (respectively 50 ng), which shows the importance of the parameter mass as well. As a matter of fact, the smaller it is, the more robust the system becomes against the thermal bath's temperature. This in turn is due to the fact that the optomechanical coupling, due to the radiation pressure, gets stronger as the displacement of the mirrors increases.

Next, to examine the dependence of entanglement on some other parameters in an optomechanical system, we show in Fig. 3 its behavior as a function of the laser driving power P as well. We notice, for instance, that for a fixed temperature, the driving laser power has a favorable effect on the quantum correlations as captured by the logarithmic negativity. For example, at $T=0.2$ (mK), we obtain $E_N=0.004$ for $P=3.8$ mW, $E_N=0.009$ for $P=6.9$ mW, and $E_N=0.018$ for $P=12$ mW. The injection of the laser increases the photon number inside the cavity. It seems that a great number of

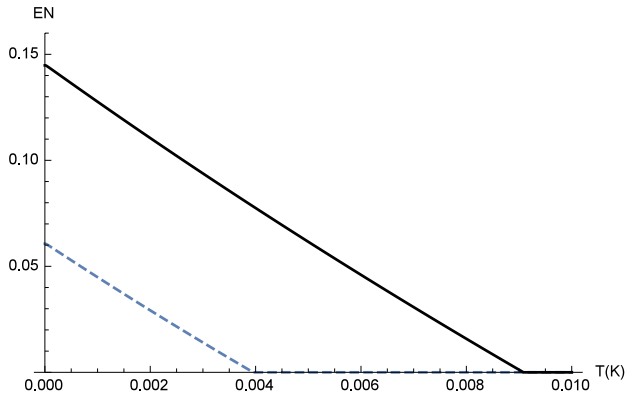

Fig. 2. Plot of the logarithmic negativity E_N versus the thermal bath temperature $T(K)$ for two values of the mass. $m=20$ ng for the black full line, and $m=50$ ng for the blue dashed line. The other parameters are chosen as follows: $\Delta=0.965\omega_m$, $P=11$ mW.

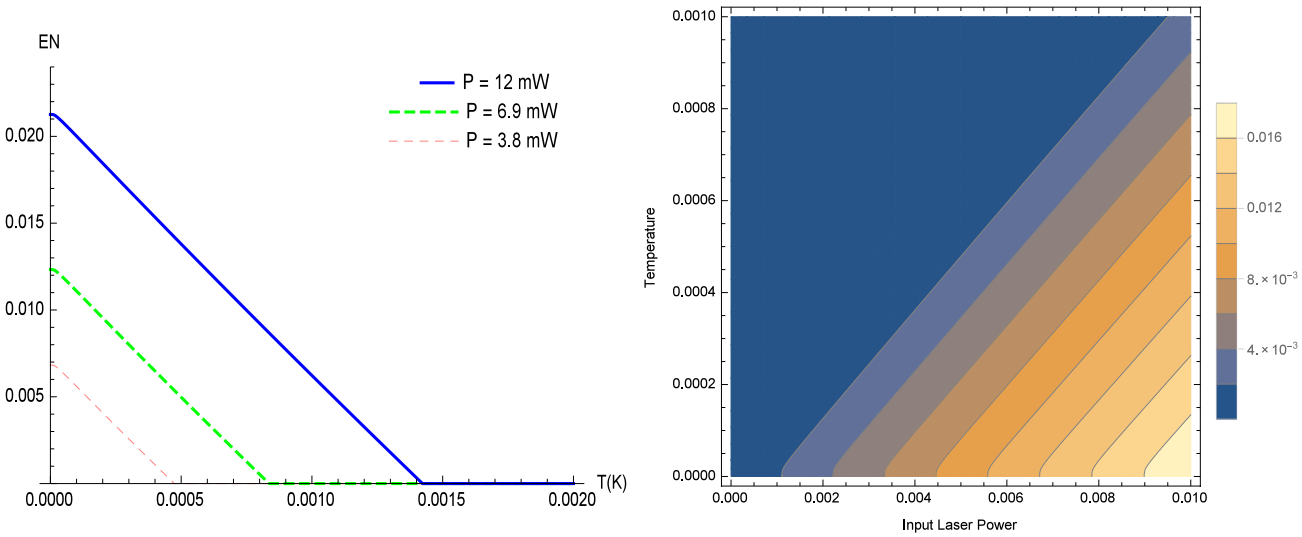

Fig. 3. (a) E_N versus T for different values of the input laser power P. (b) Contour plot of E_N versus temperature T and power P. In both plots, we use $m = 145$ ng, $\Delta = \omega_m$.

these acting on the movable mirrors leads to photon–phonon interaction, which does enhance the optomechanical coupling due to the radiation pressure that consequently allows for robust entanglement. We also see from the contour plot that the temperature at which the entanglement vanishes increases with the power, e.g., for $P = 3.8$ mW, E_N vanishes at $T \sim 0.5$ mK; however, for $P = 12$ mW, E_N persists up to 1 mK. It is worthwhile noting that there is a minimum power from which the two modes can be entangled; this what we can see in the contour plot $E_N \neq 0$ from $p \geq 1$ mW for a very small value of T. Notice that a significant entanglement could be achieved at a considerably lower driving power and also without using a squeezed vacuum light source, as the case in Ref. [19]. It is worthwhile noting that with the increase in thermal phonon number, entanglement gradually decreases, but it can persist up to a much higher number as it is quantified by some parameters such as the laser pumping power and the mass of the movable mirrors. Adjusting and optimizing a bipartite entanglement in a thermal environment might contribute to various applications in quantum information processing and communication.

4. GAUSSIAN QUANTUM DISCORD AND QUANTUM MUTUAL INFORMATION

Based solely on the entanglement, we can conclude that the states of the two modes are entangled if $E_N > 0$; otherwise, the states are separable or classically correlated. Nevertheless, it was proved [47–49] that even separable states may contain quantum correlations; thus, the notion of quantum discord was introduced as capturing the overall quantum correlations, even those beyond entanglement. In this section, we use Gaussian quantum discord [34,50], which is considered as a genuine measure of nonclassical correlations between the optical mode(a) and the relative mechanical mode(m), which can be different from zero even for separable states, i.e., $E_N = 0$. By definition, Gaussian quantum discord is the difference between quantum mutual information and classical correlations. Indeed, quantum mutual information quantifies the information that subsystems ρ_A and ρ_B share; it evaluates how much we know about one single part by observing the other. This is related to the correlations between the two modes that can be measures by quantum mutual information or conditional entropies [51].

Quantum mutual information is defined as

$$I_M(\rho_{AB}) = S_V(\rho_A) + S_V(\rho_B) - S_V(\rho_{AB}), \tag{19}$$

where $S_V(\rho_{AB})$, $S_V(\rho_A)$, and $S_V(\rho_B)$ are the von Neumann entropies of the two mode Gaussian state ρ_{AB} and that of subsystems ρ_A and ρ_B, respectively. These can be expressed in terms of symplectic invariants [Eq. (16)] as $S_V(\rho_A) = g(\sqrt{I_1})$, $S_V(\rho_B) = g(\sqrt{I_2})$, and $S_V(\rho_{AB}) = g(\nu_+) + g(\nu_-)$ [50], where g is a function defined by

$$g(x) = \left(x + \frac{1}{2}\right) \mathrm{Ln}\left(x + \frac{1}{2}\right) - \left(x - \frac{1}{2}\right) \mathrm{Ln}\left(x - \frac{1}{2}\right), \tag{20}$$

and $\nu_\pm$ are the symplectic eigenvalues of V:

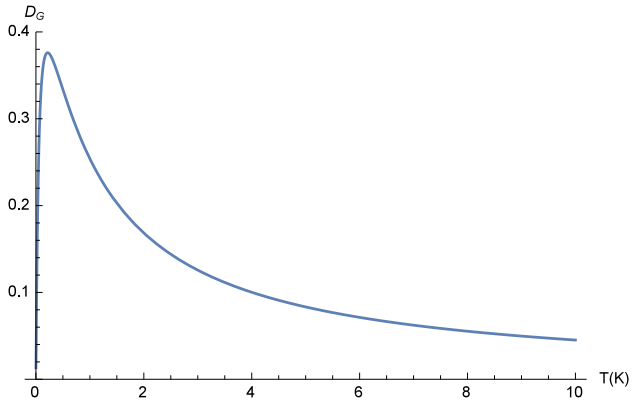

Fig. 4. Plot of the Gaussian quantum discord versus the temperature $T(K)$. We chose $m = 145$ ng, $P = 3.8$ mW, $\Delta = \omega_m$.

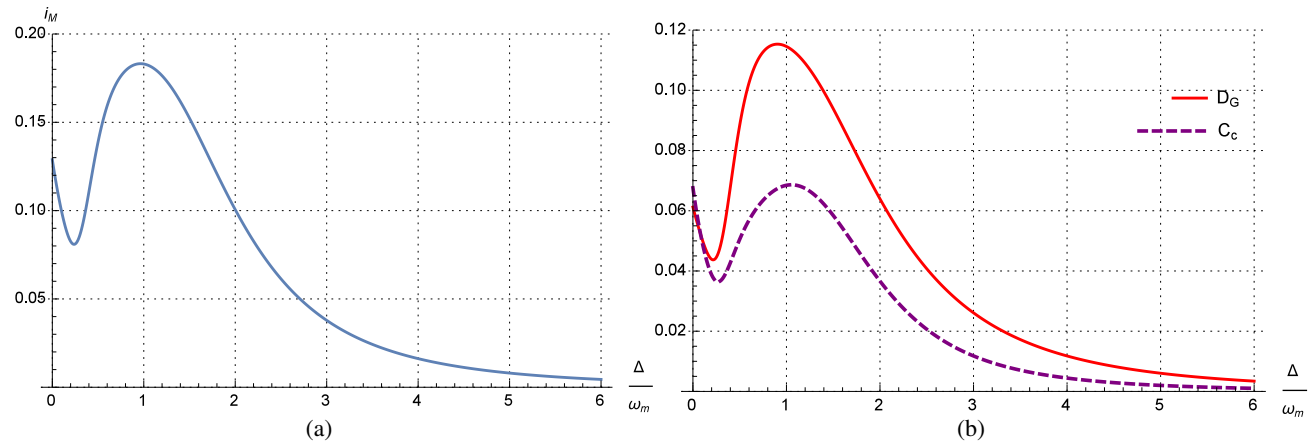

Fig. 5. (a) Mutual information. (b) Gaussian quantum discord and classical correlation. In both plots, the temperature of the environment is taken as $T = 6$ mK, with the other parameters similar to those in Fig. 4.

$$\nu_{\pm} = \frac{1}{2}\sqrt{\Gamma^{\pm}\sqrt{\Gamma^2 - 4I_4}}, \tag{21}$$

with $\Gamma = I_1 + I_2 + 2I_3$.

The quantum mutual information shared by the relative mechanical mode and the optical mode is then expressed as

$$I_M(ma) = g(\sqrt{I_1}) + g(\sqrt{I_2}) - g(\nu_+) - g(\nu_-). \tag{22}$$

The total amount of correlation is captured by the quantum mutual information, which can be divided into a classical part and a quantum part, known as Gaussian quantum discord, which can be evaluated by the following difference:

$$D_G(m|a) = I_M(ma) - C(m|a), \tag{23}$$

where $C(m|a)$ refers to the one-way classical correlation between the relative mechanical mode and the optical cavity mode.

By performing Gaussian measurement, the Gaussian quantum discord for Gaussian bipartite systems can be expressed as [34,51]

$$D_G(m|o) = g(\sqrt{I_2}) - g(\nu_+) - g(\nu_-) + g(\sqrt{W}), \tag{24}$$

$$W = \begin{cases} \frac{2|I_3| + \sqrt{4I_3^2 + (4I_2 - 1)(4I_4 - I_1)}^2}{(4I_2 - 1)} & \text{if } \frac{4(I_1 I_2 - I_4)^2}{(I_1 + 4I_4)(1 + 4I_2)I_3^2} \leq 1 \\ \frac{I_1 I_2 + I_4 - I_3^2 - \sqrt{(I_1 I_2 + I_4 - I_3^2)^2 - 4I_1 I_2 I_4}}{2I_2} & \text{otherwise.} \end{cases} \tag{25}$$

Figure 4 shows Gaussian quantum discord versus temperature, confirming that, generally, the discord decreases as T increases. Nevertheless, one can see from the figure that the discord increases initially for smaller values of temperature, which is characterized by a small number of thermal phonon fluctuations. In fact, a few of these are actually needed and do enhance the photon–phonon interaction via radiation pressure force and allows to have a strong optomechanical coupling that consequently allows for robust quantum correlations. But further increase in temperature is accompanied by an increase in the number these thermal phonons, which has the reverse effect and does not benefit the quantum correlations, as the phenomenon of decoherence enters into play and is responsible for the latter decrease in quantum discord. Furthermore, we note that while E_N vanishes at $T \sim 0.5$ mK (see Fig. 3) and since we have chosen the same parameters, Gaussian quantum discord survives beyond this temperature. Notice also that this latter remains nonzero for large values of T and does not undergo a sudden suppression or the so-called phenomenon of sudden death, as is the case for entanglement. This explains the existence of quantum correlations in the system even for separable states, i.e., $E_N = 0$, and also shows the robustness of Gaussian quantum discord against the influence of the environment.

While quantum correlations are captured by Gaussian quantum discord, the total correlations can be evaluated by using the expression of quantum mutual information [50].

Figures 5 shows, respectively, the behavior of the mutual information I_M and that of the quantum Gaussian discord D_G and the classical correlation C_c versus Δ/ω_m. The three quantities behave similarly and reach their maximum in the vicinity of $\Delta \sim \omega_m$, then they decrease with increasing Δ/ω_m. In fact, when $\Delta = \omega_m$, the cavity drive frequency is detuned to the red of the cavity resonance by an amount of ω_m; if we assume that $G << \omega_m$, where G is the many-photon optomechanical coupling, which is stronger than the single photon optomechanical coupling g by a factor of $|\alpha_s|$, we can make a rotating wave approximation and keep only energy conserving terms. In this case, the dynamics of the Hamiltonian creates phonons and photons in pairs, and leads to photon–phonon correlation, thus allowing to generate correlations between the light field and the mechanics. Furthermore, for fixed values of Δ/ω_m, we have I_M always greater than D_G and C_c, which is logical since I_M measures both the classical and quantum correlations present in the system.

5. CONCLUSION

In this work, we have studied the quantum correlations in a steady state of an optomechanical system. In our case, this latter is a ring cavity, with a fixed mirror and two movable ones, pumped by a laser source. In addition, the system under study

is experimentally feasible. The linearized quantum Langevin equations were used in order to obtain the bipartite covariance matrix at the stationary state fully describing the Gaussian state of the two subsystems, the optical mode and the relative mechanical mode.

In addition to that, we have studied the effect of the thermal bath temperature on quantum entanglement, which is measured by logarithmic negativity. It was found that the entanglement decreases with increasing temperature and mass of the two mechanical harmonic oscillators.

Then, the total amount of correlations present in the system under consideration were quantified by quantum mutual information, a measure englobing both classical correlations and quantum discord. It was found that quantum mutual information, quantum discord, and classical correlations decrease with increasing Δ/ω_m, and they reach their maximum when Δ is around ω_m. As expected, when the entanglement vanishes (which is characteristic of a separable state), the system still has a nonzero value of Gaussian quantum discord. This shows that Gaussian quantum discord is a measure of all quantum correlations, including entanglement, and confirms the robustness of this measure and the feebleness of logarithmic negativity against the fluctuations of the bath environment.

Disclosures. The authors declare no conflicts of interest.

REFERENCES

1. E. Schrödinger, "Discussion of probability relations between separated systems," Proc. Cambridge Philos. Soc. **31**, 555–563 (1935).
2. R. Horodecki, P. Horodecki, M. Horodecki, and K. Horodecki, "Quantum entanglement," Rev. Mod. Phys. **81**, 865–942 (2009).
3. A. Streltsov, U. Singh, H. S. Dhar, M. N. Bera, and G. Adesso, "Measuring quantum coherence with entanglement," Phys. Rev. Lett. **115**, 020403 (2015).
4. S. L. Braunstein and P. van Loock, "Quantum information with continuous variables," Rev. Mod. Phys. **77**, 513–577 (2005).
5. G. Giedke, M. M. Wolf, O. Krüger, R. F. Werner, and J. I. Cirac, "Entanglement of formation for symmetric Gaussian states," Phys. Rev. Lett. **91**, 107901 (2003).
6. D. Vitali, S. Gigan, A. Ferreira, H. R. Böhm, P. Tombesi, A. Guerreiro, V. Vedral, A. Zeilinger, and M. Aspelmeyer, "Optomechanical entanglement between a movable mirror and a cavity field," Phys. Rev. Lett. **98**, 030405 (2007).
7. D. Bouwmeester, A. Ekert, and A. Zeilinger, *The Physics of Quantum Information* (Springer, 2000).
8. H. Häffner, W. Hänsel, C. F. Roos, J. Benhelm, D. Chek-al-kar, M. Chwalla, T. Körber, U. D. Rapol, M. Riebe, P. O. Schmidt, C. Becher, O. Gühne, W. Dür, and R. Blatt, "Scalable multiparticle entanglement of trapped ions," Nature **438**, 643–646 (2005).
9. D. Estève, J.-M. Raimond, and J. Dalibard, eds., *Quantum Entanglement and Information Processing* (Elsevier, 2003).
10. V. Vedral, "High-temperature macroscopic entanglement," New J. Phys. **6**, 102 (2004).
11. B. Deb and G. S. Agarwal, "Entanglement of two distant Bose-Einstein condensates by detection of Bragg-scattered photons," Phys. Rev. A **78**, 013639 (2008).
12. A. Sørensen, L.-M. Duan, J. I. Cirac, and P. Zoller, "Many-particle entanglement with Bose-Einstein condensates," Nature **409**, 63–66 (2001).
13. S. Bose, K. Jacobs, and P. L. Knight, "Scheme to probe the decoherence of a macroscopic object," Phys. Rev. A **59**, 3204–3210 (1999).
14. J. Zhang, K. Peng, and S. L. Braunstein, "Quantum-state transfer from light to macroscopic oscillators," Phys. Rev. A **68**, 013808 (2003).
15. S. Mancini, V. Giovannetti, D. Vitali, and P. Tombesi, "Entangling macroscopic oscillators exploiting radiation pressure," Phys. Rev. Lett. **88**, 120401 (2002).
16. D. Vitali, S. Mancini, L. Ribichini, and P. Tombesi, "Macroscopic mechanical oscillators at the quantum limit through optomechanical cooling," J. Opt. Soc. Am. B **20**, 1054–1065 (2003).
17. S. Chakraborty and A. K. Sarma, "Entanglement dynamics of two coupled mechanical oscillators in modulated optomechanics," Phys. Rev. A **97**, 022336 (2018).
18. S. Chakraborty and A. K. Sarma, "Qubit assisted enhancement of quantum correlations in an optomechanical system," Ann. Phys. **392**, 39–48 (2018).
19. S. Huang and G. S. Agarwal, "Entangling nanomechanical oscillators in a ring cavity by feeding squeezed light," New J. Phys. **11**, 103044 (2009).
20. R.-J. Xiao, G.-X. Pan, and L. Zhou, "Multiple optomechanically induced transparency in a ring cavity optomechanical system assisted by atomic media," Int. J. Theor. Phys. **54**, 3665–3675 (2015).
21. Y. Han, J. Cheng, and L. Zhou, "Electromagnetically induced transparency in a cavity optomechanical system with an atomic medium," J. Phys. B **44**, 165505 (2011).
22. T. Qi, Y. Han, and L. Zhou, "Electromagnetically induced transparency in cavity optomechanical system with Λ-type atomic medium," J. Mod. Opt. **60**, 431–436 (2013).
23. J. D. Teufel, D. Li, M. S. Allman, K. Cicak, A. J. Sirois, J. D. Whittaker, and R. W. Simmonds, "Circuit cavity electromechanics in the strong-coupling regime," Nature **471**, 204–208 (2011).
24. S. Weis, R. Rivière, S. Deléglise, E. Gavartin, O. Arcizet, A. Schliesser, and T. J. Kippenberg, "Optomechanically induced transparency," Science **330**, 1520–1523 (2010).
25. M. Aspelmeyer, T. J. Kippenberg, and F. Marquardt, "Cavity optomechanics," Rev. Mod. Phys. **86**, 1391–1452 (2014).
26. P. Meystre, "A short walk through quantum optomechanics," Ann. Phys. (Berlin) **525**, 215–233 (2013).
27. C. M. Caves, "Quantum-mechanical radiation-pressure fluctuations in an interferometer," Phys. Rev. Lett. **45**, 75–79 (1980).
28. T. Corbitt, D. Ottaway, E. Innerhofer, J. Pelc, and N. Mavalvala, "Measurement of radiation-pressure-induced optomechanical dynamics in a suspended Fabry-Perot cavity," Phys. Rev. A **74**, 021802 (2006).
29. R. Ghobadi, A. R. Bahrampour, and C. Simon, "Quantum optomechanics in the bistable regime," Phys. Rev. A **84**, 033846 (2011).
30. L. Henderson and V. Vedral, "Classical, quantum and total correlations," J. Phys. A **34**, 6899–6905 (2001).
31. A. Farace, F. Ciccarello, R. Fazio, and V. Giovannetti, "Steady-state entanglement activation in optomechanical cavities," Phys. Rev. A **89**, 022335 (2014).
32. W. H. Zurek, "Einselection and decoherence from an information theory perspective," Ann. Phys. (Leipzig) **9**, 855–864 (2000).
33. H. Ollivier and W. H. Zurek, "Quantum discord: a measure of the quantumness of correlations," Phys. Rev. Lett. **88**, 017901 (2001).
34. G. Adesso and A. Datta, "Quantum versus classical correlations in Gaussian states"," Phys. Rev. Lett. **105**, 030501 (2010).
35. P. Giorda and M. G. A. Paris, "Gaussian quantum discord," Phys. Rev. Lett. **105**, 020503 (2010).
36. D. F. Walls and G. J. Milburn, *Quantum Optics* (Springer, 1994).
37. V. Giovannetti and D. Vitali, "Phase-noise measurement in a cavity with a movable mirror undergoing quantum Brownian motion," Phys. Rev. A **63**, 023812 (2001).
38. R. Benguria and M. Kac, "Quantum Langevin equation," Phys. Rev. Lett. **46**, 1–4 (1981).
39. E. X. DeJesus and C. Kaufman, "Routh-Hurwitz criterion in the examination of eigenvalues of a system of nonlinear ordinary differential equations," Phys. Rev. A **35**, 5288–5290 (1987).
40. A. Mari and J. Eisert, "Gently modulating optomechanical systems," Phys. Rev. Lett. **103**, 213603 (2009).
41. S. Olivares, M. G. A. Paris, and A. R. Rossi, "Optimized teleportation in Gaussian noisy channels," Phys. Lett. A **319**, 32–43 (2003).
42. A. V. Dodonov, V. V. Dodonov, and S. S. Mizrahi, "Separability dynamics of two-mode Gaussian states in parametric conversion and amplification," J. Phys. A **38**, 683–696 (2005).

43. G. Vidal and R. F. Werner, "Computable measure of entanglement," Phys. Rev. A **65**, 032314 (2002).
44. G. Adesso, A. Serafini, and F. Illuminati, "Extremal entanglement and mixedness in continuous variable systems," Phys. Rev. A **70**, 022318 (2004).
45. R. Simon, "Peres-Horodecki separability criterion for continuous variable systems," Phys. Rev. Lett. **84**, 2726–2729 (2000).
46. S. Gröblacher, K. Hammerer, M. R. Vanner, and M. Aspelmeyer, "Observation of strong coupling between a micromechanical resonator and an optical cavity field," Nature **460**, 724–727 (2009).
47. B. P. Lanyon, M. Barbieri, M. P. Almeida, and A. G. White, "Experimental quantum computing without entanglement," Phys. Rev. Lett. **101**, 200501 (2008).
48. S. L. Braunstein, C. M. Caves, R. Jozsa, N. Linden, S. Popescu, and R. Schack, "Separability of very noisy mixed states and implications for NMR quantum computing," Phys. Rev. Lett. **83**, 1054–1057 (1999).
49. A. Datta and G. Vidal, "Role of entanglement and correlations in mixed-state quantum computation," Phys. Rev. A **75**, 042310 (2007).
50. S. Olivares, "Quantum optics in the phase space," Eur. Phys. J. Spec. Top. **203**, 3–24 (2012).
51. D. Slepian and J. K. Wolf, "Noiseless coding of correlated information sources," IEEE Trans. Inf. Theory **19**, 471–480 (1973).

Chapter 4

Detection of genuine tripartite entanglement of an atoms-optomechanical cavity

This part of thesis is devoted to the study of genuine tripartite entanglement. In the previous chapter, we present the behavior of the quantum correlations in ring optomechanical cavity. Which is the main idea of the thesis. In this part, we study an ongoing investigation, where the system under consideration corresponds to an hybrid optomechanical system formed of a ring cavity where an atomic ensemble is placed inside. These systems, can be coherently manipulated by pumping the cavity with an external laser field with the goal of controlling the interaction between electromagnetic radiation and motion. The central thought of this chapter is to explore the impact of the atomic ensemble on the entanglement. Since, we can generate a strongly quantum entanglement between the atomic ensemble and a vibrating mirror by increasing the coupling strength. Another point of interest in this part is to investigate the genuine tripartite entanglement being possibly shared by the four subsystems (cavity field – atomic ensemble and two vibrating mirrors). This chapter is organized as follow, at first glance, we illustrates the realization of the theoretical atom-optomechanical system, then we analysis the dynamics that allow to obtain the multimode covariance matrix. Hence, we simulate the bipartite entanglement between any pair of the multipartite system using the logarithmic negativity. In final analysis, we generate the genuine tripartite entanglement which is the broad plan of this chapter.

4.1 Model and Hamiltonian

4.1.1 Model

As depicted in Fig. 4.1, the system studied here is an Atom-Optomechanical system, made of a ring cavity with length L, and an atomic ensemble of two-level atoms placed inside the cavity. This latter is driven by a squeezed light source with frequency ω_s and a coherent laser source with strength E_L. The optical cavity is composed of two movable mirrors perfectly transmitting and a fixed one partially transmitting in a triangular design.

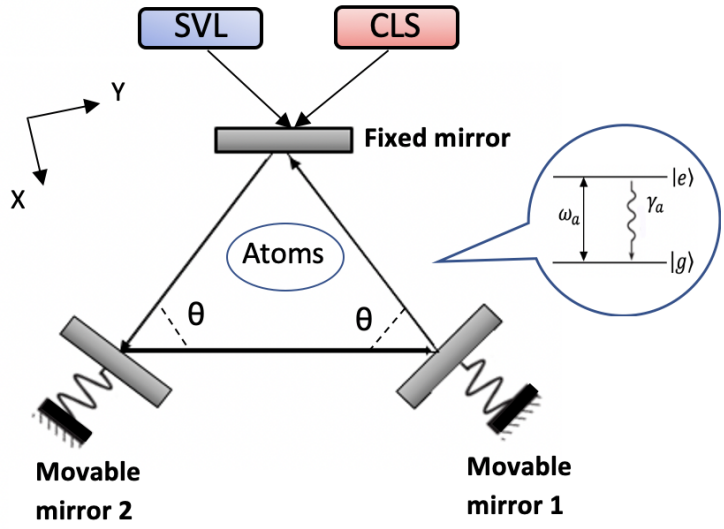

Figure 4.1: Schematic illustration of the Atom-optomechanical system.

It is worth mentioning that systems based on atom-optomechanical models are experimentally feasible [102–104]. In this background, i attempt to summarize in this chapter research on the optomechanics of atoms within optical cavities, we adopt a ring configuration to facilitate the generation of entanglement, that can be strengthened by the displacement of the mirror and an increase of the photon number.

4.1.2 Basics of light-atom interaction

The proposed system, is an Atom-Optomechanical system. For more clarification, we begin by a brief description of the interaction of a single atom on one mode cavity. In figure 4.2, we present a theoretical model to describe the exchanging atomic processes. Indeed, the atom-light interaction in a cavity comes in form of the Jaynes-Cummings model. This model, was originally developed in 1963 by Edwin Jaynes and Fred Cummings to describe the system of a two-level

atom interacting with an electromagnetic field in order to investigate the process of absorption of photons and spontaneous emission in a cavity.

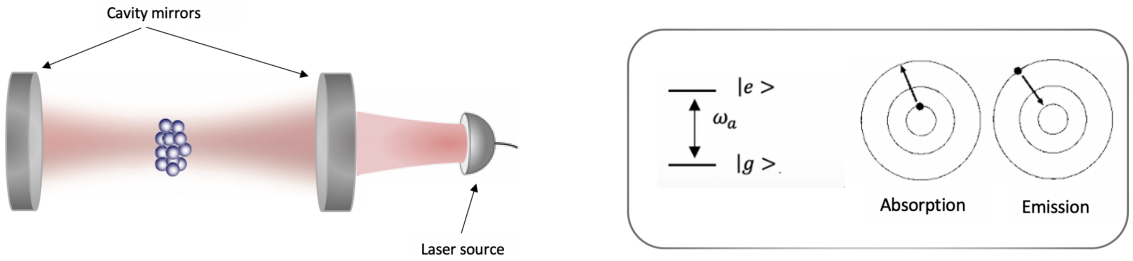

Figure 4.2: Single atom interacting mechanically with a coherently electromagnetic cavity field.

The Jaynes–Cummings model is of great interest to quantum optics, recall in this part to introduce the basic equations which lead us to the strongly coupled single-mode cavity field. The Hamiltonian of the model is given by

$$H_{JC} = H_{atom} + H_{field} + H_{int}, \tag{4.1}$$

H_{atom} is the two level atom Hamiltonian with ground state $|g\rangle$ and excited state $|e\rangle$, defined as.

$$H_{atom} = \hbar\omega_a S_z, \tag{4.2}$$

the frequency ω_a is the transition between the ground state $|g\rangle$ and the excited state $|e\rangle$, having respectively the following energies $E_g = -\frac{\hbar\omega_a}{2}$ and $E_e = \frac{\hbar\omega_a}{2}$. S_z and $S_\pm$ are the spin operators $S_{z,\pm} = \sum_{i=1}^{N_a} \sigma^i_{z,\pm}$, with N_a is the two-level atoms, $\sigma^i_{z,\pm}$ are the Pauli matrices defined by $\sigma^i_z = |e\rangle^{(i)(i)} \langle e|$, $\sigma^i_+ = |e\rangle^{(i)(i)} \langle g|$ and $\sigma^i_- = |g\rangle^{(i)(i)} \langle e|$ and satisfying the commutation relations $[\sigma^i_+, \sigma^i_-] = \sigma^i_z$ and $[\sigma^i_z, \sigma^i_\pm] = \pm 2\sigma^i_\pm$. H_{field} is the Hamiltonian of the optical cavity mode already introduced in the previous sections given by

$$H_{field} = \hbar\omega_c \hat{a}^\dagger \hat{a}, \tag{4.3}$$

and H_{int} is the Jaynes–Cummings interaction Hamiltonian

$$H_{int} = \hbar g_c (S_+ \hat{a} + S_- \hat{a}^\dagger) \tag{4.4}$$

g_c design the atom-cavity coupling constant defined as $g_c = \mu\sqrt{\frac{\omega_c}{2\hbar\epsilon_0 V}}$ with μ being the dipole moment of the atomic transition, V is the volume of the cavity.

Now we can go back to our system modeled in figure 4.1 to describe the full Hamiltonian in the next part.

4.1.3 Hamiltonian

The total Hamiltonian of the optomechanical system under study can be expressed as

$$H = H_0 + H_{interaction} + H_{Drive} \tag{4.5}$$

with

$$\begin{aligned} H_0 &= \hbar\omega_c \hat{a}^\dagger \hat{a} + \frac{\hbar\omega_{m1}}{2}(q_1^2 + p_1^2) + \frac{\hbar\omega_{m2}}{2}(q_2^2 + p_2^2) + \frac{\hbar\omega_a}{2} S_z, & (4.6)\\ H_{Interaction} &= \hbar g_c (S_+ \hat{a} + S_- \hat{a}^\dagger) + \hbar\, g\, \hat{a}^\dagger \hat{a} \cos^2(\theta/2)(q_1 - q_2), & (4.7)\\ H_{Drive} &= i\hbar E_L (\hat{a}^\dagger e^{-i\omega_L t} - \hat{a} e^{i\omega_L t}). & (4.8) \end{aligned}$$

H_0 represents the free Hamiltonian, the first term of which describes the cavity mode. The second and third term represent the Hamiltonian of the two mechanical resonators, that are considered as quantum harmonic oscillators fully described in the previous case. The last one, describe the Hamiltonian of the atomic ensemble.

The first term of $H_{Interaction}$ represents the coupling Hamiltonian, where the atoms interact with the two mechanical oscillators via the coupling with the intracavity field expressed as g_c, the second term takes into account the interaction of the two mechanical resonators motion with the electromagnetic field confined in the cavity due to the radiation pressure force.

The part H_{Drive} represents the drive laser input, remain unchanged with the previous descriptions in the previous section.

Working in the rotating frame at the input laser frequency ω_L, the Hamiltonian of the system simplifies to

$$\begin{aligned} H =& \hbar\Delta_0 a^\dagger a + \frac{\hbar\omega_{m1}}{2}(q_1^2 + p_1^2) + \frac{\hbar\omega_{m2}}{2}(q_2^2 + p_2^2) + \hbar\Delta_a c^\dagger c + \hbar G_a (c^\dagger a + c a^\dagger) \\ &+ \hbar g a^\dagger a \cos^2(\theta/2)(q_1 - q_2) + i\hbar E_L (a^\dagger - a), \end{aligned} \tag{4.9}$$

with $\Delta_0 = \omega_c - \omega_L$ and $\Delta_a = \omega_a - \omega_L$ are respectively the cavity mode and atomic detuning. For simplification, we choose the low atomic excitation limit, *i.e.,* when the atoms are initially in the ground state and the average number of photons is much smaller in the excited state, so that $S_Z \approx< S_Z >\approx -N_a$. In addition to that, we suppose the excitation probability of a

single atom to be small. In this limit, the atomic polarization can be defined in terms of the bosonic annihilation and creation operators $c = \frac{S_-}{\sqrt{|<S_Z>|}}$, which satisfy the bosonic commutation relations $[c, c^\dagger] = 1$ [105]. We define $G_a = g_c\sqrt{N_a}$, the atom-cavity coupling strength.

4.2 System dynamics

For a clear analysis of the dynamics of the system, we determine the Heisenberg equations of motion which can be obtained from the Hamiltonian 4.9. Taking into consideration the effects of noise and the dissipation terms as detailed in chapter 3 section 2.5.2. Therfore, we get the following Heisenberg-Langevin equations

$$\begin{aligned}
\dot{q_1} &= \omega_m\ p_1, \\
\dot{q_2} &= \omega_m\ p_2, \\
\dot{p_1} &= -\omega_m q_1 - g a^\dagger a \cos^2(\theta/2) - \gamma_m\ p_1 + \xi, \\
\dot{p_2} &= -\omega_m q_2 + g a^\dagger a \cos^2(\theta/2) - \gamma_m\ p_2 + \xi, \\
\dot{a} &= -(\kappa + i\Delta_0)a - iG_a c - ig\cos^2(\theta/2)(q_1 - q_2)a + E_L + \sqrt{2\kappa}a_{in}, \\
\dot{c} &= -(\gamma_a + i\Delta_a)c - iG_a a + \sqrt{2\gamma_a}c_{in}.
\end{aligned} \tag{4.10}$$

For the sake of simplicity and without loss of generality, We choose $\omega_{m_1} = \omega_{m_2} = \omega_m$, $\gamma_{m1} = \gamma_{m2} = \gamma_m$. The noise operator corresponding to the atomic ensemble with zero mean value, c_{in}, appearing in (4.10) , satisfy the non-vanishing correlations function $\langle c_{in}(t)c_{in}^\dagger(t')\rangle = \delta(t - t')$ [106].

The vacuum input noise of the optical operator a_{in} defined in section 2.5.2 is different of a_{in} presented here. In fact, the system under study is fed by squeezed light that corresponds to the nonzero time-domain correlation functions [107].

$$\begin{aligned}
\langle \delta a_{in}^\dagger(t)\delta a_{in}(t')\rangle &= N\delta(t - t'), \\
\langle \delta a_{in}(t)\delta a_{in}^\dagger(t')\rangle &= (N + 1)\delta(t - t'), \\
\langle \delta a_{in}(t)\delta a_{in}(t')\rangle &= M\, \mathrm{e}^{-i\omega_m(t+t')}\, \delta(t - t'), \\
\langle \delta a_{in}^\dagger(t)\delta a_{in}^\dagger(t')\rangle &= M^*\, \mathrm{e}^{i\omega_m(t+t')}\, \delta(t - t'),
\end{aligned} \tag{4.11}$$

where $M = \sinh r \cosh r e^{i\phi}$ and $N = \sinh^2 r$, r and ϕ being respectively the strength squeezing parameter and phase of the squeezed vacuum light.

The Heisenberg-Langevin equations are in general nonsolvable analytically. So one needs the

linearization treatment by expanding each Heisenberg operator as a sum of its classical steady state value plus an additional operator of fluctuation with zero-mean value [89]:

$$q = q_s + \delta q,\ p = p_s + \delta p,\ a = a_s + \delta a,\ c = c_s + \delta c. \tag{4.12}$$

The corresponding steady-state values read

$$\begin{aligned} p_1^s &= 0, \\ p_2^s &= 0, \\ q_1^s &= \frac{-g\cos^2(\theta/2)|a_s|^2}{\omega_m}, \\ q_2^s &= \frac{g\cos^2(\theta/2)|a_s|^2}{\omega_m}, \\ c^s &= \frac{-iG_a a^s}{(\gamma_a + i\Delta_a)}, \\ a^s &= \frac{E_L}{\kappa + i\Delta + \frac{G_a^2}{\gamma_a + i\Delta_a}}, \end{aligned} \tag{4.13}$$

where $\Delta = \Delta_0 + g\cos^2(\theta/2)(q_1^s - q_2^s)$.

Inserting equation (4.12) in (4.10), and introducing $\delta X = \frac{\delta a + \delta a^\dagger}{\sqrt{2}}$, $\delta Y = \frac{\delta a - \delta a^\dagger}{i\sqrt{2}}$, $\delta x = \frac{\delta c + \delta c^\dagger}{\sqrt{2}}$, $\delta y = \frac{\delta c - \delta c^\dagger}{i\sqrt{2}}, X_{in} = \frac{a_{in} + a_{in}^\dagger}{\sqrt{2}}$, $Y_{in} = \frac{a_{in} - a_{in}^\dagger}{i\sqrt{2}}$, $x_{in} = \frac{c_{in} + c_{in}^\dagger}{\sqrt{2}}$, $y_{in} = \frac{c_{in} - c_{in}^\dagger}{i\sqrt{2}}$, allows to obtain the following linearized Langevin equations:

$$\begin{aligned} \delta\dot{q}_1 &= \omega_m\ \delta p_1, \\ \delta\dot{p}_1 &= -\omega_m \delta q_1 - \gamma_m\ \delta p_1 - G\cos^2(\theta/2)\delta X + \xi, \\ \delta\dot{q}_2 &= \omega_m\ \delta p_2, \\ \delta\dot{p}_2 &= -\omega_m \delta q_2 - \gamma_m\ \delta p_2 + G\cos^2(\theta/2)\delta X + \xi, \\ \delta\dot{X} &= -\kappa\delta X + \Delta\delta Y + G_a\delta y + \sqrt{2\kappa}X_{in}, \\ \delta\dot{Y} &= -G\cos^2(\theta/2)\delta q_1 + G\cos^2(\theta/2)\delta q_2 - \Delta\delta X - \kappa\delta Y - G_a\delta x + \sqrt{2\kappa}Y_{in}, \\ \delta\dot{x} &= G_a\delta Y - \gamma_a\delta x + \Delta_a\delta y + \sqrt{2\gamma_a}x_{in}, \\ \delta\dot{y} &= -G_a\delta X - \gamma_a\delta y - \Delta_a\delta x + \sqrt{2\gamma_a}y_{in}, \end{aligned} \tag{4.14}$$

with $G = \sqrt{2}ga^s$. The resulting evolution equations of motion for the fluctuations in (4.14) can be rewritten in the matrix form

$$\dot{u}(t) = Au(t) + n(t), \tag{4.15}$$

where $u(t)$ and $n(t)$ are respectively, the column vector of the fluctuations and the column vector of noise operators, the transpose of which are respectively given by

$$\begin{aligned} u^T(\infty) &= (\delta q_1(\infty),\, \delta p_1(\infty),\, \delta q_2(\infty),\, \delta p_2(\infty),\, \delta X(\infty),\, \delta Y(\infty),\, \delta x(\infty),\, \delta y(\infty)) \\ n^T(t) &= (0, \xi, 0, \xi, \sqrt{2\kappa}X_{in}, \sqrt{2\kappa}Y_{in}, \sqrt{2\gamma_a}x_{in}, \sqrt{2\gamma_a}y_{in}). \end{aligned} \tag{4.16}$$

The drift matrix A, reads

$$A = \begin{pmatrix} 0 & \omega_m & 0 & 0 & 0 & 0 & 0 & 0 \\ -\omega_m & -\gamma_m & 0 & 0 & -G\cos^2(\theta/2) & 0 & 0 & 0 \\ 0 & 0 & 0 & \omega_m & 0 & 0 & 0 & 0 \\ 0 & 0 & -\omega_m & -\gamma_m & G\cos^2(\theta/2) & 0 & 0 & 0 \\ 0 & 0 & 0 & 0 & -\kappa & \Delta & 0 & G_a \\ -G\cos^2(\theta/2) & 0 & G\cos^2(\theta/2) & 0 & -\Delta & -\kappa & -G_a & 0 \\ 0 & 0 & 0 & 0 & 0 & G_a & -\gamma_a & \Delta_a \\ 0 & 0 & 0 & 0 & -G_a & 0 & -\Delta_a & -\gamma_a. \end{pmatrix} \tag{4.17}$$

The solution of the differential equation (4.15), is $u(t) = Y(t)u(0) + \int_0^t dx Y(x)\eta(t-x)$, with $Y(t) = \exp\{At\}$.

Now, let's bring the covariance matrix V of the system previously explored in this thesis. It can be obtained using the following Lyapunov equation:

$$AV + VA^T = -D, \tag{4.18}$$

where D is a diagonal matrix that represents the noise correlations. It is given by

$$D = \begin{pmatrix} 0 & 0 & 0 & 0 & 0 & 0 & 0 & 0 \\ 0 & \gamma_m(2n_{th}+1) & 0 & 0 & 0 & 0 & 0 & 0 \\ 0 & 0 & 0 & 0 & 0 & 0 & 0 & 0 \\ 0 & 0 & 0 & \gamma_m(2n_{th}+1) & 0 & 0 & 0 & 0 \\ 0 & 0 & 0 & 0 & 2\kappa(Re[M]+N+\frac{1}{2}) & 2\kappa Im[M] & 0 & 0 \\ 0 & 0 & 0 & 0 & 2\kappa Im[M] & 2\kappa(-Re[M]+N+\frac{1}{2}) & 0 & 0 \\ 0 & 0 & 0 & 0 & 0 & 0 & \gamma_a & 0 \\ 0 & 0 & 0 & 0 & 0 & 0 & 0 & \gamma_a \end{pmatrix} \tag{4.19}$$

The Covariance Matrix V can be written in a block form:

$$V = \begin{pmatrix} V_{m_1} & V_{m_1 m_2} & V_{m_1 op} & V_{m_1 a} \\ V_{m_1 m_2}^T & V_{m_2} & V_{m_2 op} & V_{m_2 a} \\ V_{m_1 op}^T & V_{m_2 op}^T & V_{op} & V_{opa} \\ V_{m_1 a}^T & V_{m_2 a}^T & V_{opa}^T & V_a \end{pmatrix}, \tag{4.20}$$

where V_a, $V_{m_j} (j = 1, 2)$, and V_{op} are the covariance matrices of the atomic mode, the $(j = 1, 2)$ mechanical mode and the optical mode, respectively. When interested in studying the behavior of only two subsystems (and their correlations, among other things), the global 8×8 covariance matrix V (4.20) can be reduced to a 4×4 submatrix V_S, containing only the covariance matrices of the subsystems of interest:

$$V_S = \begin{pmatrix} A & C \\ C^T & B \end{pmatrix}, \tag{4.21}$$

with A and B being the 2×2 covariance matrices describing the single modes and C the 2×2 covariance matrix of the quantum correlations between the two subsystems.

The system being comprised of four modes: atomic (a), optical (op) and the two mechanical modes (m_1 and m_2), it allows the study of various types of entanglements mainly focused throughout this thesis.

4.3 Entanglement analysis

We still want to shed light on entanglement in this chapter. Bipartite entanglement, which is generally the type that is thoroughly studied in the literature, can be investigated in this case, using any bi-partition of the system. Moreover, tripartite entanglement can also be discussed in detail using the different tri-partitions of the system. The benefit from such a general study is that the comparison of the different types of entanglement brings more insight into their general behavior and their mutual influence.

4.3.1 Bipartite entanglement

To quantify the bipartite stationary entanglement between any two modes x and y ($x, y = a, m_1, m_2$ or op), we use the logarithmic negativity E_N

$$E_N = \max[0, -\ln 2\tilde{\eta}], \tag{4.22}$$

with

$$\tilde{\eta} = \min\left\{\text{eig} \mid \oplus_{j=1}^{2} (-\sigma_y) P V_S P|\right\}, \tag{4.23}$$

where σ_y is the y-Pauli matrix, V_S is the 4×4 covariance matrix of the two subsystems and $P = \sigma_z \oplus 1$, with σ_z being the z-Pauli matrix.

In order to evaluate numerically the logarithmic negativity. we choose, the power of the driven laser $P = 35mW$, the masses and the frequencies of two oscillators are respectively $m = 10\ ng$ and $\omega_m = 2\pi \times 10^7 H_z$, the laser wavelength is $\lambda = 1064\ nm$, $\theta = \frac{\pi}{3}$, the cavity decay rate $\kappa = \pi \times 10^7 H_z$, the mechanical damping rate $\gamma_m = 2\pi \times 10^2 H_z$, the length of the cavity $l = 1mm$, the phase of the squeezed vacuum light $\phi = 0$. We choose the parameter of the atoms to be $G_a = 12\pi \times 10^6 H_z$ and $\gamma_a = \pi \times 10^7 H_z$. In addition, we consider that the atoms are resonant: $\Delta_a = -\omega_m$. Some parameters are taken from the set of experiments [108–110].

It is important to note that, the symmetry between the mechanical modes is reflected in the expressions of the logarithmic negativities involving these modes. For instance, the logarithmic negativity between any mechanical mode and the optical mode are the same, $E_{m1op} = E_{m2op}$, and the same with respect to the atomic mode, $E_{m1a} = E_{m2a}$. Next, we investigate the stationary entanglement as a function of the thermal bath's temperature T.

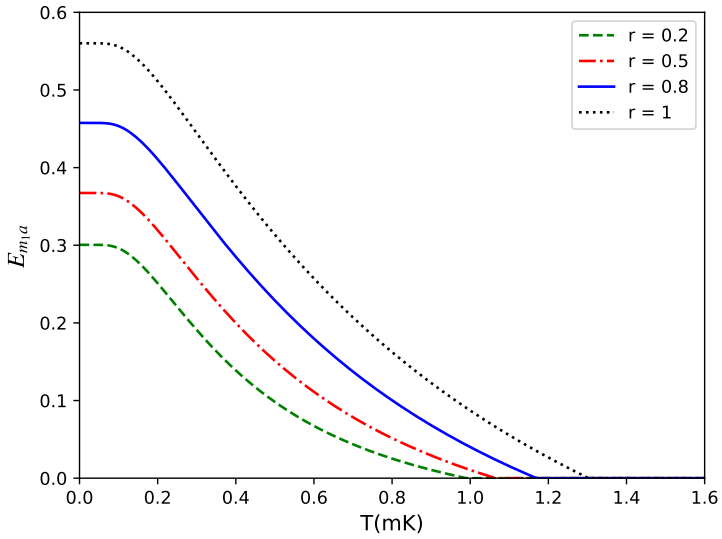

Figure 4.3: Plot of the bipartite entanglement $E_{m_1 a}$, between m_1 and a, versus the thermal bath temperature $T(K)$, for different values of the input field squeezing parameter r.

Figure 4.3 shows the bipartite stationary entanglement $E_{m_1 a}$, we choose $\Delta = \omega_m$ and numerically simulate the logarithmic negativity between the mechanical mode 1 and the atomic mode

for different values of the squeezing parameter r. This will allow us to distinguish the impact of the atomic medium on hybrid optomechanical systems. It is worth noting, that the atoms are indirectly coupled to the mechanical resonators through their common interaction with the input field. In fact, when atoms are present within the cavity, they have the ability to interact coherently with the electromagnetic field mode. They respond to the cavity field by spontaneously emitting photons, increasing their overall number in the cavity. The collisions of the photons on the surfaces of the movable mirrors generate a strong optomechanical coupling due to the radiation pressure force. Consequently, a stronger optomechanical coupling can be achieved by increasing the number of atoms resulting in a more resilient atom-mirror entanglement.

It is well known that the entanglement decreases with the effect of the environment's temperature due to thermal fluctuations; this is confirmed in the behavior of E_{m_1a} in Figure 4.3. Interestingly, for such systems in the presence of the atomic medium, a collective interaction can emerge between atoms and the cavity field mode, giving rise to the phenomenon of superradiance [111, 112], responsible for the creation of entangled states involving the atoms and cavity. Simultaneously, the optical field being coupled to the mechanical oscillator, the presence of the atomic ensemble enhances the cooperativity between the optical mode and the mechanical mode, enabling the generation of a significant amount of entanglement. In addition, the ring structure can minimize optical losses compared to other cavity geometries, leading to higher finesse and powerful interaction against decoherence as is clearly seen in the plateau observed for the entanglement at low temperatures. For that reason, adding an atomic ensemble to a cavity allows for a stronger optomechanical coupling. Besides this, the atom-field coupling strength and the excitation number has an important influence on the atomic effective damping rate of the mechanical resonators [113].

The numerical simulation results show that the progressive injection of the squeezed light increases the entanglement, and it becomes more robust against the environment temperature, *e.g.*, for low temperatures, when $r = 0.2$, the numerical value of the entanglement is $E_{m_1a} = 0.3$, whereas, for $r = 1$, it is $E_{m_1a} = 0.56$. Moreover, it is noticeable that, the entanglement in the case of $r = 1$ persists against the bath environment more than in the case where the parameter of squeezing $r = 0.2$. This explains the impact of the squeezed vacuum light on entanglement due to the light-matter interaction. Indeed, the increase of the photon number in the cavity leads to a stronger radiation pressure force and does enhance the quantum correlations transfer from squeezed light to the subsystems.

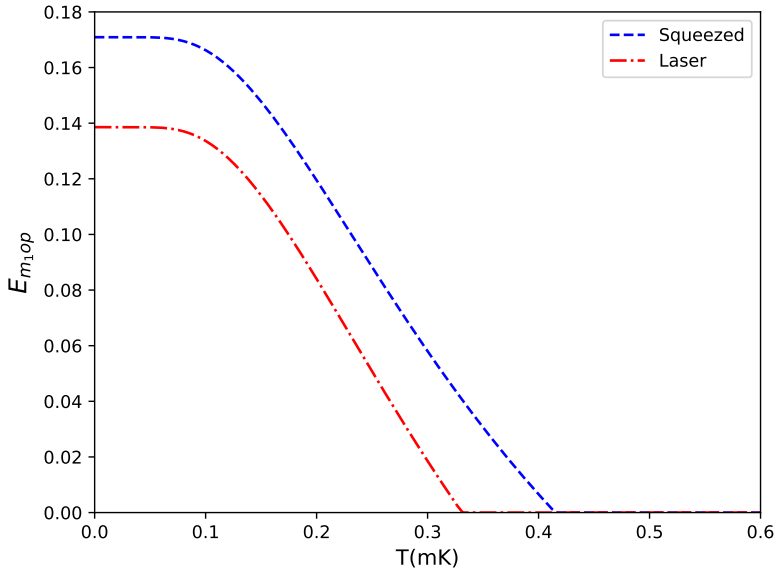

Figure 4.4: The logarithmic negativity E_{m_1op}, between m_1 and op versus the thermal bath temperature $T(K)$; the other parameters are chosen as in Figure 4.3.

In Figure 4.4, we plot the logarithmic negativity E_{m_1op} which expresses the entanglement between the mechanical mode 1 and the optical mode. In the following, we analyze the influence injecting the squeezed light in the system. The red line representing the entanglement when there is no squeezing and only the laser field is injected ($r = 0$), shows that the entanglement vanishes around $T \simeq 0.35mk$. However, the blue line representing the squeezed vacuum light with ($r = 0.1$), shows that the entanglement survives until $T \simeq 0.42mk$. We remark that for low temperatures we have $E_{m_1op} = 0.14$ (when $r = 0$) and $E_{m_1op} = 0.17$ (when $r = 0.1$). A relatively significant entanglement is reached for a sufficiently large number of photons from the two sources, as they allow for a robust photon-phonon interaction via the radiation pressure. Indeed, the photons exert a small push on the surface of the movable mirror and change the cavity's length, which in turn, modifies the intensity of the field and does enhance the radiation pressure force allowing for a strong optomechanical coupling that optimizes entanglement [65].

Overall, the injection of laser and squeezed vacuum light that increases the number of photons, in conjunction with the atomic ensemble placed inside the cavity that scatter photons through stimulated re-emission is of crucial importance for the motion of the mechanical oscillator. It should be noted that quantum fluctuations occur within the cavity as a result of the interaction between the pumped photons and the photons scattered by the atom, while thermal fluctuations originating from the mechanical bath environment contribute to decoherence. Since any feasible system couples with its own environment to some extent, a large number of photons

is needed to overcome the decohering effects of the quantum fluctuations and to strengthen the resulting entanglement.

4.3.2 Tripartite entanglement

In order to study the existence of genuine tripartite entanglement we adopt a quantitative measure of tripartite negativity, which for a tripartite system (ABC) is given by (see 1.5.4)

$$\mathcal{E}_{ABC} = (E_{A|BC}\ E_{B|AC}\ E_{C|AB})^{1/3}. \tag{4.24}$$

In our case A, B and C can be one of the mechanical modes, optical mode or atomic mode. Moreover, for the sake of simplicity we will use the following compact notations $\mathcal{E}_1 \equiv \mathcal{E}_{m_1 m_2 a}$, $\mathcal{E}_2 \equiv \mathcal{E}_{a\, m_1 op} = \mathcal{E}_{a\, m_2 op}$ and $\mathcal{E}_3 \equiv \mathcal{E}_{m_1 m_2 op}$.

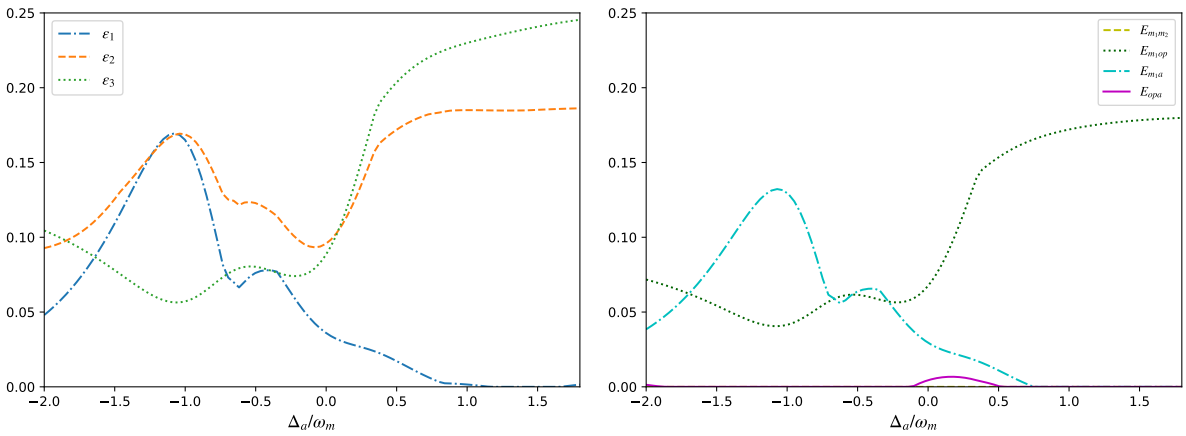

(a) (b)

Figure 4.5: Effect of the normalized atomic detuning on the (a) tripartite logarithmic negativities $\mathcal{E}_1$, $\mathcal{E}_2$ and $\mathcal{E}_3$ and (b) bipartite negativities ($E_{m_1 m_2}$, $E_{m_1 op}$, $E_{m_1 a}$ and $E_{op\, a}$) . In all the cases we choose $\Delta = \omega_m$, $P = 10mW$, $r = 0.1$ and the temperature $T = 0.1mK$.

We plot in figure 4.5a, the tripartite entanglement as captured by the logarithmic negativity 4.24 versus the normalized atomic detuning. The three logarithmic negativities react quite differently, and broadly speaking, it depends on whether the atomic mode is involved or not. For instance, $\mathcal{E}_1$ and $\mathcal{E}_2$ have their maximum close to the region where $\Delta_a = -\omega_m$ whereas, $\mathcal{E}_3$ decreases in this interval and actually reaches its minimum in this region. It is remarkable that

the tripartite entanglement between the optical mode, the atomic mode and the mechanical mode ($\mathcal{E}_2$), is the one that remains significant in a broader interval. This is due to the absorption and remission of photons by the atoms. On the other hand, the more photons we have in the cavity, the more the photon-phonon interaction is enhanced via the radiation pressure force due to the effect of the vibrating mirror. Under the atom-photon-phonon interaction, not only the region of the effective detuning is wider, but also a significant entanglement is obtained. These collective bosonic modes form an optimal quantum tripartite system that ensures a strong entanglement sharing, more easily realized and observed in experiment.

It is worth noticing that, when $\Delta_a > 0$, both $\mathcal{E}_2$ and $\mathcal{E}_3$ asymptotically increase, while $\mathcal{E}_1$ is negligible *i.e.*, the tripartite $\{m_1, m_2, a\}$ entanglement is not present in this area. This result might be interpreted as a result of the negative value of the effective atomic detuning being a convenient choice since it regulates the evolution of the atomic quadrature [114].

This collective tripartite behavior can be explained by the corresponding underlying bipartite entanglement shown in Figure 4.5b. As a matter of fact, the behavior of $\mathcal{E}_1 \equiv \mathcal{E}_{m1m2a}$ in Figure 4.5a is identical to that of E_{m_1a} in Figure 4.5b because the other bipartite entanglement $E_{m_1m_2}$ involved in $\mathcal{E}_1$ is shown in Figure 4.5b to be negligible. Similarly, $\mathcal{E}_3 \equiv \mathcal{E}_{m1m2op}$, relies on the *mechanical-optical*, entanglement, E_{m_1op}, and the negligible *mechanical-mechanical* entanglement, $E_{m_1m_2}$. This results in the behavior of $\mathcal{E}_3$ resembling that of E_{m_1op}. In contrast, $\mathcal{E}_2 \equiv \mathcal{E}_{m1a\,op}$, depends on three bipartite entanglements E_{m_1op}, E_{m_1a} and $E_{op\,a}$, the last one of which is shown to be negligible in Figure 4.5b. $\mathcal{E}_2$ is thus mainly driven by E_{m_1op} and E_{m_1a}; henceforth, the behavior of $\mathcal{E}_2$ in Figure 4.5a is a hybrid of that of E_{m_1op} and E_{m_1a} in Figure 4.5b.

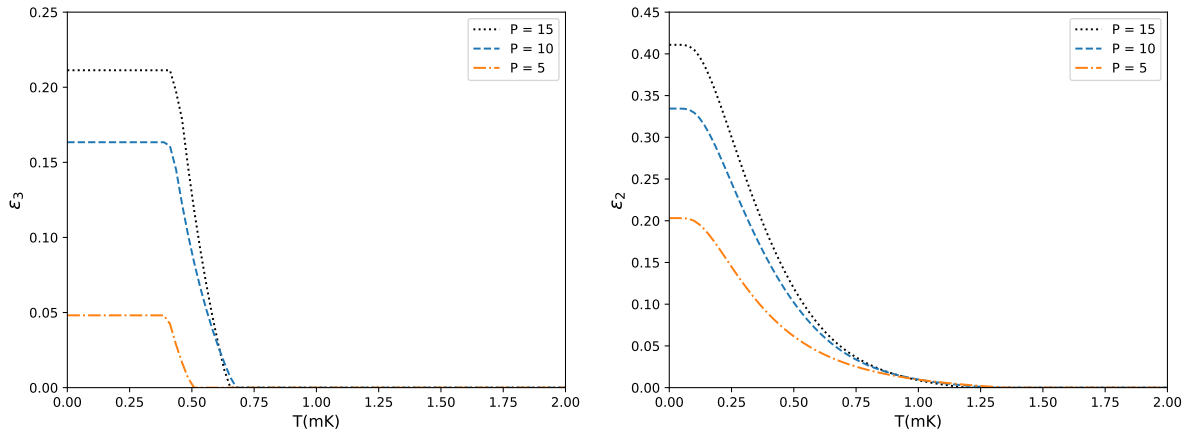

(a) (b)

Figure 4.6: (a) $\mathcal{E}_3$ and (b) $\mathcal{E}_2$ as a function of the temperature $T(mK)$ for different values of the pumping power P (measured in mW). $\Delta = 0.5\omega_m$ and the other parameters are chosen as in Figure 4.5.

To analyze the influence of the pumping power, we plotted in Figure 4.6 $\mathcal{E}_2$ and $\mathcal{E}_3$ as a function of the environment temperature T, for different values of P. With the increase of driving power, the values of logarithmic negativity increase and, relatively, resist better the environment-induced decoherence. We also find that, for $P = 15mW$, $\mathcal{E}_3$ vanishes at $T \simeq 0.65mk$, while $\mathcal{E}_2$ survives until $T \simeq 1.2mk$, so $\mathcal{E}_3$ vanishes quicker than $\mathcal{E}_2$ due to the thermal environment. On the other hand, for $P = 5mW$ and for a fixed temperature $T = 0.27mk$, $\mathcal{E}_3 = 0.048$ while $\mathcal{E}_2 = 0.13$, which shows that, compared to $\mathcal{E}_2$, $\mathcal{E}_3$ requires a much higher value of power that increases the number of photons in the cavity and a very low number of thermal phonons, *i.e.*, temperature.

It is an intuitive fact that entanglement is highly sensitive to fluctuations, with the mechanical modes being much noisier and the fluctuations of the atomic mode being less noisy resulting from the collision between photons of the light source and the photons emitted by the atoms. This partly explains the reason of the fragility of $\mathcal{E}_3$ compared to $\mathcal{E}_2$ as the latter depends less on the much more fragile correlations involving the mechanical modes than the former. Moreover, we have an additional squeezed vacuum light, the injection of which reduces the fluctuations and results in stronger correlations when it is involved; this illustrates well the usefulness of squeezed light.

The system under consideration is an optical ring cavity, which is characterized by a high-quality factor and efficient coupling between the optical and mechanical modes since the use of two movable mirrors enhances the field-mirrors interaction. Indeed, the pumping power circulation inside the cavity amplifies its intensity and the displacement of the two movable mirrors do enhance the optomechanical coupling. Lengthening the cavity provides further enhancement of the interaction. A significant values of the power increases the circulation inside the cavity, which in turn enhances the interaction and thus the entanglement, establishing the importance of the parameter of power as well.

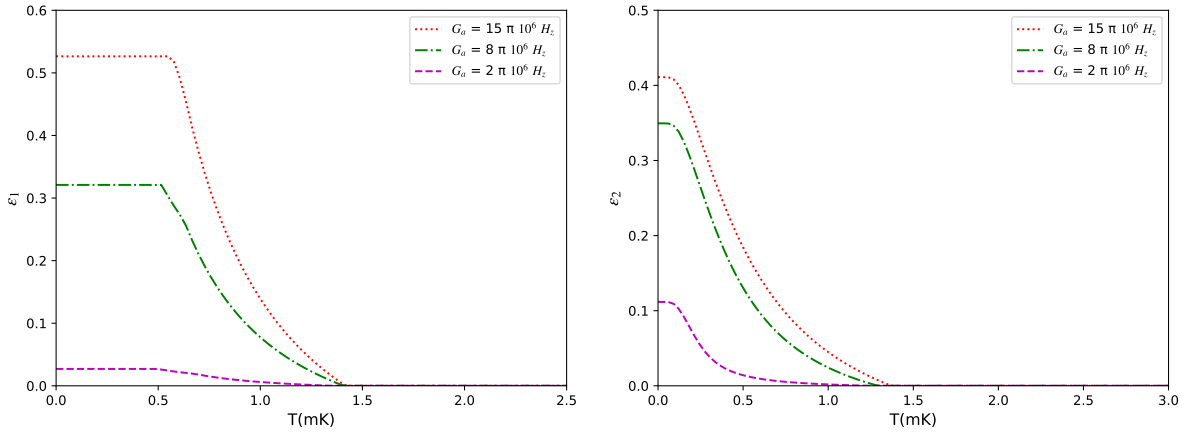

(a) (b)

Figure 4.7: The influence of the atom-cavity coupling G_a on $\mathcal{E}_1$ and $\mathcal{E}_2$ as a function of the temperature $T(mK)$. We choose $P = 35mW$, $r = 0.6$, $\Delta = \omega_m$.

Let us finally explore the effect of the atomic-field coupling strength G_a. For this purpose, we simulate the tripartite entanglement $\mathcal{E}_1$ and $\mathcal{E}_2$ versus the temperature for different values of G_a. It is observed that, for a fixed temperature *e.g.*, $T = 0.5mK$ as G_a increases, both $\mathcal{E}_1$ and $\mathcal{E}_2$ increase, and in general, one can achieve significant amounts of tripartite entanglement for high couplings. This can, for instance, be achieved by increasing the atom numbers in the cavity and with a strong driven laser that increases the number of photons as explained previously, then a well-fortified interaction is achieved leading to a strong atom-field coupling. Indeed, for high-quality cavities such as ring cavities considerable coupling can be easily realized experimentally [115].

By comparing the plots 4.7a and 4.7b, it comes out that $\mathcal{E}_1$ is more resistant than $\mathcal{E}_2$ to

the thermal-induced decoherence; *e.g.,* when $G_a = 8\pi 10^6 H_z$, $\mathcal{E}_2$ vanishes at $T \approx 1.3mk$ while $\mathcal{E}_1$ vanishes at $T \approx 1.5mk$ all the while maintaining a significant amount and plateauing over a longer interval. It is clearly seen that $\mathcal{E}_1$ *i.e.,* the $\{m_1, m_2, a\}$ entanglement which is of interest in this paper is greater than $\mathcal{E}_2$ *i.e.,* $\{a, m_1, op\}$ even though atoms and mirrors are only indirectly coupled in the Hamiltonian 4.9. As a matter of fact, $\mathcal{E}_1$ enhances at the expanse of the field-mirror interaction via the radiation pressure as in [116].

As explained in the previous sections, the ring geometry provides a closed-loop configuration for the light circulating within the cavity. This feedback mechanism allows for powerfull interaction between the atomic ensemble and cavity field leading to a stronger coupling. As the atoms absorb energy from the cavity field, they can undergo spontaneous emission. This process involves the atom transitioning back to a lower energy state and releasing a photon into the cavity field. In addition to spontaneous emission, stimulated emission can also occur. If the atom is already in an excited state, an incoming photon from the cavity field can stimulate the atom to emit a photon that is in phase and coherent with the incoming photon. This allows to avoid a large number of photons interacting with the mechanical oscillators and get a stronger and more persistent correlation between optical and mechanical modes. This enhances $\mathcal{E}_1$ and results in the large plateau being less affected by the temperature effects.

All these results, confirm that a significant entanglement is established with a strong atom-field coupling and can be optimized by the optical field squeezing.

As a conclusion, in this chapter we have proposed a theoretical scheme for the study of steady state bipartite and tripartite entanglement. The system consists of a ring cavity with a fixed mirror and two movable mirrors, as well as an atomic ensemble composed of two-level atoms that are confined within the cavity. This latter is pumped with a coherent laser source and a squeezed vacuum light allowing to enhance the quantum correlations. A proper analysis of the dynamics of the coupled system is carried out, allowing for the derivation of the set of quantum Langevin equations. These equations are then linearized to obtain the 8×8 steady state covariance matrix that is fully describing the hybrid optomechanical system (cavity field – atomic ensemble - two vibrating mirrors). The bipartite and tripartite logarithmic negativity is used to evaluate the entanglement of the multimode system.

An analysis of the bipartite and tripartite entanglement shared by the coupled system confirms the negative influence of the environment's temperature on the different types of entanglement. Some types of entanglement are more resilient than others. In particular, the benefits of adding the atomic ensemble in the cavity are observed as it allows for a more resistant entan-

glement. In this regard, we have shown that a stronger atomic-field coupling allows for a better entanglement. On the other hand, with the increase of the power of the driving laser, significant entanglement and broader effective detuning region can be achieved. In addition to that, we have shown the needfulness of the squeezed light source since this latter allows for a strong optomechanical coupling. The combination of an atomic ensemble, strong optomechanical coupling and optimized cavity design makes the system less susceptible to thermal fluctuations. As a result, entanglement is preserved even at higher temperatures. In our case, we obtain a large plateau for entanglement against temperature. This is achieved because of the fact that the atoms can extract thermal energy from the mechanical oscillator. This energy transfer occurs when the atoms absorb phonons from the mechanical motion, effectively reducing temperature and cooling the mechanical oscillator [117,118]. This process provides a strong and stable system against environment fluctuations.

Such a scheme will open new perspectives for the application of quantum teleportation in cavity optomechanics, the implementation of quantum memories [119] and quantum routers [120] for continuous variable quantum information processing. The enhancement of the entanglement in the cavity will prove critical for the cavity optomechanical sensing [121, 122]. The presence of strong multipartite entanglement can be exploited to realize teleportation in optomechanical ring cavities, similar to what was achieved in [123]. The added advantage here is the ability to teleport quantum states between a multitude of modes.

Chapter 5

Observation of Non-Gaussianity on nonlinear optomechanical cavity

This chapter of the thesis seems to be the most different chapter of this work. While many studies undergo through the linearization process, as previously explored in this thesis, this chapter, focuses on shedding light on the nonlinear interaction between the optical field and the mechanical element within the optical cavity. Indeed, the light-matter interaction induced by radiation pressure force is inherently nonlinear [124–126]. The nonlinear characteristic of optomechanical systems have been frequently used for the creation of non-Gaussian states. This latter exhibit to have an excellent sensing. Several optomechanical systems have been implemented to exploit properties of nonlinearities, such as [127–129]. Therefore, it is of utmost importance to determine how the nonlinearity can be further enhanced, or rather, how can we enhance the amount of non-Gaussianity in an optomechanical system. Against this background, we quantify the amount of non-Gaussianity between the two mechanical modes and the optical mode. Building upon the foundation laid by the work of [130, 131], where the authors quantify the non-Gaussianty of the system, suggesting a viable mechanism for increasing the non-Gaussianity of optomechanical systems even in the presence of noise.

The chapter is organised as follows. We begin by introducing the ring optomechanical system and presenting the nonlinear Hamiltonian. Next in section 5.2 we solve the resulting dynamics and provide a comprehensive calculation of the covariance matrix. That allows as to evaluate the non-Gaussianity between the two-mode and three-mode scenarios (see section 5.3). Finally, in section 5.3 we plot the non-Gaussianty as function of the time τ and finalize the chapter with a discussion and concluding remarks.

5.1 System and model

We consider the ring cavity illustrated in Fig. 5.1, as previously depicted.

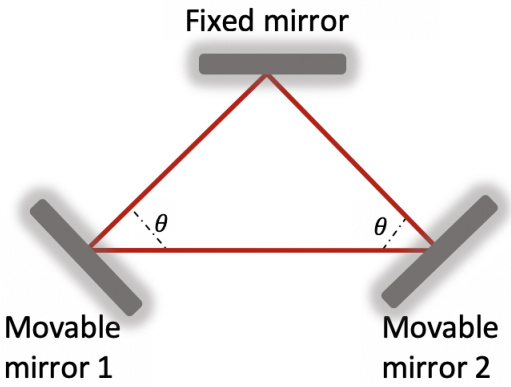

Figure 5.1: Scheme of the optomechanical system under analysis.

5.2 Dynamics

Hamiltonian

The Hamiltonian of the system is given by

$$\hat{H} = \hbar\omega_c \hat{a}^\dagger \hat{a} + \hbar\omega_m \hat{b}_1^\dagger \hat{b}_1 + \hbar\omega_m \hat{b}_2^\dagger \hat{b}_2 + \hbar g(t)\hat{a}^\dagger \hat{a}\cos^2(\theta/2)(\hat{b}_1^\dagger + \hat{b}_1) - \hbar g(t)\hat{a}^\dagger \hat{a}\cos^2(\theta/2)(\hat{b}_2^\dagger + \hat{b}_2), \tag{5.1}$$

where $\hat{H}$ is the free Hamiltonian already studied in the previous chapter. Now let's rescale the Hamiltonian and introduce dimensionless quantities to simplify the notation and graphical representation of the system dynamics. This action involves transitioning from t to τ, where $\tau = \omega_m t$ is the new, dimensionless time. And the optical frequency becomes $\Omega_c := \omega_c/\omega_m$. In addition, the coupling become $g(t) = g(\omega_m t)/\omega_m$. We also rescale the Hamiltonian by $\hbar$, and gets

$$\frac{\hat{H}}{\hbar\omega_m} = \Omega_c \hat{a}^\dagger \hat{a} + \hat{b}_1^\dagger \hat{b}_1 + \hat{b}_2^\dagger \hat{b}_2 + g(\tau)\hat{a}^\dagger \hat{a}\cos^2(\theta/2)(\hat{b}_1^\dagger + \hat{b}_1) - g(\tau)\hat{a}^\dagger \hat{a}\cos^2(\theta/2)(\hat{b}_2^\dagger + \hat{b}_2). \tag{5.2}$$

Now let's move to solve the dynamics induced by 5.2.

Time evolution of the system

To determine the expression for the time evolution operator $U(t)$ for a system undergoing evolution as described by 5.2. The unitary time-evolution operator reads

$$\hat{U}(\tau) := \vec{T} \exp\left[-i \int_0^\tau d\tau' H(\tau')\right], \tag{5.3}$$

where $\vec{T}$ is the time-ordering operator [132]. The foundation for decoupling the operator involves identifying a set of generators $\hat{G}_i$ that form a Lie algebra and drive the process of time-evolution. This Lie algebra must be closed under commutation, that is, either $[\hat{G}_j, \hat{G}_k] \propto \hat{G}_l$, or $[\hat{G}_j, \hat{G}_k] = m$ where m is a scalar.

We begin by proposing the ansatz that the evolution operator 5.3 can be written as

$$\hat{U}(\tau) = \prod_j \hat{U}_j(\tau) = \prod_j \mathrm{e}^{-iF_j \hat{G}_j}, \tag{5.4}$$

where F_j are coefficients corresponding to each of the generators $\hat{G}_j$. Our objective involves determining the coefficients F_j.

We initiate the process by establishing the operators $\hat{G}_j$ within the algebra :

$$\begin{aligned}
&\hat{N}_a := \hat{a}^\dagger \hat{a} && \hat{N}_a^2 := (\hat{a}^\dagger \hat{a})^2 \\
&\hat{N}_{b1} := \hat{b}_1^\dagger \hat{b}_1 && \hat{N}_{b2} := \hat{b}_2^\dagger \hat{b}_2 \\
&\hat{N}_a \hat{B}_{+1} := \hat{N}_a(\hat{b}_1^\dagger + \hat{b}_1) && \hat{N}_a \hat{B}_{-1} := i\hat{N}_a(\hat{b}_1^\dagger - \hat{b}_1) \\
&\hat{N}_a \hat{B}_{+2} := \hat{N}_a(\hat{b}_2^\dagger + \hat{b}_2) && \hat{N}_a \hat{B}_{-2} := i\hat{N}_a(\hat{b}_2^\dagger - \hat{b}_2)
\end{aligned} \tag{5.5}$$

It can be confirmed that the operators described in 5.5 constitute a closed Lie algebra through commutation. Using these operators, our ansatz can be expressed as follows

$$\hat{U}(\tau) = \hat{U}_a(\tau)\hat{U}_{b_1}(\tau)\hat{U}_{b_2}(\tau)\hat{U}_a^2(\tau)\hat{U}_{+1}(\tau)\hat{U}_{-1}(\tau)\hat{U}_{+2}(\tau)\hat{U}_{-2}(\tau), \tag{5.6}$$

where we identify

$$\begin{aligned}
&\hat{U}_a(\tau) = \mathrm{e}^{-iF_{\hat{N}_a}\hat{N}_a} && \hat{U}_{b_1}(\tau) = \mathrm{e}^{-iF_{N_{b1}}\hat{N}_{b1}} && \hat{U}_{b_2}(\tau) = \mathrm{e}^{-iF_{N_{b2}}\hat{N}_{b2}} \\
&\hat{U}_a^2(\tau) = \mathrm{e}^{-iF_{\hat{N}_a^2}\hat{N}_a^2} && \hat{U}_{+1}(\tau) = \mathrm{e}^{-iF_{\hat{N}_a\hat{B}_{+1}}\hat{N}_a\hat{B}_{+1}} && \hat{U}_{-1}(\tau) = \mathrm{e}^{-iF_{\hat{N}_a\hat{B}_{-1}}\hat{N}_a\hat{B}_{-1}} \\
&\hat{U}_{+2}(\tau) = \mathrm{e}^{-iF_{\hat{N}_a\hat{B}_{+2}}\hat{N}_a\hat{B}_{+2}} && \hat{U}_{-2}(\tau) = \mathrm{e}^{-iF_{\hat{N}_a\hat{B}_{-2}}\hat{N}_a\hat{B}_{-2}}
\end{aligned} \tag{5.7}$$

To find the coefficients, we note the following equivalence:

$$\vec{T}\exp\left[-i\int_0^\tau d\tau^{'}H(\tau^{'})\right] = \mathrm{e}^{-iF_{\hat{N}_a}\hat{N}_a}\ \mathrm{e}^{-iF_{N_{b1}}\hat{N}_{b1}}\ \mathrm{e}^{-iF_{N_{b2}}\hat{N}_{b2}}\ \mathrm{e}^{-iF_{\hat{N}_a^2}\hat{N}_a^2}\ \mathrm{e}^{-iF_{\hat{N}_a\hat{B}_{+1}}\hat{N}_a\hat{B}_{+1}}$$
$$\mathrm{e}^{-iF_{\hat{N}_a\hat{B}_{-1}}\hat{N}_a\hat{B}_{-1}}\ \mathrm{e}^{-iF_{\hat{N}_a\hat{B}_{+2}}\hat{N}_a\hat{B}_{+2}}\ \mathrm{e}^{-iF_{\hat{N}_a\hat{B}_{-2}}\hat{N}_a\hat{B}_{-2}}. \tag{5.8}$$

Upon differentiation of both sides, the Hamiltonian 5.2 emerges on the left side, expressed in terms of the generators. Subsequently, multiplying both sides by $U^\dagger$ yields the ensuing differential equation:

$$\Omega_c\hat{N}_a + \hat{N}_{b1} + \hat{N}_{b2} + g(\tau)\cos^2(\theta/2)\hat{N}_a\hat{B}_{+1} - g(\tau)\cos^2(\theta/2)\hat{N}_a\hat{B}_{+2} = \dot{F}_{\hat{N}_a}\hat{N}_a + \dot{F}_{\hat{N}_{b1}}\hat{U}_a(\tau)\hat{N}_{b1}$$
$$\hat{U}_a^\dagger(\tau) + \dot{F}_{\hat{N}_{b2}}\hat{U}_a(\tau)\hat{U}_{b_1}(\tau)\hat{N}_{b2}\hat{U}_{b_1}^\dagger(\tau)\hat{U}_a^\dagger(\tau) + \dot{F}_{\hat{N}_a^2}\hat{U}_a(\tau)\hat{U}_{b_1}(\tau)\hat{U}_{b_2}(\tau)\hat{N}_a^2\hat{U}_{b_2}^\dagger(\tau)\hat{U}_{b_1}^\dagger(\tau)\hat{U}_a^\dagger(\tau) +$$
$$\dot{F}_{\hat{N}_a\hat{B}_{+1}}\hat{U}_a(\tau)\hat{U}_{b_1}(\tau)\hat{U}_{b_2}(\tau)\hat{U}_a^2(\tau)\hat{N}_a\hat{B}_{+1}\hat{U}_a^{2\dagger}(\tau)\hat{U}_{b_2}^\dagger(\tau)\hat{U}_{b_1}^\dagger(\tau)\hat{U}_a^\dagger(\tau) + \dot{F}_{\hat{N}_a\hat{B}_{-1}}\hat{U}_a(\tau)\hat{U}_{b_1}(\tau)\hat{U}_{b_2}(\tau)$$
$$\hat{U}_a^2(\tau)\hat{U}_{+1}(\tau)\hat{N}_a\hat{B}_{-1}\hat{U}_{+1}^\dagger(\tau)\hat{U}_a^{2\dagger}(\tau)\hat{U}_{b_2}^\dagger(\tau)\hat{U}_{b_1}^\dagger(\tau)\hat{U}_a^\dagger(\tau) + \dot{F}_{\hat{N}_a\hat{B}_{+2}}\hat{U}_a(\tau)\hat{U}_{b_1}(\tau)\hat{U}_{b_2}(\tau)\hat{U}_a^2(\tau)\hat{U}_{+1}(\tau)$$
$$\hat{U}_{-1}(\tau)\hat{N}_a\hat{B}_{+2}\hat{U}_{-1}^\dagger(\tau)\hat{U}_{+1}^\dagger(\tau)\hat{U}_a^{2\dagger}(\tau)\hat{U}_{b_2}^\dagger(\tau)\hat{U}_{b_1}^\dagger(\tau)\hat{U}_a^\dagger(\tau) + \dot{F}_{\hat{N}_a\hat{B}_{-2}}\hat{U}_a(\tau)\hat{U}_{b_1}(\tau)\hat{U}_{b_2}(\tau)\hat{U}_a^2(\tau)\hat{U}_{+1}(\tau)$$
$$\hat{U}_{-1}(\tau)\hat{U}_{+2}(\tau)\hat{N}_a\hat{B}_{-2}\hat{U}_{+2}^\dagger(\tau)\hat{U}_{-1}^\dagger(\tau)\hat{U}_{+1}^\dagger(\tau)\hat{U}_a^{2\dagger}(\tau)\hat{U}_{b_2}^\dagger(\tau)\hat{U}_{b_1}^\dagger(\tau)\hat{U}_a^\dagger(\tau). \tag{5.9}$$

Note that, $\dot{F}_i = \frac{d}{dt}F_i$. Solving this equation and using the commutation of the operators we can determine the coefficients and get :

$$\begin{aligned}
F_{\hat{N}_a} &= \Omega_c\tau,\\
F_{\hat{N}_{b1}} &= \tau,\\
F_{\hat{N}_{b2}} &= \tau,\\
F_{\hat{N}_a\hat{B}_{+1}} &= \int_0^\tau g(\tau^{'})\cos^2(\theta/2)\cos\Big(\tau^{'}\Big)d\tau^{'},\\
F_{\hat{N}_a\hat{B}_{-1}} &= \int_0^\tau g(\tau^{'})\cos^2(\theta/2)\sin\Big(\tau^{'}\Big)d\tau^{'},\\
F_{\hat{N}_a\hat{B}_{+2}} &= -\int_0^\tau g(\tau^{'})\cos^2(\theta/2)\cos\Big(\tau^{'}\Big)d\tau^{'},\\
F_{\hat{N}_a\hat{B}_{-2}} &= -\int_0^\tau g(\tau^{'})\cos^2(\theta/2)\sin\Big(\tau^{'}\Big)d\tau^{'},\\
F_{\hat{N}_a^2} &= -4\int_0^\tau \cos^4(\theta/2)g(\tau^{'})\sin\Big(\tau^{'}\Big)\int_0^{\tau^{'}} d\tau^{''}g(\tau^{''})\cos\Big(\tau^{''}\Big).
\end{aligned} \tag{5.10}$$

We can now use these equations to find the simplified form of $\hat{U}(\tau)$. Furthermore, these coefficients will be frequently used, such as in quantifying the non-Gaussianity measure. Next, we will examine the measure of non-Gaussianity based on the relative entropy of an initially Gaussian

state.

Calculation using the covariance matrix formalism

When evaluating the degree of non-Gaussianity, it's valuable to calculate the symplectic eigenvalues of the covariance matrix that refers to the second moments of a quantum state [133], and can be used to fully characterise a Gaussian state [134]. First, let's find the elements $\sigma_{nm}(\tau)$ of the 6×6 covariance matrix $\sigma(\tau)$ given by:

$$\sigma = \begin{pmatrix} \sigma_1 & \varepsilon_{12} & \varepsilon_{13} \\ \varepsilon_{12}^T & \sigma_2 & \varepsilon_{23} \\ \varepsilon_{13}^T & \varepsilon_{23}^T & \sigma_3 \end{pmatrix}, \tag{5.11}$$

where, σ_1, σ_2 and σ_3 are the local covariance matrix of the single-mode subsystems (optical field, oscillating mirror 1, oscillating mirror 2), and ε represents their correlations. In a specific choice of basics $\hat{\mathbb{X}} = (\hat{a}, \hat{b}_1, \hat{b}_2, \hat{a}^\dagger, \hat{b}_1^\dagger, \hat{b}_2^\dagger)^T$ the elements $\sigma_{nm}(\tau)$ are defined as $\sigma_{nm}(\tau) := \langle\{\hat{X}_n, \hat{X}_m^\dagger\}\rangle - 2\langle\hat{X}_n\rangle\langle\hat{X}_m^\dagger\rangle$. We get :

$$
\begin{aligned}
\sigma_{11} &= \sigma_{44} = 1 + 2\langle \hat{a}^\dagger \hat{a} \rangle - 2\langle \hat{a}^\dagger \rangle \langle \hat{a} \rangle \\
\sigma_{12} &= \sigma_{54} = 2\langle \hat{a}^\dagger \hat{b}_1 \rangle - 2\langle \hat{a}^\dagger \rangle \langle \hat{b}_1 \rangle \\
\sigma_{13} &= \sigma_{64} = 2\langle \hat{a}^\dagger \hat{b}_2 \rangle - 2\langle \hat{a}^\dagger \rangle \langle \hat{b}_2 \rangle \\
\sigma_{14} &= 2\langle \hat{a}^{\dagger 2} \rangle - 2\langle \hat{a}^\dagger \rangle^2 \\
\sigma_{15} &= \sigma_{24} = 2\langle \hat{a}^\dagger \hat{b}_1^\dagger \rangle - 2\langle \hat{a}^\dagger \rangle \langle \hat{b}_1^\dagger \rangle \\
\sigma_{16} &= 2\langle \hat{a}^\dagger \hat{b}_2^\dagger \rangle - 2\langle \hat{a}^\dagger \rangle \langle \hat{b}_2^\dagger \rangle \\
\sigma_{22} &= \sigma_{55} = 1 + 2\langle \hat{b}_1^\dagger \hat{b}_1 \rangle - 2\langle \hat{b}_1^\dagger \rangle \langle \hat{b}_1 \rangle \\
\sigma_{21} &= 2\langle \hat{b}_1^\dagger \hat{a} \rangle - 2\langle \hat{b}_1^\dagger \rangle \langle \hat{a} \rangle \\
\sigma_{23} &= 2\langle \hat{b}_1^\dagger \hat{b}_2 \rangle - 2\langle \hat{b}_1^\dagger \rangle \langle \hat{b}_2 \rangle \\
\sigma_{25} &= 2\langle \hat{b}_1^{\dagger 2} \rangle - 2\langle \hat{b}_1^\dagger \rangle^2 \\
\sigma_{26} &= 2\langle \hat{b}_1^\dagger \hat{b}_2^\dagger \rangle - 2\langle \hat{b}_1^\dagger \rangle \langle \hat{b}_2^\dagger \rangle \\
\sigma_{31} &= \sigma_{46} = 2\langle \hat{b}_2^\dagger \hat{a} \rangle - 2\langle \hat{b}_2^\dagger \rangle \langle \hat{a} \rangle \\
\sigma_{32} &= 2\langle \hat{b}_2^\dagger \hat{b}_1 \rangle - 2\langle \hat{b}_2^\dagger \rangle \langle \hat{b}_1 \rangle \\
\sigma_{33} &= 1 + 2\langle \hat{b}_2^\dagger \hat{b}_2 \rangle - 2\langle \hat{b}_2^\dagger \rangle \langle \hat{b}_2 \rangle \\
\sigma_{34} &= 2\langle \hat{a}^\dagger \hat{b}_2^\dagger \rangle - 2\langle \hat{a}^\dagger \rangle \langle \hat{b}_2^\dagger \rangle \\
\sigma_{35} &= 2\langle \hat{b}_2^\dagger \hat{b}_1^\dagger \rangle - 2\langle \hat{b}_2^\dagger \rangle \langle \hat{b}_1^\dagger \rangle \\
\sigma_{36} &= 2\langle \hat{b}_2^{\dagger 2} \rangle - 2\langle \hat{b}_2^\dagger \rangle^2 \\
\sigma_{41} &= 2\langle \hat{a}^2 \rangle - 2\langle \hat{a} \rangle^2 \\
\sigma_{51} &= \sigma_{42} = 2\langle \hat{a} \hat{b}_1 \rangle - 2\langle \hat{a} \rangle \langle \hat{b}_1 \rangle \\
\sigma_{61} &= \sigma_{43} = 2\langle \hat{a} \hat{b}_2 \rangle - 2\langle \hat{a} \rangle \langle \hat{b}_2 \rangle \\
\sigma_{45} &= 2\langle \hat{a} \hat{b}_1^\dagger \rangle - 2\langle \hat{a} \rangle \langle \hat{b}_1^\dagger \rangle \\
\sigma_{52} &= 2\langle \hat{b}_1^2 \rangle - 2\langle \hat{b}_1 \rangle^2 \\
\sigma_{53} &= \sigma_{62} = 2\langle \hat{b}_1 \hat{b}_2 \rangle - 2\langle \hat{b}_1 \rangle \langle \hat{b}_2 \rangle \\
\sigma_{63} &= 2\langle \hat{b}_2^2 \rangle - 2\langle \hat{b}_2 \rangle^2 \\
\sigma_{56} &= 2\langle \hat{b}_1 \hat{b}_2^\dagger \rangle - 2\langle \hat{b}_1 \rangle \langle \hat{b}_2^\dagger \rangle \\
\sigma_{65} &= 2\langle \hat{b}_2 \hat{b}_1^\dagger \rangle - 2\langle \hat{b}_2 \rangle \langle \hat{b}_1^\dagger \rangle \\
\sigma_{66} &= 1 + 2\langle \hat{b}_2^\dagger \hat{b}_2 \rangle - 2\langle \hat{b}_2^\dagger \rangle \langle \hat{b}_2 \rangle .
\end{aligned}
\tag{5.12}
$$

To compute the expectation values of components illustrated in 5.12, it is necessary to initially

determinate the time evolution of the mode operators $\hat{a}$, $\hat{b}_1$ and $\hat{b}_2$ induced by the Hamiltonian.

In the Heisenberg picture, the time evolution of the mode operators can be considered basically $\hat{a}(t) := \hat{U}^\dagger(t)\,\hat{a}\,\hat{U}(t)$, $\hat{b}_1(t) := \hat{U}^\dagger(t)\,\hat{b}_1\,\hat{U}(t)$ and $\hat{b}_2(t) := \hat{U}^\dagger(t)\,\hat{b}_2\,\hat{U}(t)$. Given the case when the optical mode is a coherent state and the two mechanical modes are a thermal coherent states, which we denote $|\mu_c\rangle$, $|\mu_{m1}\rangle$ and $|\mu_{m2}\rangle$. These states satisfy the relations :

$$\begin{cases} \hat{a}\,|\mu_c\rangle = \mu_c\,|\mu_c\rangle\,, \\ \hat{b}_1\,|\mu_{m1}\rangle = \mu_{m1}\,|\mu_{m1}\rangle\,, \\ \hat{b}_2\,|\mu_{m2}\rangle = \mu_{m2}\,|\mu_{m2}\rangle\,. \end{cases} \tag{5.13}$$

The assumption that the optical field is a coherent state is an available resource, since coherent state model laser light quite well. For The mechanical element in optomechanical systems is most often found in a thermal state. Our choice of initial coherent state and thermal coherent state can be generalised by the initial state $|\psi(0)\rangle$:

$$|\psi(0)\rangle = |\mu_c\rangle \otimes |\mu_{m1}\rangle \otimes |\mu_{m2}\rangle\,. \tag{5.14}$$

Now, let's go back to the time evolution of the mode operators $\hat{a}(t)$, $\hat{b}_1(t)$ and $\hat{b}_2(t)$. Using 5.6 we explicitly find in terms of the generators of the Lie algebra :

$$\begin{aligned} \hat{a}(t) :=\ & \mathrm{e}^{-iF_{\hat{N}_a}}\,\mathrm{e}^{-iF_{\hat{N}_a^2}}\,\mathrm{e}^{-2i(F_{\hat{N}_a^2}+F_{\hat{N}_a\hat{B}_{+1}}F_{\hat{N}_a\hat{B}_{-1}}+F_{\hat{N}_a\hat{B}_{+2}}F_{\hat{N}_a\hat{B}_{-2}})\hat{N}_a}\,\mathrm{e}^{-iF_{\hat{N}_a\hat{B}_{+1}}\hat{B}_{+1}}\,\mathrm{e}^{-iF_{\hat{N}_a\hat{B}_{-1}}\hat{B}_{-1}} \\ & \mathrm{e}^{-iF_{\hat{N}_a\hat{B}_{+2}}\hat{B}_{+2}}\,\mathrm{e}^{-iF_{\hat{N}_a\hat{B}_{-2}}\hat{B}_{-2}}\,\hat{a}, \\ \hat{b}_1(t) :=\ & \mathrm{e}^{-iF_{N_{b1}}}\,(\hat{b}_1 + (F_{\hat{N}_a\hat{B}_{-1}} - iF_{\hat{N}_a\hat{B}_{+1}})\hat{N}_a), \\ \hat{b}_2(t) :=\ & \mathrm{e}^{-iF_{N_{b2}}}\,(\hat{b}_2 + (F_{\hat{N}_a\hat{B}_{-2}} - iF_{\hat{N}_a\hat{B}_{+2}})\hat{N}_a). \end{aligned} \tag{5.15}$$

For simplicity, this expressions can be rewritten as :

$$\begin{aligned} \hat{a}(t) :=\ & \mathrm{e}^{-iF_{\hat{N}_a}}\,\mathrm{e}^{-i\theta_a(\hat{N}_a+\frac{1}{2})}\,\hat{D}_b(F_1^*)\hat{D}_b(F_2^*)\hat{a}, \\ \hat{b}_1(t) :=\ & \mathrm{e}^{-iF_{N_{b1}}}\,(\hat{b}_1 + F_1^*\hat{N}_a), \\ \hat{b}_2(t) :=\ & \mathrm{e}^{-iF_{N_{b2}}}\,(\hat{b}_2 + F_2^*\hat{N}_a), \end{aligned} \tag{5.16}$$

where $\hat{D}_b$ is a Weyl displacement operator and where we have introduces the quantities

$$\begin{aligned}
\theta_a &= 2(F_{\hat{N}_a^2} + F_{\hat{N}_a\hat{B}_{+1}}F_{\hat{N}_a\hat{B}_{-1}} + F_{\hat{N}_a\hat{B}_{+2}}F_{\hat{N}_a\hat{B}_{-2}}),\\
F_1 &= F_{\hat{N}_a\hat{B}_{-1}} + iF_{\hat{N}_a\hat{B}_{+1}},\\
F_2 &= F_{\hat{N}_a\hat{B}_{-2}} + iF_{\hat{N}_a\hat{B}_{+2}}.
\end{aligned} \tag{5.17}$$

Ignoring the global phases $\Omega_c\tau$, and by transforming 5.16 into a rotating frame rotation with $\Omega_c\hat{a}^\dagger\hat{a}$, we obtain :

$$\begin{aligned}
\langle\hat{a}(t)\rangle &:= \mathrm{e}^{-i\frac{1}{2}\theta_a}\,\mathrm{e}^{|\mu_c|^2(\mathrm{e}^{-i\theta_a}-1)}\,\mathrm{e}^{-\frac{1}{2}|F_1|^2}\,\mathrm{e}^{F_1^*\mu_{m1}^*-F_1\mu_{m1}}\,\mathrm{e}^{-\frac{1}{2}|F_2|^2}\,\mathrm{e}^{F_2^*\mu_{m2}^*-F_2\mu_{m2}}\,\mu_c\\
\langle\hat{b}_1(t)\rangle &:= \mathrm{e}^{-i\tau}(\mu_{m1}+F_1^*|\mu_c|^2)\\
\langle\hat{b}_2(t)\rangle &:= \mathrm{e}^{-i\tau}(\mu_{m2}+F_2^*|\mu_c|^2)\\
\langle\,\hat{b}_1^2(t)\rangle &:= \mathrm{e}^{-2i\tau}(\mu_{m1}+F_1^*|\mu_c|^2)^2 + \mathrm{e}^{-2i\tau}\,F_1^{*2}|\mu_c|^2\\
\langle\,\hat{b}_2^2(t)\rangle &:= \mathrm{e}^{-2i\tau}(\mu_{m2}+F_2^*|\mu_c|^2)^2 + \mathrm{e}^{-2i\tau}\,F_2^{*2}|\mu_c|^2\\
\langle\hat{a}^\dagger(t)\hat{a}(t)\rangle &:= |\mu_c|^2\\
\langle\hat{b}_1^\dagger(t)\hat{b}_1(t)\rangle &:= \left|\mu_{m1}+F_1^*|\mu_c|^2\right|^2 + |F_1|^2|\mu_c|^2\\
\langle\hat{b}_2^\dagger(t)\hat{b}_2(t)\rangle &:= \left|\mu_{m2}+F_2^*|\mu_c|^2\right|^2 + |F_2|^2|\mu_c|^2\\
\langle\hat{a}^2(t)\rangle &:= \mathrm{e}^{-2i\theta_a}\,\mathrm{e}^{|\mu_c|^2(\mathrm{e}^{-2i\theta_a}-1)}\,\mathrm{e}^{2(F_1^*\mu_{m1}^*-F_1\mu_{m1})}\,\mathrm{e}^{-2|F_1|^2}\,\mathrm{e}^{2(F_2^*\mu_{m2}^*-F_2\mu_{m2})}\,\mathrm{e}^{-2|F_2|^2}\,{\mu_c}^2\\
\langle\hat{a}(t)\hat{b}_1(t)\rangle &:= \mathrm{e}^{-i\frac{1}{2}\theta_a}\,\mathrm{e}^{|\mu_c|^2(\mathrm{e}^{-i\theta_a}-1)}\,\mathrm{e}^{-\frac{1}{2}|F_1|^2}\,\mathrm{e}^{F_1^*\mu_{m1}^*-F_1\mu_{m1}}\,\mathrm{e}^{-\frac{1}{2}|F_2|^2}\,\mathrm{e}^{F_2^*\mu_{m2}^*-F_2\mu_{m2}}\,\mathrm{e}^{-i\tau}\,\mu_c(\mu_{m1}+\\
&\quad(|\mu_c|^2\,\mathrm{e}^{-i\theta_a}+1)F_1^*)\\
\langle\hat{a}(t)\hat{b}_2(t)\rangle &:= \mathrm{e}^{-i\frac{1}{2}\theta_a}\,\mathrm{e}^{|\mu_c|^2(\mathrm{e}^{-i\theta_a}-1)}\,\mathrm{e}^{-\frac{1}{2}|F_1|^2}\,\mathrm{e}^{F_1^*\mu_{m1}^*-F_1\mu_{m1}}\,\mathrm{e}^{-\frac{1}{2}|F_2|^2}\,\mathrm{e}^{F_2^*\mu_{m2}^*-F_2\mu_{m2}}\,\mathrm{e}^{-i\tau}\,\mu_c(\mu_{m2}+\\
&\quad(|\mu_c|^2\,\mathrm{e}^{-i\theta_a}+1)F_2^*)\\
\langle\hat{a}(t)\hat{b}_1^\dagger(t)\rangle &:= \mathrm{e}^{-i\frac{1}{2}\theta_a}\,\mathrm{e}^{|\mu_c|^2(\mathrm{e}^{-i\theta_a}-1)}\,\mathrm{e}^{-\frac{1}{2}|F_1|^2}\,\mathrm{e}^{F_1^*\mu_{m1}^*-F_1\mu_{m1}}\,\mathrm{e}^{-\frac{1}{2}|F_2|^2}\,\mathrm{e}^{F_2^*\mu_{m2}^*-F_2\mu_{m2}}\,\mathrm{e}^{i\tau}\,\mu_c(\mu_{m1}^*+\\
&\quad|\mu_c|^2\,\mathrm{e}^{-i\theta_a}\,F_1)\\
\langle\hat{a}(t)\hat{b}_2^\dagger(t)\rangle &:= \mathrm{e}^{-i\frac{1}{2}\theta_a}\,\mathrm{e}^{|\mu_c|^2(\mathrm{e}^{-i\theta_a}-1)}\,\mathrm{e}^{-\frac{1}{2}|F_1|^2}\,\mathrm{e}^{F_1^*\mu_{m1}^*-F_1\mu_{m1}}\,\mathrm{e}^{-\frac{1}{2}|F_2|^2}\,\mathrm{e}^{F_2^*\mu_{m2}^*-F_2\mu_{m2}}\,\mathrm{e}^{i\tau}\,\mu_c(\mu_{m2}^*+\\
&\quad|\mu_c|^2\,\mathrm{e}^{-i\theta_a}\,F_2).
\end{aligned} \tag{5.18}$$

Providing a complete calculation of the time evolution operators allows to calculate the

elements of the covariance matrix 5.12, subsequently yielding:

$$
\begin{aligned}
\sigma_{11} &= \sigma_{44} = 1 + 2|\mu_c|^2(1 - \mathrm{e}^{-4|\mu_c|^2 \sin^2 \frac{\theta_a}{2}} \mathrm{e}^{-|F_1|^2} \mathrm{e}^{-|F_2|^2}) \\
\sigma_{12} &= \sigma_{54} = 2\,\mathrm{e}^{i\frac{\theta_a}{2}} \mathrm{e}^{|\mu_c|^2(\mathrm{e}^{i\theta_a}-1)} \mathrm{e}^{-\frac{1}{2}|F_1|^2} \mathrm{e}^{-\frac{1}{2}|F_2|^2} \mathrm{e}^{F_1\mu_{m1} - F_1^*\mu_{m1}^*} \mathrm{e}^{F_2\mu_{m2} - F_2^*\mu_{m2}^*} \mathrm{e}^{-i\tau}\, \mu_c^*|\mu_c|^2 F_1^*(\mathrm{e}^{i\theta_a} - 1) \\
\sigma_{22} &= \sigma_{55} = 1 + 2|F_1|^2|\mu_c|^2 \\
\sigma_{25} &= 2\,\mathrm{e}^{2i\tau}\, F_1^2|\mu_c|^2 \\
\sigma_{26} &= 2\,\mathrm{e}^{2i\tau}\, F_2F_1|\mu_c|^2 \\
\sigma_{31} &= \sigma_{46} = 2\,\mathrm{e}^{-i\frac{\theta_a}{2}} \mathrm{e}^{|\mu_c|^2(\mathrm{e}^{-i\theta_a}-1)} \mathrm{e}^{-\frac{1}{2}|F_1|^2} \mathrm{e}^{-\frac{1}{2}|F_2|^2} \mathrm{e}^{F_1^*\mu_{m1}^* - F_1\mu_{m1}} \mathrm{e}^{F_2^*\mu_{m2}^* - F_2\mu_{m2}} \mathrm{e}^{i\tau}\, \mu_c|\mu_c|^2 F_2 \\
&\quad (\mathrm{e}^{-i\theta_a} - 1) \\
\sigma_{32} &= 2F_2F_1^*|\mu_c|^2 \\
\sigma_{33} &= \sigma_{66} = 1 + 2|F_2|^2|\mu_c|^2 \\
\sigma_{35} &= 2\,\mathrm{e}^{2i\tau}\, F_2F_1|\mu_c|^2 \\
\sigma_{36} &= 2\,\mathrm{e}^{2i\tau}\, F_2^2|\mu_c|^2 \\
\sigma_{41} &= 2\mu_c^2\, \mathrm{e}^{-|F_1|^2} \mathrm{e}^{-|F_2|^2} \mathrm{e}^{2(F_1^*\mu_{m1}^* - F_1\mu_{m1})} \mathrm{e}^{2(F_2^*\mu_{m2}^* - F_2\mu_{m2})} \mathrm{e}^{-i\theta_a} (\mathrm{e}^{-i\theta_a} \mathrm{e}^{|\mu_c|^2(\mathrm{e}^{-2i\theta_a}-1)} \mathrm{e}^{-|F_1|^2} \mathrm{e}^{-|F_2|^2} \\
&\quad - \mathrm{e}^{2|\mu_c|^2(\mathrm{e}^{-i\theta_a}-1)}) \\
\sigma_{51} &= \sigma_{42} = 2\,\mathrm{e}^{-i\frac{\theta_a}{2}} \mathrm{e}^{|\mu_c|^2(\mathrm{e}^{-i\theta_a}-1)} \mathrm{e}^{-\frac{1}{2}|F_1|^2} \mathrm{e}^{-\frac{1}{2}|F_2|^2} \mathrm{e}^{F_1^*\mu_{m1}^* - F_1\mu_{m1}} \mathrm{e}^{F_2^*\mu_{m2}^* - F_2\mu_{m2}} \mathrm{e}^{-i\tau}\, \mu_c F_1^* \\
&\quad (|\mu_c|^2(\mathrm{e}^{-i\theta_a} - 1) + 1) \\
\sigma_{61} &= \sigma_{43} = 2\,\mathrm{e}^{-i\frac{\theta_a}{2}} \mathrm{e}^{|\mu_c|^2(\mathrm{e}^{-i\theta_a}-1)} \mathrm{e}^{-\frac{1}{2}|F_1|^2} \mathrm{e}^{-\frac{1}{2}|F_2|^2} \mathrm{e}^{F_1^*\mu_{m1}^* - F_1\mu_{m1}} \mathrm{e}^{F_2^*\mu_{m2}^* - F_2\mu_{m2}} \mathrm{e}^{-i\tau}\, \mu_c F_2^* \\
&\quad (|\mu_c|^2(\mathrm{e}^{-i\theta_a} - 1) + 1) \\
\sigma_{45} &= 2\,\mathrm{e}^{-i\frac{\theta_a}{2}} \mathrm{e}^{|\mu_c|^2(\mathrm{e}^{-i\theta_a}-1)} \mathrm{e}^{-\frac{1}{2}|F_1|^2} \mathrm{e}^{-\frac{1}{2}|F_2|^2} \mathrm{e}^{F_1^*\mu_{m1}^* - F_1\mu_{m1}} \mathrm{e}^{F_2^*\mu_{m2}^* - F_2\mu_{m2}} \mathrm{e}^{i\tau}\, \mu_c F_1 \\
&\quad |\mu_c|^2(\mathrm{e}^{-i\theta_a} - 1) \\
\sigma_{52} &= 2\,\mathrm{e}^{-2i\tau}\, F_1^{*2}|\mu_c|^2 \\
\sigma_{63} &= 2\,\mathrm{e}^{-2i\tau}\, F_2^{*2}|\mu_c|^2 \\
\sigma_{56} &= 2F_2F_1^*|\mu_c|^2
\end{aligned}
\tag{5.19}
$$

We have calculated the second moments and the covariance matrix $\sigma(\tau)$. our next step involves quantifying the amount of non-Gaussianity of this state. To initiate this process, we need to determine the symplectic eigenvalues by following these steps:

1. Calculate the covariance matrix σ.

2. Find the eigenvalues and eigenvectors of the covariance matrix σ by solving the character-

istic equation : $Det(\sigma - \lambda I) = 0$

$$\begin{pmatrix} \sigma_{11}-\lambda_1 & \sigma_{12} & \sigma_{13} & \sigma_{14} & \sigma_{15} & \sigma_{16} \\ \sigma_{21} & \sigma_{22}-\lambda_2 & \sigma_{23} & \sigma_{24} & \sigma_{25} & \sigma_{26} \\ \sigma_{31} & \sigma_{32} & \sigma_{33}-\lambda_3 & \sigma_{34} & \sigma_{35} & \sigma_{36} \\ \sigma_{41} & \sigma_{42} & \sigma_{43} & \sigma_{44}-\lambda_4 & \sigma_{45} & \sigma_{46} \\ \sigma_{51} & \sigma_{52} & \sigma_{53} & \sigma_{54} & \sigma_{55}-\lambda_5 & \sigma_{56} \\ \sigma_{61} & \sigma_{62} & \sigma_{63} & \sigma_{64} & \sigma_{65} & \sigma_{66}-\lambda_6 \end{pmatrix} \tag{5.20}$$

3. The eigenvectors constitute a novel set of orthogonal mode functions for the system, while the eigenvalues ($\lambda_1, \lambda_2, \lambda_3, \lambda_4, \lambda_5$ and λ_6) represent the variance of the quadrature operators within these emergent modes.

4. The covariance matrix can be written in the form of a block matrix where each block corresponds to one of the modes

$$\begin{pmatrix} \sigma_1 & 0 & 0 \\ 0 & \sigma_2 & 0 \\ 0 & 0 & \sigma_3 \end{pmatrix}, \tag{5.21}$$

with $\sigma_1 = \begin{pmatrix} \lambda_1 & 0 \\ 0 & \lambda_2 \end{pmatrix}$, $\sigma_2 = \begin{pmatrix} \lambda_3 & 0 \\ 0 & \lambda_4 \end{pmatrix}$, $\sigma_3 = \begin{pmatrix} \lambda_5 & 0 \\ 0 & \lambda_6 \end{pmatrix}$.

5. The three nonnegative symplectic eigenvalues is subsequently derived employing the following formula: $\Lambda_i = \sqrt{\det \sigma_i}$.

Utilizing these symplectic eigenvalues, we are able to find the expression of the non-Gaussianity, which will be presented comprehensively in the following section.

5.3 Measures of deviation from quantum Gaussianity

To apply a suitable measure of deviation from Gaussianity. We choose to employ a measure denoted as δ, originally suggested in Refs [130,131,135,136]. Based on the comparaison between the entropy of the final state and that of a suitably chosen reference Gaussian state [135,136]. Given an Hamiltonian $\hat{H}$, and an initial Gaussian state $\hat{\rho}(0)$ that evolves into the state $\hat{\rho}(\tau)$ at time τ. The nonlinear dynamics of our system expect an initial Gaussian state, to become a non-Gaussian state at later times. Moreover, the only way to preserve its Gaussianity is to

evolve through a linear transformation, induced by a Hamiltonian with at most quadratic terms in the quadrature operators [134]. Introducing the previously obtained elements, we can derive analytic expressions for the first and second moments of $\hat{\rho}(\tau)$. Then, we construct a state $\hat{\rho}_G(\tau)$, which is the Gaussian state defined by the first and second moments that coincide with those of $\hat{\rho}(\tau)$. Accordingly, the measure $\delta(\tau)$ that quantifies how $\hat{\rho}(\tau)$ deviates from $\hat{\rho}_G(\tau)$:

$$\delta(\tau) := S(\hat{\rho}_G(\tau)) - S(\hat{\rho}(\tau)), \tag{5.22}$$

with $S(\hat{\rho})$ is the von Neumann of a state $\hat{\rho}$, defined as $S(\hat{\rho}) := -\operatorname{Tr}(\hat{\rho}\ln\hat{\rho})$, it vanishes if and only if $\hat{\rho}(\tau)$ is a Gaussian state [135]. The von Neumann entropy $S(\sigma)$ in terms of symplectic eigenvalues is given by $S(\sigma) = \sum_i f(\nu_i)$, where ν_i are the symplectic eigenvalues and $f(x) = \frac{x+1}{2}\ln\left(\frac{x+1}{2}\right) - \frac{x-1}{2}\ln\left(\frac{x-1}{2}\right)$. The exact solution of $\delta(\tau)$ is too long and cumbersome to be reprinted here, but we plot the amount of non-Gaussianity over $0 < \tau < 2\pi$ in the case where $|\mu_c| \gg 1$ and $\mu_m = 0$. The explanation will be presented in the following section.

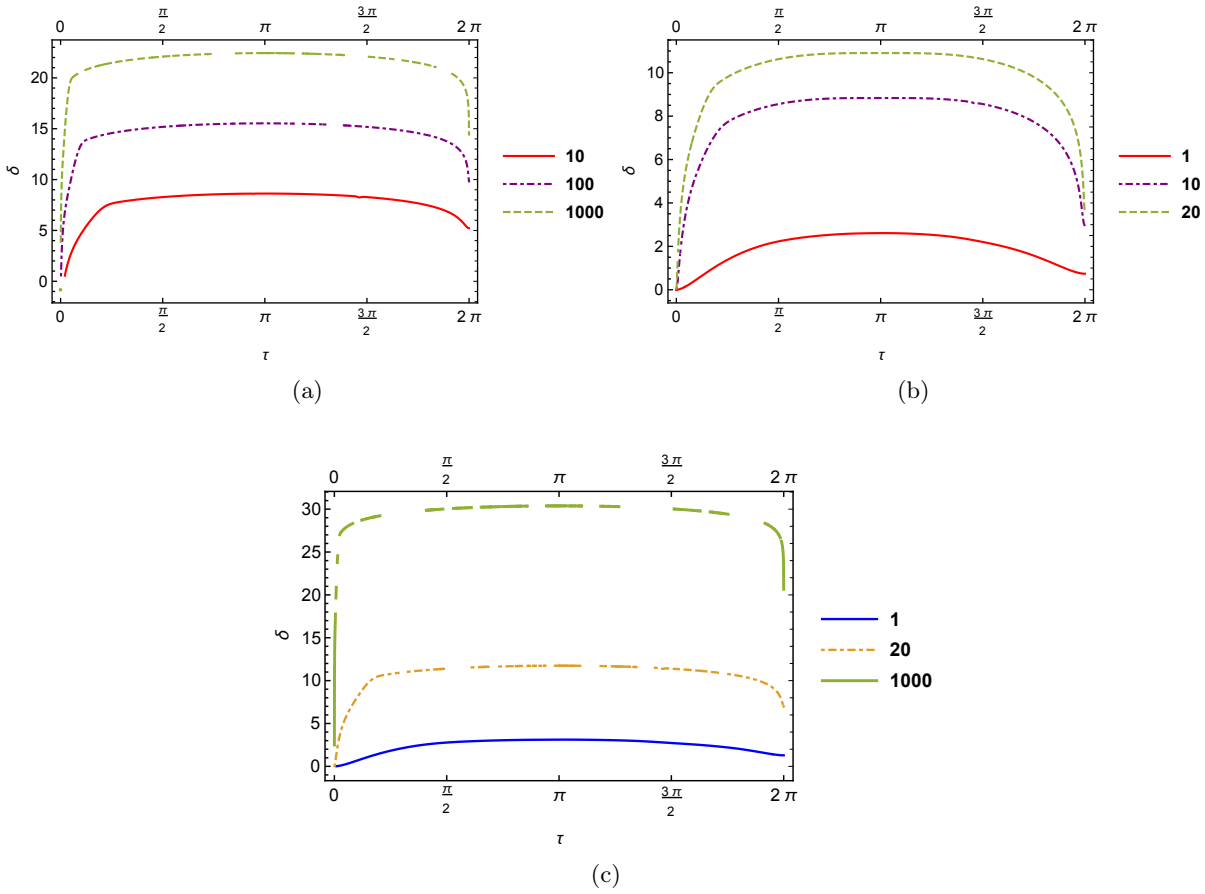

Figure 5.2: The measure of non-Gaussianity $\delta(\tau)$ versus time τ for different values of μ_c. (a) corresponds to the non-Gaussianity of the optical and the mechanical mode 1. (b) represent the non-Gaussianity between the two mechanical modes. (c) corresponds to the 3 modes non-Gaussianity of the optomechanical system (optical, mechanical 1 and mechanical 2).

In figure 5.2, we shall examine the bi-mode and multimode non-Gaussianity for different values of the coherent state parameter μ_c in the case where the nonlinear light–matter interaction is constant: $g(\tau) = g_0 = 1$. To a significant extent, this holds true for the majority of experimental systems. From the three graphs as μ_c increases the amount of non-Gaussianity increases which is evident from the constructive or destructive interference of the optical field, resulting a variation to deviation of the Gaussianity. We also see that the system reaches its maximum level of non-Gaussianity. Then it conserve the same amount until $\tau = 2\pi$, as seen on the plateau. Meaning that, there will be a rapid decrease of non-Gaussianity before the system revives once again. The main idea of this part of chapter, is to enhance the amount of non-Gaussianity. Since this latter constitute an important resource for quantum computation [137,138], quantum teleportation protocols [139] and entanglement distillation [140–142]. As shown in figure 5.2 the

higher amount of non-Gaussianity corresponds to the three-modes (optical and two mechanical modes). This illustrates well the convienient choice of a ring cavity.

5.4 Summary

In this chapter, we solved the time-evolution of a non-linear optomechanical ring cavity to quantify the non-Gaussianity of both the two-mode and three-mode of the system. Our solution is based on identifying a closed Lie algebra that facilitates calculations for the quantification of non-Gaussianity. The measure relies on the relative entropy of a state to characterize the deviation from Gaussianity within the system. First, we present the nonlinear Hamiltonian and extract the symplectic eigen values from the covariance matrix to assess the amount of non-Gaussianity of the state. We plot the evolution of non-Gaussianity over time in the case where the nonlinear optomechanical coupling is constant. Subsequently, we analyze the observed behavior and discuss the results. These findings carry significant implications for quantum control of nonlinear optomechanical systems [143, 144].

Conclusion and future works

In conclusion, this thesis has explored two distinct concepts: the processes occurring the non-linear regime that can be applied to study the non-Gaussianity of optomechanical modes. The notion of nonlinearity refers to deviations from purely linear coupling between the optical field and the mechanical displacement. Consequently, this can lead to a diverse range of behaviors generated for various applications, such as generation of non-classical states, and quantum sensing. The second process involves to perform a linearization technique. In the language of cavity optomechanics, many systems exhibit linear dynamics. Linearization simplifies the equations of motion by approximating nonlinear terms as linear ones around a particular operating point or equilibrium position. This allows for the production and manipulation of correlated states and generation of a fundamental concept widely used throughout this thesis, namely, "Entanglement" [145–148]. This latter plays a crucial role in quantum information processing and quantum technologies.

To fully quantify and measure the quantum correlations, including entanglement and Gaussian quantum discord within optomechanical ring cavity. I begin by presenting the design and construction of a ring cavity and trying to answer the question. Why ring cavity? The cavity's geometry comprising two movable mirrors can minimize optical losses compared to other cavity geometries, leading to higher finesse and powerful interaction against decoherence. Indeed, the circulation of the optical power inside the cavity amplifies its intensity and the displacement of the two movable mirrors do enhance the optomechanical coupling. That, exhibits advantageous behavior towards the quantum correlations between the optical and mechanical modes. To better analyze the properties of the entanglement generated by the intra-cavity mode and the mechanical elements, I adopt a measure of entanglement based on an analytical solution of the quantum Langevin equations, which is valid within the full parameter range of a stable

cavity. Our findings reveal that ring optomechanical cavities possess a remarkable steady-state entanglement that remains robust against temperature fluctuations. Moreover, entanglement can be optimized under a particular parameter condition. Another concept, widely exploited in coupled optomechanical systems, is aimed at shedding light on the possibilities of constructing entangled states between the macroscopic and subatomic realms. For this reason, I attempt to study this novel type of hybrid systems, whereby an atomic ensemble is placed inside the ring cavity. The integration of the atomic ensemble essentially forms a well-fortified environment to generate multipartite entanglement.

In addition to quantum entanglement, I studied Gaussian quantum discord, which is a measure of total quantum correlations, including entanglement. It can arise due to non-classical correlations between the optical and mechanical modes. It has been demonstrated that some separable states do contain some amount of quantum correlations. The exploration of Gaussian quantum discord has revealed the subtler aspects of quantum correlations, highlighting their role in non-classical information transfer and processing [64, 149].

In the next part of the thesis, I introduce the field of theoretical nonlinear optomechanics, where I define the notions of nonlinear as opposed to linear dynamics. I studied the mathematical description and application of cavity optomechanical systems evolving in the nonlinear regime. I solved the dynamics of the nonlinear Hamiltonian and used the solutions to derive the covariance matrix. Through these calculations I computed the non-Gaussianity of the optomechanical state using a relative entropy measure. And conclude that, optomechanical systems provide an inherent nonlinear coupling that, when sufficiently strong, may lead to significant deviations from Gaussianity in the evolved state. I hope that the results presented here will aid the theoretical understanding of nonlinear optomechanical systems and motivate the developments of future optomechanical experiments. Furthermore, it has been established that there is a connection between the non-Gaussianity of a state and its Wigner function [150, 151]. This means that the measure often requires supplementation with another metric of non-classicality, such as assessing the negativity of the Wigner function to indicate when non-Gaussian states are suitable for quantum information tasks. This proposition can be effectively incorporated in our system in next work.

Finally, my future research perspectives will center around a well-established task in quantum metrology: enhancing measurement precision using quantum Fisher information in ring cavity. I will direct my focus towards investigating the relationship between entanglement and quantum Fisher information in the context of cavity optomechanics.

Bibliography

[1] Johannes Kepler. 1619. de cometis libelli tres.

[2] Peter Lebedew. Untersuchungen über die druckkräfte des lichtes. *Annalen der Physik*, 311(11):433–458, 1901.

[3] Ernest Fox Nichols and Gordon Ferrie Hull. A preliminary communication on the pressure of heat and light radiation. *Physical Review (Series I)*, 13(5):307, 1901.

[4] Albert Einstein. On the development of our views concerning the nature and constitution of radiation. *Phys. Z*, 10(22):817–825, 1909.

[5] VB Braginski and AB Manukin. Ponderomotive effects of electromagnetic radiation. *Sov. Phys. JETP*, 25(4):653–655, 1967.

[6] VB Braginskiĭ, Anatoli B Manukin, and M Yu Tikhonov. Investigation of dissipative ponderomotive effects of electromagnetic radiation. *Soviet Journal of Experimental and Theoretical Physics*, 31:829, 1970.

[7] Vladimir Borisovich Braginskiĭ, Valerij Pavlovič Mitrofanov, and Vladimir Ivanovich Panov. *Systems with small dissipation*. University of Chicago Press, 1985.

[8] VB Braginskii, Yu I Vorontsov, and F Ya Khalili. Optimal quantum measurements in detectors of gravitation radiation. *JETP Lett*, 27(5), 1978.

[9] Vladimir B Braginsky, Yuri I Vorontsov, and Kip S Thorne. Quantum nondemolition measurements. *Science*, 209(4456):547–557, 1980.

[10] A Dorsel, John D McCullen, Pierre Meystre, E Vignes, and H Walther. Optical bistability and mirror confinement induced by radiation pressure. *Physical Review Letters*, 51(17):1550, 1983.

[11] Monika H Schleier-Smith, Ian D Leroux, Hao Zhang, Mackenzie A Van Camp, and Vladan Vuletić. Optomechanical cavity cooling of an atomic ensemble. *Physical review letters*, 107(14):143005, 2011.

[12] Yue Chang, T Shi, Yu-xi Liu, CP Sun, and Franco Nori. Multistability of electromagnetically induced transparency in atom-assisted optomechanical cavities. *Physical Review A*, 83(6):063826, 2011.

[13] Dan M Stamper-Kurn. Cavity optomechanics with cold atoms. In *Cavity Optomechanics: Nano-and Micromechanical Resonators Interacting with Light*, pages 283–325. Springer, 2014.

[14] William D Phillips and Harold Metcalf. Laser deceleration of an atomic beam. *Physical Review Letters*, 48(9):596, 1982.

[15] Harold J Metcalf, Peter van der Straten, Harold J Metcalf, and Peter van der Straten. Deceleration of an atomic beam. *Laser Cooling and Trapping*, pages 73–86, 1999.

[16] Justin B Spring, W Steven Kolthammer, James C Gates, Nathan K Langford, Xian-Min Jin, Peter C Humphreys, Benjamin J Metcalf, Ian A Walmsley, Marco Barbieri, Nicholas Thomas-Peter, et al. Experimental boson sampling. *Science*, 339(arXiv: 1212.2622):798–801, 2012.

[17] Jing Zhang, Kunchi Peng, and Samuel L Braunstein. Quantum-state transfer from light to macroscopic oscillators. *Physical Review A*, 68(1):013808, 2003.

[18] Michel Pinard, Y Hadjar, and Antoine Heidmann. Effective mass in quantum effects of radiation pressure. *The European Physical Journal D-Atomic, Molecular, Optical and Plasma Physics*, 7:107–116, 1999.

[19] Pierre Meystre and Murray Sargent. *Elements of quantum optics*. Springer Science & Business Media, 2007.

[20] Paolo Piergentili, Letizia Catalini, Mateusz Bawaj, Stefano Zippilli, Nicola Malossi, Riccardo Natali, David Vitali, and Giovanni Di Giuseppe. Two-membrane cavity optomechanics. *New Journal of Physics*, 20(8):083024, 2018.

[21] E Hecht. Optics 4th edition by eugene hecht reading. *MA: Addison-Wesley Publishing Company*, 1:2001, 2001.

[22] Kamran Ullah. Electro-optomechanical switch via tunable bistability and four-wave mixing. *Chinese Physics B*, 28(11):114209, 2019.

[23] Weijian Yang, Stephen Adair Gerke, Kar Wei Ng, Yi Rao, Christopher Chase, and Connie J Chang-Hasnain. Laser optomechanics. *Scientific reports*, 5(1):13700, 2015.

[24] Cheng-Hua Bai, Dong-Yang Wang, Hong-Fu Wang, Ai-Dong Zhu, and Shou Zhang. Robust entanglement between a movable mirror and atomic ensemble and entanglement transfer in coupled optomechanical system. *Scientific reports*, 6(1):33404, 2016.

[25] Christian Weedbrook, Stefano Pirandola, Raúl García-Patrón, Nicolas J Cerf, Timothy C Ralph, Jeffrey H Shapiro, and Seth Lloyd. Gaussian quantum information. *Reviews of Modern Physics*, 84(2):621, 2012.

[26] Pieter Kok and Brendon W Lovett. *Introduction to optical quantum information processing*. Cambridge university press, 2010.

[27] Michael A Nielsen and Isaac L Chuang. Quantum computation and information theory, 2010.

[28] Rodney Loudon. *The quantum theory of light*. OUP Oxford, 2000.

[29] Klaus Jöns. *Optical and quantum optical properties of site-controlled and strain-tuned quantum dots*. Verlag Dr. Hut, 2013.

[30] Ioannis Kogias. *Entanglement, Einstein-Podolsky-Rosen steering and cryptographical applications*. PhD thesis, University of Nottingham, 2016.

[31] Shohini Ghose and Barry C Sanders. Non-gaussian ancilla states for continuous variable quantum computation via gaussian maps. *Journal of Modern Optics*, 54(6):855–869, 2007.

[32] Nicolas J Cerf, Gerd Leuchs, and Eugene S Polzik. *Quantum information with continuous variables of atoms and light*. World Scientific, 2007.

[33] Samuel L Braunstein and Peter Van Loock. Quantum information with continuous variables. *Reviews of modern physics*, 77(2):513, 2005.

[34] Gerardo Adesso and Fabrizio Illuminati. Entanglement in continuous-variable systems: recent advances and current perspectives. *Journal of Physics A: Mathematical and Theoretical*, 40(28):7821, 2007.

[35] R Simon, ECG Sudarshan, and N Mukunda. Gaussian-wigner distributions in quantum mechanics and optics. *Physical Review A*, 36(8):3868, 1987.

[36] Reinhard F Werner and Michael M Wolf. Bound entangled gaussian states. *Physical review letters*, 86(16):3658, 2001.

[37] John Williamson. On the algebraic problem concerning the normal forms of linear dynamical systems. *American journal of mathematics*, 58(1):141–163, 1936.

[38] Gerardo Adesso, Alessio Serafini, and Fabrizio Illuminati. Entanglement, purity, and information entropies in continuous variable systems. *Open Systems & Information Dynamics*, 12(2):189–205, 2005.

[39] Mauro Paternostro, David Vitali, Sylvain Gigan, MS Kim, Caslav Brukner, Jens Eisert, and Markus Aspelmeyer. Creating and probing multipartite macroscopic entanglement with light. *Physical Review Letters*, 99(25):250401, 2007.

[40] Andrea Mari and Jens Eisert. Gently modulating optomechanical systems. *Physical Review Letters*, 103(21):213603, 2009.

[41] A Mari and Jens Eisert. Opto-and electro-mechanical entanglement improved by modulation. *New Journal of Physics*, 14(7):075014, 2012.

[42] Michel Pinard, Aurelien Dantan, David Vitali, Olivier Arcizet, Tristan Briant, and Antoine Heidmann. Entangling movable mirrors in a double-cavity system. *Europhysics Letters*, 72(5):747, 2005.

[43] Claudiu Genes, A Mari, P Tombesi, and D Vitali. Robust entanglement of a micromechanical resonator with output optical fields. *Physical Review A*, 78(3):032316, 2008.

[44] Christopher Wipf, Thomas Corbitt, Yanbei Chen, and Nergis Mavalvala. Route to ponderomotive entanglement of light via optically trapped mirrors. *New Journal of Physics*, 10(9):095017, 2008.

[45] David Vitali, Stefano Mancini, and Paolo Tombesi. Stationary entanglement between two movable mirrors in a classically driven fabry–perot cavity. *Journal of Physics A: Mathematical and Theoretical*, 40(28):8055, 2007.

[46] Maciej Lewenstein, Dagmar Bruß, Juan Ignacio Cirac, Barbara Kraus, Marek Kuś, Jan Samsonowicz, Anna Sanpera, and Rolf Tarrach. Separability and distillability in composite quantum systems-a primer. *Journal of Modern Optics*, 47(14-15):2481–2499, 2000.

[47] Thomas Beth and Gerd Leuchs. *Quantum information processing*. Wiley Online Library, 2005.

[48] S Alnujaim, A Bouhemadou, A Bedjaoui, S Bin-Omran, Y Al-Douri, R Khenata, and S Maabed. Ab initio prediction of the elastic, electronic and optical properties of a new family of diamond-like semiconductors, li2hgms4 (m= si, ge and sn). *Journal of Alloys and Compounds*, 843:155991, 2020.

[49] I SHAKENNOTST. 1 is there a perfect cipher? In *Challenges For The 21st Century, Procs Of The Intl Conf On Fundamental Sciences: Mathematics And Theoretical Physics*, page 339. World Scientific, 2001.

[50] Charles H Bennett, David P DiVincenzo, John A Smolin, and William K Wootters. Mixed-state entanglement and quantum error correction. *Physical Review A*, 54(5):3824, 1996.

[51] Guifré Vidal and Reinhard F Werner. Computable measure of entanglement. *Physical Review A*, 65(3):032314, 2002.

[52] Alessio Serafini, S De Siena, Fabrizio Illuminati, and Matteo GA Paris. Minimum decoherence cat-like states in gaussian noisy channels. *Journal of Optics B: Quantum and Semiclassical Optics*, 6(6):S591, 2004.

[53] Alessio Serafini, Fabrizio Illuminati, Matteo GA Paris, and Silvio De Siena. Entanglement and purity of two-mode gaussian states in noisy channels. *Physical Review A*, 69(2):022318, 2004.

[54] Sabrina Maniscalco, Stefano Olivares, and Matteo GA Paris. Entanglement oscillations in non-markovian quantum channels. *Physical Review A*, 75(6):062119, 2007.

[55] Ruggero Vasile, Stefano Olivares, Matteo GA Paris, and Sabrina Maniscalco. Continuous-variable-entanglement dynamics in structured reservoirs. *Physical Review A*, 80(6):062324, 2009.

[56] Gerardo Adesso, Davide Girolami, and Alessio Serafini. Measuring gaussian quantum information and correlations using the rényi entropy of order 2. *Physical review letters*, 109(19):190502, 2012.

[57] Gerardo Adesso and Fabrizio Illuminati. Gaussian measures of entanglement versus negativities: Ordering of two-mode gaussian states. *Physical Review A*, 72(3):032334, 2005.

[58] F Anza, Benedetto Militello, and Antonino Messina. Tripartite thermal correlations in an inhomogeneous spin–star system. *Journal of Physics B: Atomic, Molecular and Optical Physics*, 43(20):205501, 2010.

[59] Carlos Sabín and Guillermo García-Alcaine. A classification of entanglement in three-qubit systems. *The european physical journal D*, 48:435–442, 2008.

[60] Fabrizio Buscemi and Paolo Bordone. Measure of tripartite entanglement in bosonic and fermionic systems. *Physical Review A*, 84(2):022303, 2011.

[61] Leah Henderson and Vlatko Vedral. Classical, quantum and total correlations. *Journal of physics A: mathematical and general*, 34(35):6899, 2001.

[62] Harold Ollivier and Wojciech H Zurek. Quantum discord: a measure of the quantumness of correlations. *Physical review letters*, 88(1):017901, 2001.

[63] Stefano Olivares. Quantum optics in the phase space: a tutorial on gaussian states. *The European Physical Journal Special Topics*, 203(1):3–24, 2012.

[64] Gerardo Adesso and Animesh Datta. Quantum versus classical correlations in gaussian states. *Physical review letters*, 105(3):030501, 2010.

[65] Markus Aspelmeyer, Tobias J Kippenberg, and Florian Marquardt. Cavity optomechanics. *Reviews of Modern Physics*, 86(4):1391, 2014.

[66] Olivier Arcizet, P-F Cohadon, Tristan Briant, Michel Pinard, and Antoine Heidmann. Radiation-pressure cooling and optomechanical instability of a micromirror. *Nature*, 444(7115):71–74, 2006.

[67] Sumei Huang and GS Agarwal. Entangling nanomechanical oscillators in a ring cavity by feeding squeezed light. *New Journal of Physics*, 11(10):103044, 2009.

[68] Alexandre Brieussel, Yong Shen, Geoff Campbell, Giovanni Guccione, Jiri Janousek, Boris Hage, BC Buchler, Nicolas Treps, Christian Fabre, FZ Fang, et al. Squeezed light from a diamond-turned monolithic cavity. *Optics Express*, 24(4):4042–4056, 2016.

[69] Simon Chelkowski, Henning Vahlbruch, Boris Hage, Alexander Franzen, Nico Lastzka, Karsten Danzmann, and Roman Schnabel. Experimental characterization of frequency-dependent squeezed light. *Physical Review A*, 71(1):013806, 2005.

[70] Anthony E Siegman. New developments in laser resonators. In *Optical resonators*, volume 1224, pages 2–14. Spie, 1990.

[71] A Yariv. Quantum electronics. 3ˆ rd ed. *New York: John Wiley& Sins*, 1989.

[72] Claude Cohen-Tannoudji, Bernard Diu, and Franck Laloë. Mecanique quantique hermann, 1973.

[73] Jun John Sakurai and Eugene D Commins. Modern quantum mechanics, revised edition, 1995.

[74] Pau Mestres Junque. *Cavity optomechanics with optically trapped particles.* PhD thesis, Universitat Politecnica de Catalunya Barcelona, 2017.

[75] Andrew N Cleland and Michael R Geller. Superconducting qubit storage and entanglement with nanomechanical resonators. *Physical review letters*, 93(7):070501, 2004.

[76] Eyob A Sete, Hichem Eleuch, and CH Raymond Ooi. Light-to-matter entanglement transfer in optomechanics. *JOSA B*, 31(11):2821–2828, 2014.

[77] B Diu, C Guthmann, D Lederer, and B Roulet. Eléments de physique statistique, physique statistique, deuxieme cycle. *Hermann, Editeurs des sciences et des arts*, 1996.

[78] Aurélien G Kuhn. *Optomécanique en cavité cryogénique avec un micro-pilier pour l'observation du régime quantique d'un résonateur mécanique macroscopique.* PhD thesis, Université Pierre et Marie Curie-Paris VI, 2013.

[79] Claude Cohen-Tannoudji, Jacques Dupont-Roc, and Gilbert Grynberg. *Photons et atomes. Introduction à l'électrodynamique quantique: Introduction à l'électrodynamique quantique.* EDP sciences, 2012.

[80] MD LaHaye, Olivier Buu, Benedetta Camarota, and KC Schwab. Approaching the quantum limit of a nanomechanical resonator. *Science*, 304(5667):74–77, 2004.

[81] Alex Abramovici, William E Althouse, Ronald WP Drever, Yekta Gürsel, Seiji Kawamura, Frederick J Raab, David Shoemaker, Lisa Sievers, Robert E Spero, Kip S Thorne, et al. Ligo: The laser interferometer gravitational-wave observatory. *science*, 256(5055):325–333, 1992.

[82] Carlo Bradaschia, R Del Fabbro, A Di Virgilio, A Giazotto, H Kautzky, V Montelatici, D Passuello, A Brillet, O Cregut, P Hello, et al. The virgo project: a wide band antenna for gravitational wave detection. *Nuclear Instruments and Methods in Physics Research Section A: Accelerators, Spectrometers, Detectors and Associated Equipment*, 289(3):518–525, 1990.

[83] Thomas Corbitt, Christopher Wipf, Timothy Bodiya, David Ottaway, Daniel Sigg, Nicolas Smith, Stanley Whitcomb, and Nergis Mavalvala. Optical dilution and feedback cooling of a gram-scale oscillator to 6.9 mk. *Physical Review Letters*, 99(16):160801, 2007.

[84] Tobias J Kippenberg and Kerry J Vahala. Cavity optomechanics: back-action at the mesoscale. *science*, 321(5893):1172–1176, 2008.

[85] Florian Marquardt and Steven M Girvin. Optomechanics. *Physics*, 2:40, 2009.

[86] CK Law. Interaction between a moving mirror and radiation pressure: A hamiltonian formulation. *Physical Review A*, 51(3):2537, 1995.

[87] Rafael Benguria and Mark Kac. Quantum langevin equation. *Physical review letters*, 46(1):1, 1981.

[88] Vittorio Giovannetti and David Vitali. Phase-noise measurement in a cavity with a movable mirror undergoing quantum brownian motion. *Physical Review A*, 63(2):023812, 2001.

[89] DF Walls. Gj milburn, quantum optics (springer, berlin, 1994.

[90] David Vitali, Sylvain Gigan, Anderson Ferreira, HR Böhm, Paolo Tombesi, Ariel Guerreiro, Vlatko Vedral, Anton Zeilinger, and Markus Aspelmeyer. Optomechanical entanglement between a movable mirror and a cavity field. *Physical review letters*, 98(3):030405, 2007.

[91] Edmund X DeJesus and Charles Kaufman. Routh-hurwitz criterion in the examination of eigenvalues of a system of nonlinear ordinary differential equations. *Physical Review A*, 35(12):5288, 1987.

[92] Roohollah Ghobadi, AR Bahrampour, and C Simon. Quantum optomechanics in the bistable regime. *Physical Review A*, 84(3):033846, 2011.

[93] Gerardo Adesso, Alessio Serafini, and Fabrizio Illuminati. Extremal entanglement and mixedness in continuous variable systems. *Physical Review A*, 70(2):022318, 2004.

[94] Rajiah Simon. Peres-horodecki separability criterion for continuous variable systems. *Physical Review Letters*, 84(12):2726, 2000.

[95] Kater W Murch, Kevin L Moore, Subhadeep Gupta, and Dan M Stamper-Kurn. Observation of quantum-measurement backaction with an ultracold atomic gas. *Nature Physics*, 4(7):561–564, 2008.

[96] Jasper Chan, TP Alegre, Amir H Safavi-Naeini, Jeff T Hill, Alex Krause, Simon Gröblacher, Markus Aspelmeyer, and Oskar Painter. Laser cooling of a nanomechanical oscillator into its quantum ground state. *Nature*, 478(7367):89–92, 2011.

[97] John D Teufel, Tobias Donner, Dale Li, Jennifer W Harlow, MS Allman, Katarina Cicak, Adam J Sirois, Jed D Whittaker, Konrad W Lehnert, and Raymond W Simmonds. Sideband cooling of micromechanical motion to the quantum ground state. *Nature*, 475(7356):359–363, 2011.

[98] Ewold Verhagen, Samuel Deléglise, Stefan Weis, Albert Schliesser, and Tobias J Kippenberg. Quantum-coherent coupling of a mechanical oscillator to an optical cavity mode. *Nature*, 482(7383):63–67, 2012.

[99] BD Cuthbertson, ME Tobar, EN Ivanov, and DG Blair. Parametric back-action effects in a high-q cyrogenic sapphire transducer. *Review of Scientific Instruments*, 67(7):2435–2442, 1996.

[100] Simon Gröblacher, Klemens Hammerer, Michael R Vanner, and Markus Aspelmeyer. Observation of strong coupling between a micromechanical resonator and an optical cavity field. *Nature*, 460(7256):724–727, 2009.

[101] Dustin Kleckner, Brian Pepper, Evan Jeffrey, Petro Sonin, Susanna M Thon, and Dirk Bouwmeester. Optomechanical trampoline resonators. *Optics express*, 19(20):19708–19716, 2011.

[102] C Genes, D Vitali, and P Tombesi. Emergence of atom-light-mirror entanglement inside an optical cavity. *Physical Review A*, 77(5):050307, 2008.

[103] Long Chang, Xiaoshun Jiang, Shiyue Hua, Chao Yang, Jianming Wen, Liang Jiang, Guanyu Li, Guanzhong Wang, and Min Xiao. Parity–time symmetry and variable optical isolation in active–passive-coupled microresonators. *Nature photonics*, 8(7):524–529, 2014.

[104] Ivan S Grudinin, Hansuek Lee, Oskar Painter, and Kerry J Vahala. Phonon laser action in a tunable two-level system. *Physical review letters*, 104(8):083901, 2010.

[105] T Holstein and Hl Primakoff. Field dependence of the intrinsic domain magnetization of a ferromagnet. *Physical Review*, 58(12):1098, 1940.

[106] Crispin W Gardiner. Springer series in synergetics, 2009.

[107] CW Gardiner. Inhibition of atomic phase decays by squeezed light: A direct effect of squeezing. *Physical review letters*, 56(18):1917, 1986.

[108] Schwab Gigan, HR Böhm, Mauro Paternostro, Florian Blaser, G Langer, JB Hertzberg, Keith C Schwab, Dieter Bäuerle, Markus Aspelmeyer, and Anton Zeilinger. Self-cooling of a micromirror by radiation pressure. *Nature*, 444(7115):67–70, 2006.

[109] Olivier Arcizet, P-F Cohadon, T Briant, M Pinard, A Heidmann, J-M Mackowski, Christine Michel, L Pinard, O Français, and L Rousseau. High-sensitivity optical monitoring of a micromechanical resonator with a quantum-limited optomechanical sensor. *Physical review letters*, 97(13):133601, 2006.

[110] Thomas Corbitt, Christopher Wipf, Timothy Bodiya, David Ottaway, Daniel Sigg, Nicolas Smith, Stanley Whitcomb, and Nergis Mavalvala. Optical dilution and feedback cooling of a gram-scale oscillator to 6.9 mk. *Physical Review Letters*, 99(16):160801, 2007.

[111] T Kipf and GS Agarwal. Superradiance and collective gain in multimode optomechanics. *Physical Review A*, 90(5):053808, 2014.

[112] Robert H Dicke. Coherence in spontaneous radiation processes. *Physical review*, 93(1):99, 1954.

[113] Wei Zeng, Wenjie Nie, Ling Li, and Aixi Chen. Ground-state cooling of a mechanical oscillator in a hybrid optomechanical system including an atomic ensemble. *Scientific reports*, 7(1):17258, 2017.

[114] Gabriele De Chiara, Mauro Paternostro, and G Massimo Palma. Entanglement detection in hybrid optomechanical systems. *Physical Review A*, 83(5):052324, 2011.

[115] Rui-Jie Xiao, Gui-Xia Pan, and Ling Zhou. Multiple optomechanically induced transparency in a ring cavity optomechanical system assisted by atomic media. *International Journal of Theoretical Physics*, 54:3665–3675, 2015.

[116] Sh Barzanjeh, MH Naderi, and M Soltanolkotabi. Steady-state entanglement and normal-mode splitting in an atom-assisted optomechanical system with intensity-dependent coupling. *Physical Review A*, 84(6):063850, 2011.

[117] Ralf Riedinger, Sungkun Hong, Richard A Norte, Joshua A Slater, Juying Shang, Alexander G Krause, Vikas Anant, Markus Aspelmeyer, and Simon Gröblacher. Non-classical correlations between single photons and phonons from a mechanical oscillator. *Nature*, 530(7590):313–316, 2016.

[118] Remi Riviere, Samuel Deleglise, Stefan Weis, Emanuel Gavartin, Olivier Arcizet, Albert Schliesser, and Tobias J Kippenberg. Optomechanical sideband cooling of a micromechanical oscillator close to the quantum ground state. *Physical Review A*, 83(6):063835, 2011.

[119] X Maitre, E Hagley, G Nogues, C Wunderlich, P Goy, M Brune, JM Raimond, and S Haroche. Quantum memory with a single photon in a cavity. *Physical review letters*, 79(4):769, 1997.

[120] Cong Cao, Yu-Wen Duan, Xi Chen, Ru Zhang, Tie-Jun Wang, and Chuan Wang. Implementation of single-photon quantum routing and decoupling using a nitrogen-vacancy center and a whispering-gallery-mode resonator-waveguide system. *Optics Express*, 25(15):16931–16946, 2017.

[121] Bei-Bei Li, Lingfeng Ou, Yuechen Lei, and Yong-Chun Liu. Cavity optomechanical sensing. *Nanophotonics*, 10(11):2799–2832, 2021.

[122] Fabienne Schneiter, Sofia Qvarfort, Alessio Serafini, André Xuereb, Daniel Braun, Dennis Rätzel, and David Edward Bruschi. Optimal estimation with quantum optomechanical systems in the nonlinear regime. *Physical Review A*, 101(3):033834, 2020.

[123] Sebastian G Hofer, Witlef Wieczorek, Markus Aspelmeyer, and Klemens Hammerer. Quantum entanglement and teleportation in pulsed cavity optomechanics. *Physical Review A*, 84(5):052327, 2011.

[124] Stefano Mancini, VI Man'Ko, and Paolo Tombesi. Ponderomotive control of quantum macroscopic coherence. *Physical Review A*, 55(4):3042, 1997.

[125] Sougato Bose, Kurt Jacobs, and Peter L Knight. Preparation of nonclassical states in cavities with a moving mirror. *Physical Review A*, 56(5):4175, 1997.

[126] Max Ludwig, Björn Kubala, and Florian Marquardt. The optomechanical instability in the quantum regime. *New Journal of Physics*, 10(9):095013, 2008.

[127] Ivan Favero and Khaled Karrai. Optomechanics of deformable optical cavities. *Nature Photonics*, 3(4):201–205, 2009.

[128] PF Barker and MN Shneider. Cavity cooling of an optically trapped nanoparticle. *Physical Review A*, 81(2):023826, 2010.

[129] Zhang-qi Yin, Tongcang Li, Xiang Zhang, and LM Duan. Large quantum superpositions of a levitated nanodiamond through spin-optomechanical coupling. *Physical Review A*, 88(3):033614, 2013.

[130] Sofia Qvarfort, Alessio Serafini, André Xuereb, Dennis Rätzel, and David Edward Bruschi. Enhanced continuous generation of non-gaussianity through optomechanical modulation. *New Journal of Physics*, 21(5):055004, 2019.

[131] Sofia Qvarfort, Alessio Serafini, André Xuereb, Daniel Braun, Dennis Rätzel, and David Edward Bruschi. Time-evolution of nonlinear optomechanical systems: Interplay of mechanical squeezing and non-gaussianity. *Journal of Physics A: Mathematical and Theoretical*, 53(7):075304, 2020.

[132] David Edward Bruschi, Antony R Lee, and Ivette Fuentes. Time evolution techniques for detectors in relativistic quantum information. *Journal of Physics A: Mathematical and Theoretical*, 46(16):165303, 2013.

[133] Gerardo Adesso, Sammy Ragy, and Antony R Lee. Continuous variable quantum information: Gaussian states and beyond. *Open Systems & Information Dynamics*, 21(01n02):1440001, 2014.

[134] Alessio Serafini. *Quantum continuous variables: a primer of theoretical methods*. CRC press, 2017.

[135] Marco G Genoni, Matteo GA Paris, and Konrad Banaszek. Quantifying the non-gaussian character of a quantum state by quantum relative entropy. *Physical Review A*, 78(6):060303, 2008.

[136] Jiyong Park, Jaehak Lee, Kyunghyun Baek, Se-Wan Ji, and Hyunchul Nha. Faithful measure of quantum non-gaussianity via quantum relative entropy. *Physical Review A*, 100(1):012333, 2019.

[137] Seth Lloyd and Samuel L Braunstein. Quantum information with continuous variables, 1999.

[138] Nicolas C Menicucci, Peter Van Loock, Mile Gu, Christian Weedbrook, Timothy C Ralph, and Michael A Nielsen. Universal quantum computation with continuous-variable cluster states. *Physical review letters*, 97(11):110501, 2006.

[139] Fabio Dell'Anno, Silvio De Siena, Gerardo Adesso, and Fabrizio Illuminati. Teleportation of squeezing: Optimization using non-gaussian resources. *Physical Review A*, 82(6):062329, 2010.

[140] Jens Eisert and Martin B Plenio. Conditions for the local manipulation of gaussian states. *Physical review letters*, 89(9):097901, 2002.

[141] Jaromír Fiurášek. Gaussian transformations and distillation of entangled gaussian states. *Physical review letters*, 89(13):137904, 2002.

[142] Géza Giedke and J Ignacio Cirac. Characterization of gaussian operations and distillation of gaussian states. *Physical Review A*, 66(3):032316, 2002.

[143] Ryuji Takagi and Quntao Zhuang. Convex resource theory of non-gaussianity. *Physical Review A*, 97(6):062337, 2018.

[144] Quntao Zhuang, Peter W Shor, and Jeffrey H Shapiro. Resource theory of non-gaussian operations. *Physical Review A*, 97(5):052317, 2018.

[145] Uzma Akram, William Munro, Kae Nemoto, and GJ Milburn. Photon-phonon entanglement in coupled optomechanical arrays. *Physical Review A*, 86(4):042306, 2012.

[146] John D Jost, JP Home, Jason M Amini, David Hanneke, Roee Ozeri, Christopher Langer, John J Bollinger, Dietrich Leibfried, and David J Wineland. Entangled mechanical oscillators. *Nature*, 459(7247):683–685, 2009.

[147] Shabir Barzanjeh, ES Redchenko, Matilda Peruzzo, Matthias Wulf, DP Lewis, G Arnold, and Johannes M Fink. Stationary entangled radiation from micromechanical motion. *Nature*, 570(7762):480–483, 2019.

[148] K Børkje, A Nunnenkamp, and SM Girvin. Proposal for entangling remote micromechanical oscillators via optical measurements. *Physical review letters*, 107(12):123601, 2011.

[149] Paolo Giorda and Matteo G. A. Paris. Gaussian quantum discord. *Phys. Rev. Lett.*, 105:020503, Jul 2010.

[150] Marco G Genoni, Mattia L Palma, Tommaso Tufarelli, Stefano Olivares, MS Kim, and Matteo GA Paris. Detecting quantum non-gaussianity via the wigner function. *Physical Review A*, 87(6):062104, 2013.

[151] Francesco Albarelli, Marco G Genoni, Matteo GA Paris, and Alessandro Ferraro. Resource theory of quantum non-gaussianity and wigner negativity. *Physical Review A*, 98(5):052350, 2018.

ROYAUME DU MAROC
Université Mohammed V - RABAT -
جامعة محمد الخامس – الرباط –
Faculté des sciences
كلية العلوم

Résumé

Cette thèse est consacrée à l'étude des corrélations quantiques au sein d'une cavité optomécanique en anneau. Cette étude met en lumière l'interaction extraordinaire entre la lumière et le mouvement mécanique au niveau quantique. Une étude théorique complète basé sur les principaux concepts de l'optomécanique est donné. Les progrès récents dans ce domaine ont ouvert de nombreuses applications dans diverses structures. Dans ce contexte, On donne une description claire du choix d'une cavité annulaire, qui présente un milieu idéal pour étudier les effets coopératifs grâce à leur interaction commune avec le mode de la cavité. Les cavités annulaires diffèrent de la conception traditionnelle des cavités Fabry-Pérot par la présence de paires de miroirs mobiles. Cela ajoute une manipulation dynamique supplémentaire du déplacement des deux résonateurs, intensifiant ainsi le champ optique intra-cavité, contrairement au cas d'une cavité linéaire. Un autre type de système présenté dans cette thèse, considéré comme une source de grande variété de phénomènes physiques, est le système atome-optomécanique, où un ensemble d'atomes est confiné à l'intérieur de la cavité, permettant des interactions à longue distance et des corrélations multipartites. Dans la deuxième partie de la thèse, l'accent est mis sur la composante non linéaire de l'Hamiltonien optomécanique. La résolution de la dynamique est effectué en excluant le traitement de linéarisation. Cette solution est basée sur l'identification d'une algèbre de Lie minimale et finie qui génère l'évolution temporelle du système, et dérive une solution analytique pour calculer la non-Gaussianité du système en fonction du temps.

Mots-clefs: Optomécanique, intrication, cavité en anneau, corrélations quantiques, non-Gaussianité.

Abstract

This thesis focuses on the fascinating realm of quantum correlations within a ring optomechanical cavity, shedding light on the extraordinary interplay between light and mechanical motion at the quantum level. A comprehensive theoretical framework based on the principal concepts of optomechanics. Recent advancements in this have opened up numerous applications in various structures. In this context, a clear description of choosing a ring cavity, which serves as an ideal testbed to exhibit cooperative effects through their common interaction with the cavity mode. Ring cavities differ from the traditional Fabry-Perot cavity design by having pairs of movable mirrors. This adds an extra dynamic manipulation of the displacement of the two resonators, thereby intensifying the intra-cavity optical field, unlike in the case of a linear cavity. Another type of system presented in this thesis, which serves as a source of a wide variety of physical phenomena, is the atom- optomechanical system, where an ensemble of atoms is confined inside the cavity, allowing for long range interactions and multipartite correlations. In the next part of the thesis, the nonlinear component of the optomechanical Hamiltonian is emphasized. The resolution of the dynamics is carried out excluding the linearization treatment. This solution is based on identifying a minimal and finite Lie algebra that generates the time-evolution of the system, and derive analytic solution to compute the non-Gaussianity of the system as function of the time.

Keywords: Optomechanics, entanglement, ring cavity, quantum correlations, non-Gaussianity.

✉ Faculté des Sciences, avenue Ibn Battouta, BP. 1014 RP, Rabat-Maroc
☎ 00212 (05) 37 77 18 76 🖷 00212 (05) 37 77 42 61; http://www.fsr.um5.ac.ma